

Local Dosing in a 3-Mercaptopropionic Acid Chemically-Induced Epileptic Seizure  
Model with Microdialysis Sampling

By

Andrew Philip Mayer

B.A. Franklin and Marshall College

Lancaster, PA, 2006

Submitted to the graduate degree program in Chemistry and the Graduate Faculty of the  
University of Kansas in partial fulfillment of the requirements for the degree of Doctor of  
Philosophy.

---

Chairperson: Craig E. Lunte

---

Susan Lunte

---

Bob Dunn

---

Michael Johnson

---

Ivan Osorio

Date Defended: November 23, 2010

The Dissertation Committee for Andrew Philip Mayer  
certifies that this is the approved version of the following dissertation:

Local Dosing in a 3-Mercaptopropionic Acid Chemically-Induced Epileptic Seizure  
Model with Microdialysis Sampling

---

Chairperson: Craig E. Lunte

Date approved: December 15, 2010

## Abstract

Andrew Philip Mayer, Ph.D.

R.N. Adams Institute for Bioanalytical Chemistry

Department of Chemistry, November 2010

The University of Kansas

The focus of this research was the development of an animal model for local administration of 3-mercaptopropionic acid (3-MPA) in a chemically-induced epileptic seizure model using microdialysis sampling with simultaneous electrocorticography recording (ECoG). Local administration of 3-MPA through the microdialysis probe was employed to elicit seizures in a localized brain region. Delivery of 3-MPA to the brain and changes in amino acid and catecholamine neurotransmitters were monitored. Simultaneous ECoG recordings were made using a microdialysis probe with an internal Ag/AgCl electrode. Local administration of a convulsant is important, as many clinical cases present with focal seizures.

Neurochemical and electrical activity were monitored in three separate brain regions: the striatum, hippocampus, and *locus coeruleus*. 3-MPA was administered through the microdialysis probe in one region, while control samples were collected in the other two. These results demonstrated that unless two brain regions were connected via efferent or afferent pathways, administration of 3-MPA in one region had no neurochemical effect in the others. In the region where 3-MPA was administered, an

increase in both glutamate, the main excitatory amino acid, and GABA, the main inhibitory amino acid, was seen. In addition, an increase in both dopamine and norepinephrine was seen.

A multiple dosing regimen of 3-MPA was developed where 3-MPA was administered twice. These results showed that there was an attenuation in the increase of glutamate and GABA during the second administration of 3-MPA, indicating a neuronal protective mechanism taking place to decrease the effect of the second 3-MPA administration.

Seizures were not detected using during local administration of 3-MPA using the microdialysis probes with an internal Ag/AgCl electrode. This was not due to the ineffectiveness of the electrodes, as they detected seizures during systemic dosing of 3-MPA. It is possible that the number of neurons excited from the local administration of 3-MPA were so limited that the signal was too small to be detected.

## Acknowledgements

First I would like to thank some of the teachers I have had in the past who made science fun, and played a large part in me deciding to study chemistry. Thanks to my high school chemistry teachers Ms. Sabatino and Mr. Kaman, turns out chemistry when you get your doctorate is slightly different than in high school, go figure! Also, special thanks to my undergraduate advisor Dr. Hess. He is the main reason I enjoy analytical chemistry so much and I will always remember to be “appropriately lazy”. Of course, thanks to Craig, I needed an advisor that was hands off and let me work things out on my own, and I got that. Also, thank you to my committee Dr. Sue Lunte, Dr. Robert Dunn, Dr. Michael Johnson, and Dr. Ivan Osorio.

Thank you to my collaborator, Dr. Ivan Osorio. I remember one of the first times I met you, you were performing a surgery in the animal room and blood ended up all over the walls, thankfully this was an isolated incident. But seriously, you have been patient explaining to me a lot of the epilepsy/seizure terminology that I knew nothing about when I started, but thankfully know “a little” about now that I’m done. Thank you to Dr. Mark Frei and Dr. Alexey Lyubushin for analyzing the ECoG data for me. Also, thank you to Dr. Mike Thompson at LMH for the brain histology slices.

I would also like to thank present and past Lunte group members as well as other friends at KU. It’s always nice to have someone to share the frustrations of graduate school with.

Finally I would like to thank my family. Has always seemed like I had science in my blood and I would end up here someday, although I never felt pressured to be someone I wasn't. My parents, Phil and Ginny, have always been supportive even in those times when I wasn't so sure I was going to make it to the end. It has been nice to have parents who understood the graduate school process and science in general. Thank you to my brother Matthew, who does not have science in his blood, but I won't hold it against him. Thank you to my mother-in-law Nancy for taking care of Emma over the years and allowing DeAnna and I to work. A BIG thank you to my wife DeAnna, obviously. I wasn't expecting to come to KU and get married and have a baby, but I got both of those and I couldn't have been luckier. She has made countless sacrifices over the years for me to finish school and I hope someday I will be able to repay all of that. Last, and most importantly, my daughter Emma, there is nothing better than getting your work done for the day and walking in the door and hearing her say "Daddy's home", that will never get old. Emma, you are the reason I plugged on day after day, contrary to popular belief it wasn't so I could buy you milk! DeAnna and Emma: I love you two very much!

## Table of Contents

### Chapter 1: Introduction

1.1 Epilepsy overview.....	1
1.2 Treatments for Epilepsy.....	1
1.3 Overview of animal seizure models.....	3
1.3.1 Electrical and chemical kindling models.....	3
1.3.2 Chemically-induced seizure models.....	6
1.4 Electrophysiology recording.....	7
1.5 Microdialysis sampling.....	8
1.5.1 Theory of microdialysis sampling.....	9
1.5.2 Microdialysis probe designs.....	10
1.5.3 Microdialysis calibration methods.....	11
1.5.4 Advantages and limitations.....	18
1.5.5 Applications.....	20
1.6 Separations.....	21
1.6.1 Liquid chromatography.....	21
1.6.1.1 Theory.....	21
1.6.1.2 Modes of separation.....	28
1.6.1.3 Modes of detection.....	30
1.7 Overview of Research.....	32
1.8 References.....	34

## Chapter 2: Methods

2.1 Introduction.....	42
2.1.1 Background and Significance.....	42
2.1.2 Amino acid neurotransmitters.....	46
2.1.3 Catecholamine neurotransmitters and their metabolites.....	47
2.1.4 Methods for the determination of neurotransmitters and their metabolites in biological samples.....	53
2.1.5 Mechanisms of action of 3-Mercaptopropionic acid.....	53
2.1.6 Current uses for 3-Mercaptopropionic acid.....	54
2.2 Materials and methods.....	54
2.2.1 Chemical and reagents.....	54
2.2.2 Microdialysis sample considerations.....	55
2.2.3 Sample derivitization scheme.....	56
2.2.4 Instrumentation.....	60
2.2.4.1 3-Mercaptopropionic acid and catecholamine neurotransmitters.....	60
2.2.4.2 Amino acid neurotransmitters.....	65



2.2.5 Surgical procedures.....	67
2.2.5.1 Animal and instrumentation preparation.....	67
2.2.5.2 Microdialysis probe implantation.....	68
2.2.6 ECoG recordings.....	69
2.3 References.....	70

**Chapter 3: 3-MPA Local Dosing in the striatum, hippocampus, and *locus coeruleus***

3.1 Introduction.....	75
3.1.1 Background and Significance.....	75
3.1.2 Striatum.....	76
3.1.3 Hippocampus.....	77
3.1.4 <i>locus coeruleus</i> .....	78
3.1.5 Neuronal projections.....	84
3.1.6 Experimental.....	84
3.2 Results and Discussion.....	85
3.2.1 3-MPA delivery in the striatum, hippocampus, and <i>locus coeruleus</i> .....	85

3.2.2 Striatum amino acids.....	90
3.2.2.1 Striatum amino acids in anesthetized rats.....	90
3.2.2.2 Striatum amino acids in awake rats.....	93
3.2.2.3 Striatum amino acid projections into the hippocampus.....	96
3.2.2.4 Striatum amino acid projections into the <i>locus coeruleus</i> .....	96
3.2.3 Hippocampus amino acids.....	100
3.2.3.1 Hippocampus amino acids in anesthetized rats.....	100
3.2.3.2 Hippocampus amino acids in awake rats.....	101
3.2.3.3 Hippocampus amino acid projections into the striatum.....	101
3.2.3.4 Hippocampus amino acids projections into <i>locus coeruleus</i> .....	105
3.2.4 <i>locus coeruleus</i> amino acids.....	108
3.2.4.1 <i>locus coeruleus</i> amino acids in anesthetized rats.....	108
3.2.4.2 <i>locus coeruleus</i> amino acid projections into	

the striatum.....	109
3.2.4.3 <i>locus coeruleus</i> amino acid projections into	
the hippocampus.....	109
3.2.5 Amino acids in anesthetized versus awake animals.....	114
3.2.6 Inhibitory surround.....	115
3.2.7 Sources of extracellular glutamate and GABA.....	119
3.2.8 GAD isoform compartmentalization.....	120
3.2.9 Striatum catecholamine neurotransmitters.....	120
3.2.9.1 Striatum catecholamines in anesthetized rats.....	120
3.2.9.2 Striatum catecholamine projections into	
the hippocampus.....	122
3.2.9.3 Striatum catecholamine projections into	
the <i>locus coeruleus</i> .....	122
3.2.10 Hippocampus catecholamine neurotransmitters.....	123
3.2.10.1 Hippocampus catecholamines in anesthetized	
rats.....	123
3.2.10.2 Hippocampus catecholamine projections	

into the striatum.....	123
3.2.10.3 Hippocampus catecholamine projections	
into the <i>locus coeruleus</i> .....	123
3.2.11 <i>locus coeruleus</i> catecholamine neurotransmitters.....	132
3.2.11.1 <i>locus coeruleus</i> catecholamines in anesthetized	
rats.....	132
3.2.11.2 <i>locus coeruleus</i> catecholamine projections	
into the striatum.....	132
3.2.11.3 <i>locus coeruleus</i> catecholamine projections	
into the hippocampus.....	133
3.2.12 ECoG results.....	137
3.2.13 Local dosing of picrotoxin.....	144
3.2.14 Brain histology.....	145
3.3 Conclusions.....	147
3.4 References.....	148

## **Chapter 4: Multiple Dosing of 3-MPA**

4.1 Introduction.....	160
4.1.1 Background and Significance.....	160
4.1.2 Desensitization.....	161
4.1.3 Sensitization.....	162
4.1.4 Long-term potentiation.....	163
4.1.5 Short-term depression.....	164
4.1.6 Regulation of enzyme activity, proteins, and transporters.....	164
4.1.7 Experimental Procedure.....	165
4.2 Results and Discussion.....	165
4.2.1 3-MPA.....	165
4.2.2 Amino acids.....	168
4.2.3 Catecholamine neurotransmitters.....	174
4.2.4 ECoG analysis.....	174
4.3 Conclusions.....	178
4.4 References.....	179

## **Chapter 5: Conclusions and Future Work**

5.1 Summary of Dissertation.....	185
5.1.1 3-MPA local dosing in the striatum, hippocampus and <i>locus coeruleus</i> .....	186
5.1.2 Multiple dosing of 3-MPA.....	189
5.2 Future Directions.....	190
5.3 References.....	192

## List of Figures

Figure 1.1 Effectiveness of treatments by AED's.....	5
Figure 1.2 Microdialysis theory.....	13
Figure 1.3 Rigid cannula microdialysis probe design for brain experiments.....	14
Figure 1.4 Alternative microdialysis probe designs.....	15
Figure 1.5 Schematic of a typical HPLC system.....	24
Figure 1.6 Capacity factor calculation from sample chromatogram.....	25
Figure 2.1 Average brain 3-MPA concentrations from systemic dosing.....	43
Figure 2.2 Changes in glutamate and GABA during systemic dosing.....	44
Figure 2.3 Structures of amino acid neurotransmitters.....	48
Figure 2.4 Metabolic synthesis and breakdown of	

glutamic acid and $\gamma$ -hydroxybutyric acid.....	49
Figure 2.5 Catecholamine neurotransmitters of interest.....	50
Figure 2.6 Biosynthesis and metabolism of catecholamine neurotransmitters of interest.....	51
Figure 2.7 Metabolites of tryptophan.....	52
Figure 2.8 NDA/CN <sup>-</sup> reaction scheme.....	58
Figure 2.9 NDA/CN <sup>-</sup> reaction times.....	59
Figure 2.10 Schematic of dual parallel working electrode.....	61
Figure 2.11 Typical chromatogram of 3-MPA.....	63
Figure 2.12 Typical LC-EC chromatogram.....	64
Figure 2.13 Typical LC-FL chromatogram.....	66
Figure 3.1 Basal ganglia coronal slice.....	80
Figure 3.2 Basal ganglia circuitry.....	81
Figure 3.3 Pathways in the hippocampus.....	82
Figure 3.4 <i>Locus coeruleus</i> projections.....	83
Figure 3.5 3-MPA Delivery in the striatum.....	87



Figure 3.6 3-MPA Delivery in the hippocampus.....	88
Figure 3.7 3-MPA Delivery in the <i>locus coeruleus</i> .....	89
Figure 3.8 Striatum neurotransmitters return to basal.....	91
Figure 3.9 aCSF control in the striatum.....	92
Figure 3.10 Striatum amino acids in anesthetized rats.....	94
Figure 3.11 Striatum amino acids in awake rats.....	95
Figure 3.12 Striatum amino acid projections into hippocampus.....	98
Figure 3.13 Striatum amino acid projections into <i>locus coeruleus</i> .....	99
Figure 3.14 aCSF control in the hippocampus.....	103
Figure 3.15 Hippocampus amino acids in anesthetized rats.....	104
Figure 3.16 Hippocampus amino acids in awake rats.....	105
Figure 3.17 Hippocampus amino acid projections into striatum.....	107
Figure 3.18 Hippocampus amino acid projections in <i>locus coeruleus</i> .....	108
Figure 3.19 <i>Locus coeruleus</i> amino acids in anesthetized rats.....	112
Figure 3.20 <i>Locus coeruleus</i> amino acid projections into striatum .....	113
Figure 3.21 <i>Locus coeruleus</i> amino acid projections into hippocampus.....	114
Figure 3.22 Glu/GABA ratio in the striatum of anesthetized rats.....	118

Figure 3.23 Schematic of the inhibitory surround.....	119
Figure 3.24 Striatum catecholamines in anesthetized rats.....	125
Figure 3.25 Circuitry of the basal ganglia.....	126
Figure 3.26 Striatum catecholamine projections into hippocampus.....	127
Figure 3.27 Striatum catecholamine projections into <i>locus coeruleus</i> .....	128
Figure 3.28 Hippocampus catecholamines in anesthetized rats.....	129
Figure 3.29 Hippocampus catecholamine projections into striatum.....	130
Figure 3.30 Hippocampus catecholamine projections into <i>locus coeruleus</i> .....	131
Figure 3.31 <i>Locus coeruleus</i> catecholamines in anesthetized rats.....	134
Figure 3.32 <i>Locus coeruleus</i> catecholamine projections into striatum.....	135
Figure 3.33 <i>Locus coeruleus</i> catecholamine projections into hippocampus.....	136
Figure 3.34 Diagram of microdialysis probe with internal electrode.....	139
Figure 3.35 ECoG raw data.....	140
Figure 3.36 ECoG data from screws on cortex during systemic dosing.....	141
Figure 3.37 ECoG data from microdialysis probe during systemic dosing.....	142
Figure 3.38 ECoG data from microdialysis probe during local dosing.....	143
Figure 3.39 Histology slices.....	146

Figure 4.1 3-MPA multiple dosing in the hippocampus.....	167
Figure 4.2 Glutamate/GABA for 3-MPA multiple dosing in hippocampus.....	172
Figure 4.3 Amino acids for 3-MPA multiple dosing in hippocampus.....	173
Figure 4.4 Catecholamine for 3-MPA multiple dosing in hippocampus.....	175
Figure 4.5 Catecholamine metabolites for 3-MPA multiple dosing.....	176
Figure 4.6 ECoG data for 3-MPA multiple dosing.....	177

## **Chapter 1**

### **Introduction**

#### **1.1 Epilepsy Overview**

Epilepsy is a neurologic disorder that affects 50 million people worldwide, approximately 1% of the world's population [1]. Epilepsy is defined as two or more unprovoked seizures, meaning they are not caused by pre-existing conditions or environmental triggers such as low blood sugar or head trauma [1]. A seizure is a surge of electrical activity from the neurons in the central nervous system (CNS). There is a fine balance in the brain between excitation and inhibition, as well as factors that propagate and restrict electrical activity. While there are many animal seizure models with systemic dosing of convulsants, there are few where seizures are generated in a specific brain region [2]. This is important because 70% of new adult-onset epilepsy patients present with focal (local) seizures [3]. Generating seizures in a localized brain region will aid in the understanding of how it and other areas of the brain respond.

#### **1.2 Treatments for Epilepsy**

The first course of therapy for epilepsy patients is anti-epileptic drugs (AEDs). Pharmacological treatments for epilepsy have many different mechanisms of action, including sodium channel blockers (carbamazepine and phenytoin), GABA receptor agonists (phenobarbital), GABA reuptake inhibitors (tiagabine), GABA Transaminase inhibitors (vigabatrin), and glutamate blockers (felbamate and topiramate). While the knowledge of the mechanism of action of these drugs as well as an increase in the

discovery of new pharmacological treatments have increased over the years, only two-thirds of the epileptic population are effectively treated by either one AED or a combination [4]. Figure 1.1 shows the percentage of the population who are seizure-free with AEDs. Clearly there is a need for different treatments for the other one-third of the population.

One such treatment is the ketogenic diet. This diet is high in fat and low in carbohydrates and is often used for treatment of children with epilepsy. Being a low-carbohydrate diet, the body must then convert fats into fatty acids and ketones as opposed to burning carbs. The ketones then pass into the brain and are used as fuel as opposed to glucose, which is reduced due to the decrease in carbohydrates in the diet. The increase in ketones is referred to as ketosis, which leads to a decrease in seizures. The ketogenic diet has proven to be effective in one-half of the patients who use it [5]. A randomized study in children has showed a 75% decrease in the number of seizures after 3 months [6]. In adults, a modified version of this diet, known as the Atkins-diet was also effective at reducing seizures [7].

A much more intrusive treatment for epilepsy is surgery. Surgery requires removing the region of the brain which is causing seizures. The benefits and risks must be considered, and surgery is an option mainly when other treatments have been exhausted. However, surgery can be especially beneficial when the cause of seizures is a localized brain tumor or region of the brain where a stroke has occurred, or if the seizures are focal (localized to a specific region). Recent studies have shown that in children undergoing surgery for seizures, 73% were seizure free after 3 years [8]. One other treatment is deep brain stimulation. Here, electrodes are placed in the brain region where

seizures are occurring and electrical impulses are sent to the brain region to stop seizures. This has been performed in many brain regions, including the thalamus, cortex, basal ganglia, hippocampus, as well as stimulation of the vagus nerve [9, 10]. Brain stimulation has proven to be an effective treatment, with a 60-90% decrease in seizures in both animal and human studies [9, 11].

### **1.3 Overview of animal seizure models**

#### *1.3.1 Electrical and chemical kindling models*

Animal models of epilepsy are invaluable in that they are a tool that allows for the study of modes of seizure onset, neurologic changes during seizure events, and new pharmacologic tools for seizure prevention. There are generally two types of animal seizure models. The first is the kindling model and the second are chemically-induced models. The kindling model can be further broken down into two sub-categories, those that are electrically stimulated and those that are chemically-induced. The electrical stimulation kindling model was first developed by Goddard in 1967 [12]. He found that daily stimulation of the amygdala portion of the brain by low intensity currents results in an increase in electrical discharges over time. These electrical discharges have been shown to cause spontaneous seizure events [13]. Similar to electrically generated seizures, kindling can be induced by subsequent injections of chemical convulsants. Animals are injected daily with small doses of a chemical convulsant below the seizure threshold. Over several days, the animal becomes more susceptible to these low doses

and seizures are generated. There are several studies using pentylenetetrazol (PTZ) as a convulsant in kindling models [14-16].

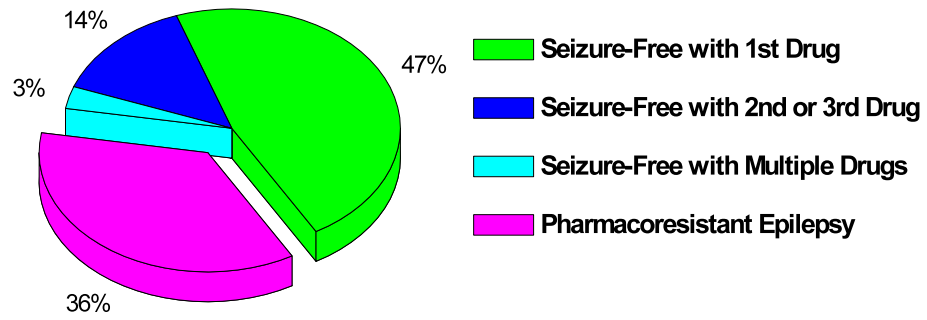


**Figure 1.1** Effectiveness of treatment by AEDs [4, 17].



### *1.3.2 Chemically-induced seizure models*

The more common seizure models are those that are chemically-induced. The majority of these models work by upsetting the excitatory/inhibitory balance in the brain. Convulsants work on both glutamate and GABAergic receptors. Agonists of glutamate receptors work by increasing glutamate, the major excitatory neurotransmitter in the brain, leading to abnormal electrical discharges. Examples of chemically-induced seizure models are those developed using kainic acid that act on ionotropic glutamate receptors [18-20] and homocysteic acid which works on metabotropic glutamate receptors [21-23]. Drugs that work on GABAergic receptors (GABA<sub>A</sub> and GABA<sub>B</sub>) act by decreasing the amount of GABA, the main inhibitory neurotransmitter in the brain. There are also seizure models which work by altering the synthesis and metabolism of GABA. Glutamic acid decarboxylase (GAD) is the enzyme which converts glutamic acid to GABA by decarboxylation. 3-mercaptopropionic acid is a well established chemical convulsant which inhibits GAD, thus increasing glutamate and decreasing GABA concentrations [24-28].

There are advantages and disadvantages for each seizure model, however chemically-induced models have several useful advantages. Seizure duration and intensity can be modulated by the concentration of the convulsant that is administered as well as the means by which it is dosed. Higher concentrations will more than likely lead to more intense seizures. Giving a single dose (whether it be sub-cutaneous, intramuscular, or intra-venous) or multiple doses will determine the time course of seizures.

The kindling model takes longer for seizures to develop as opposed to seizures occurring after several minutes with an intravenous dose. Additionally, seizures generated by kindling are less predictable, making it difficult to compare neurotransmitter changes when compared to a chemically-induced model where the concentration of convulsant can be held constant, and thus seizure intensity and duration are relatively constant. Regardless, a seizure model with a well studied mode of action is necessary to continue the discovery of AEDs and other therapeutic strategies for seizure maintenance.

#### **1.4 Electrophysiology recording**

There are two types of electrophysiology recordings typically used. The first is electroencephalography (EEG). In EEG circular electrodes are placed on the top of the scalp. EEG plots the voltage difference between two electrodes on different regions of the scalp. The EEG voltage is a summation of all the electrical activity surrounding the scalp where the electrodes are placed. EEG is extremely sensitive to body movements and these artifacts must be removed prior to analysis. In addition, the scalp creates a barrier between the brain and electrode which results in a decrease in signal.

The second method of electrophysiology recording is electrocorticography (ECoG). These measurements are made by drilling a hole in the skull so that an electrode can be placed on the cortex. The recording mechanism is similar to EEG, where the voltage difference between two electrodes is measured. ECoG, however, provides more spatial resolution than EEG. The electrodes can be placed in various brain regions, and

can be used during and after surgery to monitor brain activity and to determine if surgical removal of epileptic tissue was successful.

### **1.5 Microdialysis Sampling**

Microdialysis is an *in vivo* analytical sampling technique which measures the concentrations of unbound compounds in the extracellular space of various tissues. Microdialysis can be used to monitor the concentrations of endogenous compounds as well as exogenous compounds that have been dosed. In addition to being a sampling technique, microdialysis can be used to administer compounds into tissue as well. Since its inception, microdialysis has become a popular sampling technique in neurologic studies, and has gained popularity in pharmacokinetic (PK) and pharmacodynamic (PD) studies in various tissues [24].

The first study based upon the idea of *in vivo* dialysis was performed by Bito et al. in 1966. In this study, a dialysis sac filled with 6% dextran in saline was placed into subcutaneous neck tissue of dogs. The concentrations of free amino acids were measured based on the theory that the concentration of free amino acids were at a steady-state between the cerebrospinal fluid (CSF) and plasma. Since concentrations of the free amino acids would change rapidly in the plasma and thus would be hard to measure, it was thought that by placing the sac in the CSF for 10 weeks prior to analysis one could measure the “average” concentrations of free amino acids due to the steady-state equilibrium between the plasma and dialysis sac [29]. There have been many advances in the technique, which have decreased the size of the sampling region as well as

coupling it to various other techniques. Delgado et al. in 1972 developed the “dialytrode” by fusing two stainless steel shafts together to form inlet and outlet tubing as in a push-pull cannula with a polysulfone membrane at the tip to be used in long term studies in awake monkeys [30]. This design was modified in 1974 by Ungerstedt et al., where thin dialysis fibers were used that could be lowered into the brain for sampling [31]. The release of dopamine following amphetamine dosing was monitored in this study. Microdialysis has also been used in conjunction with behavioral studies, to monitor and correlate physiologic and neurologic changes [32, 33].

#### *1.5.1 Theory of microdialysis sampling*

Microdialysis is an *in vivo* analytical sampling technique that is based upon the principal of larger scale dialysis. Compounds diffuse down their concentration gradient across a semi-permeable membrane according to Fick’s Law. An isotonic solution, containing ions of similar concentration to those found in the targeted tissue, but void of the analytes of interest, is perfused across the membrane. This solution, called the perfusate, flows using a syringe pump at typical flow rates of 0.1-5  $\mu\text{l}/\text{min}$ . Analytes in the extracellular space diffuse across the membrane and are collected from the outlet of the probe in a solution termed the dialysate. Unlike large scale dialysis, an equilibrium is not achieved in microdialysis, rather a steady-state concentration gradient is rapidly established. The dialysate contains the free (unbound) fraction of the analyte in the extracellular space and is also free of large molecules, such as proteins, which are excluded due to the molecular weight cut-off of the membrane. Microdialysis can also be

used for introducing a drug to the tissue. In this case, the perfusate contains the drug, which diffuses across the membrane into the extracellular space. Here, a drug can be introduced to the tissue while simultaneously monitoring the changes in analyte concentration which can be collected in the dialysate. Figure 1.2 demonstrates the theory of microdialysis.

### *1.5.2 Microdialysis probe designs*

Microdialysis probes come in a variety of different designs/geometries depending upon the application. When performing experiments in the brain, a concentric/rigid probe with a cannula is used. Since the brain is a heterogeneous tissue, a probe is needed that allows for high spatial resolution. The concentric design was first developed by Zetterstrom et al. [34]. Figure 1.3 shows the design of a concentric rigid probe. The membrane is typically between 0.5-4 mm in length and has an outer diameter of 240-350  $\mu\text{m}$ . When implanted in the brain, a rigid guide cannula is used to hold the probe in place and is then held to the skull with dental cement and screws. The second type of probe has a linear design. Linear probes are used for sampling in homogenous tissues including the heart, liver, stomach, intestines and muscle [35]. In the linear probe design, the microdialysis membrane is placed between two pieces of polyamide tubing. Each end of the membrane is glued to the polyamide tubing using ultraviolet glue. The length of the membrane can be modified dependent upon the tissue in which it is being implanted. The third type of probe design is a flexible cannula. This type is mainly used for sampling in

blood vessels, but has also been used in tissue such as the liver [36, 37]. Figure 1.4 shows the flexible cannula and linear probe designs.

The other factor that plays a role in probe design is the membrane type. Membrane length and physical/chemical properties of the membrane such as the molecular weight cut-off will play a role in sampling. Membranes can be made from various materials including polycarbonate (PC), polyarylethersulphone (PAES), cuprophane, and cellulose acetate [36]. Due to the variety of chemical moieties on the analytes of interest, recovery/delivery can be greatly improved by selecting the correct membrane.

### *1.5.3 Microdialysis calibration methods*

When using microdialysis for quantitative determination of an analyte in the extracellular space, the relative recovery of the analyte across the probe must be known. Equilibrium cannot be reached between the perfusate and tissue due to the constant flow of the perfusate through the dialysis probe. Under normal perfusion conditions recovery does not reach 100% and thus the relative recovery of the analyte must be determined. Relative recovery can be calculated using equation 1.1.

$$(1.1) \quad \text{Relative Recovery} = \frac{C_{\text{dialysate}}}{C_{\text{perfusate}}}$$

The concentration of the analyte in the perfusate will always be less than the concentration of the analyte in the extracellular space (ECF). The relative recovery of the analyte can be improved by modifying several key factors. One factor is the perfusion rate of the dialysate through the probe. The slower the perfusion rate, the greater the recovery of the analyte. Another factor is the composition and molecular weight cut-off size of the dialysis membrane. Relative recovery increases with the length of the membrane. This factor can be used to your advantage, where the length of the membrane can be maximized to increase recovery of analytes in low concentrations. The one caveat to that is that the membrane length must not be larger than the target sampling site (this is especially crucial in brain experiments). Selecting the correct membrane composition is

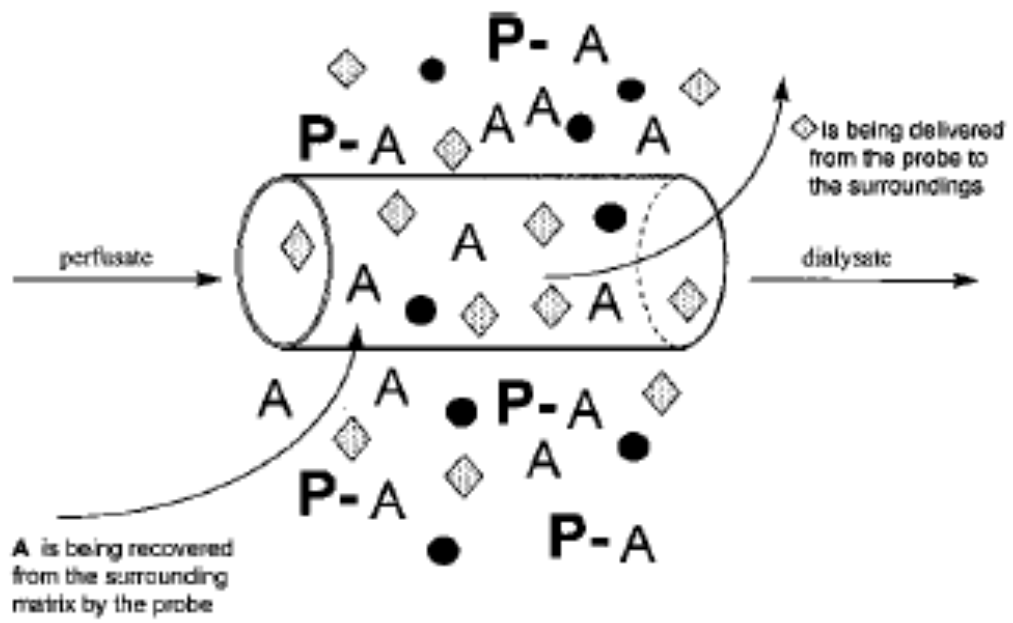
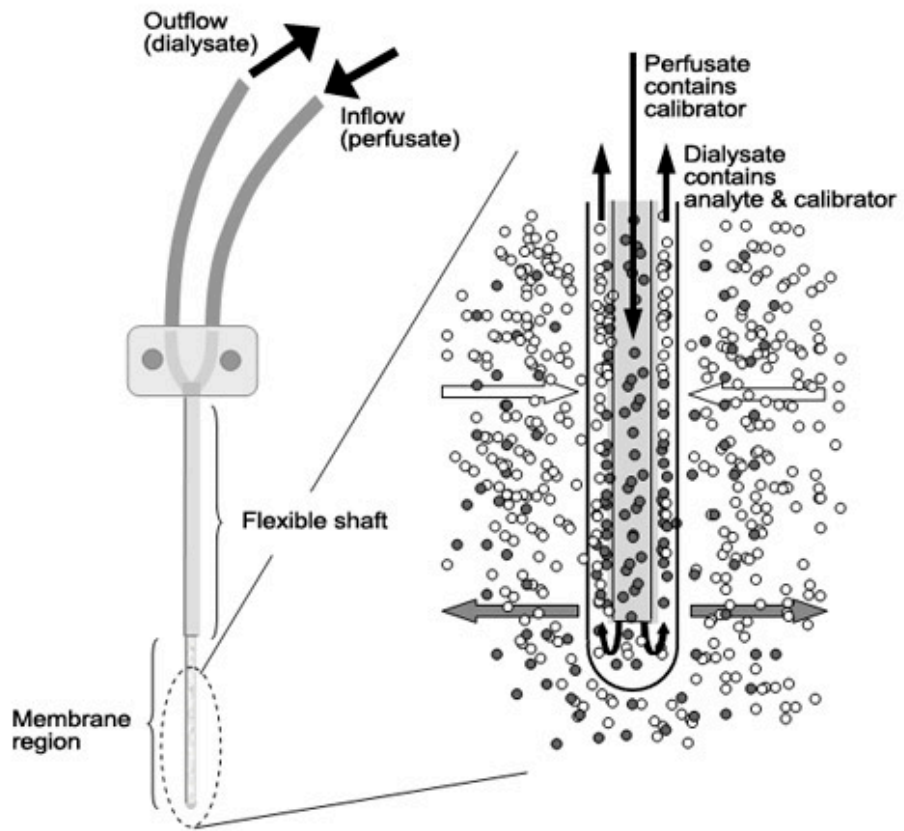
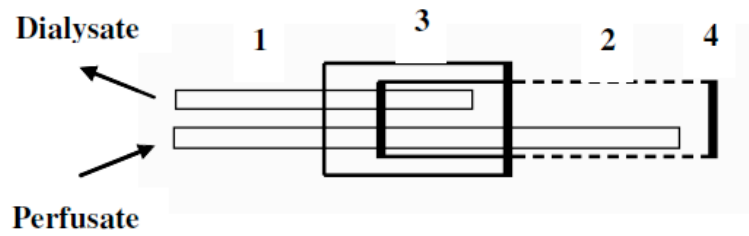


Figure 1.2 Microdialysis theory [38].

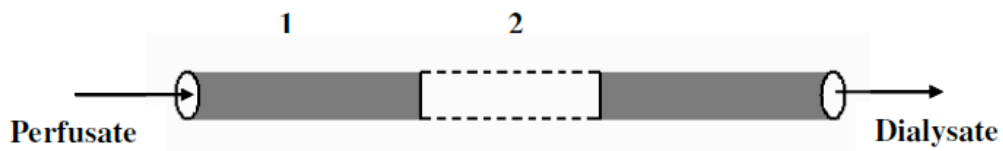




**Figure 1.3** Rigid cannula microdialysis probe design for brain experiments [39].



(A)



(B)

**Figure 1.4** (A) Flexible cannular microdialysis probe design and (B) linear microdialysis probe design. 1=polyamide tubing, 2=semi-permeable membrane, 3=MRE tubing, 4=UV glue junction [17].

also important, as studies have shown that recovery of analyte can vary as much as 20% depending on the membrane of choice [40]. In addition, the molecular weight cut-off (MWCO) of the membrane can affect recovery, as can the sampling temperature of the microenvironment and complexity of the sample matrix.

A simple experiment to determine the relative recovery of an analyte across the microdialysis membrane can be done *in vitro*. The microdialysis membrane is placed in a container containing a solution that mimics the extracellular fluid of the target tissue, such as artificial cerebral spinal fluid (aCSF) in the case of the brain. The solution is warmed to 37°C and constantly stirred. The vial contains a known concentration of the analyte and the perfusate contains no analyte. Dialysate samples are collected and the concentration of these samples are analyzed and compared with the concentration in the vial. However, due to the static and heterogeneous nature of the environment in the brain or other tissue, *in vitro* recovery cannot be equated with *in vivo* recovery. Other factors that make this comparison difficult are metabolism, vascularization of the tissue, and reuptake into cells [41]. *In vitro* probe recoveries have been calculated in other studies where the probe is placed in an agar solution to more closely mimic the environment in the brain [42].

Due to the limitations of *in vitro* microdialysis recoveries, *in vivo* calibration methods must be used to obtain quantitative data. The only true way to obtain *in vivo* recoveries is with the “no-net-flux” method described by Lonroth et al. in 1987 [43]. In this experiment, the expected concentration of the analyte *in vivo* is bracketed on both sides with varying concentrations of the analyte in the perfusate. When the concentration of the analyte in the perfusate is greater than the *in vivo* concentration, the analyte will

diffuse across the membrane and into the tissue. Likewise, if the concentration of the analyte is lower in the perfusate, then *in vivo* the analyte will diffuse into the microdialysis probe. A plot is constructed with the net change in the concentration of the analyte in the dialysate (y-axis) plotted versus the concentration of the analyte in the perfusate (x-axis). This results in a linear relationship which allows the determination of the actual concentration in the tissue, when there is “no-net-flux” of your analyte from the perfusate to the tissue. This method is time consuming, and is not practical for studies where the concentration of the analyte changes rapidly *in vivo*, such as neurotransmitters in the brain. Justice et al. described a variation on “no-net-flux” where a single concentration of analyte was perfused through various subjects as opposed to one subject being perfused with varying concentrations [44]. The data from all the subjects can then be pooled and plotted similar to the “no-net-flux” experiment. This provides a determination of the extracellular concentration with respect to time.

A simpler method for determination of probe recovery is that of calibration by delivery or retrodialysis with an internal standard. In this method, a known concentration of the analyte is placed in the perfusate. The relative delivery of the analyte is calculated using equation 1.2.

$$(1.2) \quad \text{Relative Delivery} = \frac{(C_{\text{perf usate}} - C_{\text{dialysate}})}{C_{\text{perf usate}}}$$

The recovery of the analyte can then be estimated based on the principle that the delivery across the probe membrane is the same as the recovery. This method, however, does not

allow for the determination of probe recovery throughout an experiment, and thus whether certain biologic conditions (ischemia/reperfusion etc.) change probe recovery. This can be done by retrodialysis, where an internal standard, often the exogenous compound antipyrine, is placed in the perfusate and monitored over the time course of the experiment [45, 46]. Studies by Lunte have shown that the calibration methods of no-net-flux and retrodialysis show similar results for most analytes [47].

The last method for in vivo probe calibration is the flow rate variation method [48]. In this method, the concentration of the recovered analyte is plotted against the flow rate of the perfusate. When the graph is extrapolated to zero, the concentration of the analyte as well as the probe recovery value can be estimated. The downside to this experiment is that with low flow rates, the amount of time needed to collect sufficient dialysate for analysis affects the temporal resolution. At very low flow, recovery is essentially 100% [49, 50].

#### *1.5.4 Advantages and limitations*

Microdialysis has many advantages over more conventional techniques such as tissue slicing and homogenates, as well as blood and urine sampling. Microdialysis allows for site-specific sampling of compounds in the extracellular space. This can be done in anesthetized as well as awake and freely moving animals. This is an advantage over tissue slices where the tissue of interest is removed and sampling is done *ex vivo*, removed from its native environment. Tissue homogenates, while allowing for sampling of compounds in both the intracellular and extracellular space, typically only allow for

one time point per animal. With microdialysis, one can obtain multiple time points for each animal, and each animal can be used as its own control. This greatly reduces animal to animal variability as well as the number of experiments that need to be performed. Microdialysis also provides excellent spatial resolution, which is important when sampling in a heterogeneous tissue, such as the brain, where the neurotransmitter concentrations can vary widely in two spatially close regions. Sample analysis, whether by LC or CE, can be done with no sample cleanup, due to the molecular weight cut-off of the membrane removing proteins from the sample. This is also advantageous since enzymes, which may degrade the analyte of interest, are also removed from the sample. Compared with blood and urine serial sampling, there is no net fluid loss with microdialysis. By dosing through the microdialysis probe, drugs can be introduced directly into the sampling site. Microdialysis is often used for pharmacokinetic/pharmacodynamic (PK/PD) studies [51, 52]. A probe can be placed in the blood for analysis while, another probe can be placed in the tissue.

There are some drawbacks to microdialysis sampling. One such drawback is the extraction efficiency of the membrane. Since the probe never reaches an equilibrium with the surrounding tissue, the amount of the analyte that is recovered is always less than the *in vivo* concentration. This can be problematic when the analyte is in such low concentrations that the limit of detection for the analytical method is approached. Another drawback, depending on the system being studied, is the temporal resolution. Specifically in the brain, where release of neurotransmitters occur on a sub-second time scale, by sampling on a time scale of minutes, important information could be lost [53, 54]. The issue with temporal resolution and extraction efficiency play off one another

since decreasing the flow rate through the membrane increases the extraction efficiency, but at the expense of temporal resolution. However, temporal and spatial resolution as well as the advantages of using each animal as its own control is more advantageous than tissue homogenate, which is often used.

### *1.5.5 Applications*

Microdialysis is most often used for the study of brain neurochemistry. These studies often include the analysis of major brain neurotransmitters, including amino acids [55-57], dopamine [58, 59], norepinephrine [60, 61], and serotonin [62, 63]. Studies in the brain have also looked at neuropeptides [64, 65]. Blood brain barrier permeability has been studied by systemic dosing of fluorescein and its subsequent detection in the brain after oxidative damage [66, 67]. Another area in which microdialysis has been useful is during behavioral studies. Brain neurochemical data can be correlated with behavioral data to give a broader picture of the function of the brain in addiction [68, 69] and disease states such as Huntington's and Alzheimer's [70, 71]. Microdialysis has also been coupled with on-line detection schemes to decrease sample handling and use capillary electrophoresis microchips to increase temporal resolution [59, 72]. In addition to sampling in the brain, microdialysis has been used in various other tissues including the heart [73, 74], muscle [75], stomach [76, 77], intestines [78], skin [79, 80], liver [81, 82], and eyes [83].

One area in which microdialysis has become especially prevalent is in pharmacokinetic studies. Typical absorption, distribution, metabolism and excretion

(ADME) studies involve blood, urine, and tissue collection. Taking serial blood draws and urine collections in small animals is troublesome and collecting tissue results in limited time points per animal. Using microdialysis for blood collection is advantageous because no fluid is lost during collection, meaning more time points can be taken for each animal. A drug can be dosed and its concentration can be monitored in the blood, urine, and peripheral tissues simultaneously [84, 85]. Pharmacokinetic data can also be correlated with pharmacodynamic changes as well [17, 52].

## **1.6 Separations**

While microdialysis sampling results in a rather clean sample, particularly the elimination of proteins, and decreases the need for time consuming sample cleanup when compared with tissue homogenate, an *in vivo* sample is complex. The use of separation-based techniques for the identification of analytes in a complex sample is one of the most important tools for analytical chemists. Advances in both separation techniques and detection schemes have allowed for the detection of analytes in the small sample sizes from microdialysis.

### *1.6.1 Liquid Chromatography*

#### *1.6.1.1 Theory*

Liquid chromatography (LC) has been in use since the 1960's. LC is the most widely used separation technique for non-volatile hydrophobic compounds in the liquid



phase. The separation in LC is based upon the interaction of the analyte in the mobile phase (liquid) with the solid stationary phase. Figure 1.5 shows a typical setup for liquid chromatography. The mobile phase is kept in a reservoir where it is constantly purged with an inert gas to remove oxygen. This is important for three reasons. One, with certain detection schemes, mainly electrochemical detection, oxygen can be reduced and its detection can interfere with the main analyte. Second, a major problem for pump problems with liquid chromatography is air bubbles in the pump head; removing oxygen can reduce this problem. Third, many neurotransmitters are oxidized in the presence of oxygen. From the mobile phase reservoir, the mobile phase enters the pump where solvent is delivered, up to several thousand psi, to the column. Between the pump and the column, the sample is introduced through the injector port. Once the separation is complete, detection of the analyte is performed by the detector and the data are sent to a CPU where offline analysis is performed.

Separations can be performed using anywhere from one pump, to several. When one pump and mobile phase is used, it is termed an isocratic separation. This is the simplest separation. However, when compounds have widely varying retention times, a gradient separation can be performed, where two or more pumps and mobile phases are used. By using a gradient, late eluting compounds can have their partitioning diminished, and separation of compounds with widely varying chemical properties can be performed in the same run.

Retention of the analyte on the column is described by the capacity factor,  $k'$ , which describes the amount of time spent in the mobile phase relative to the stationary phase. Equation 1.3 is for calculating the capacity factor, where  $t_r$  is the retention time

for the analyte of interest and  $t_m$  is the retention time for any unretained compounds.

Figure 1.6 shows a chromatogram illustrating  $t_r$  and  $t_m$ .

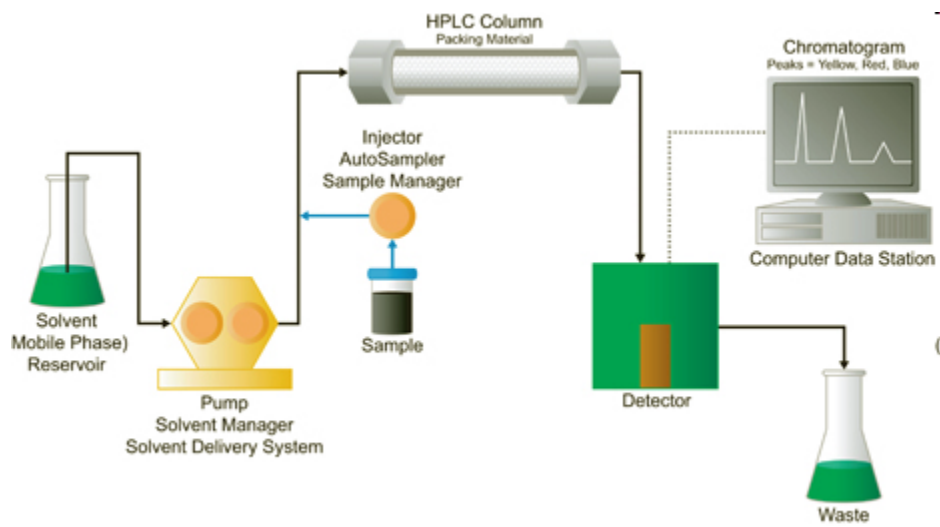


**Figure 1.5** Schematic of a typical HPLC system [86].

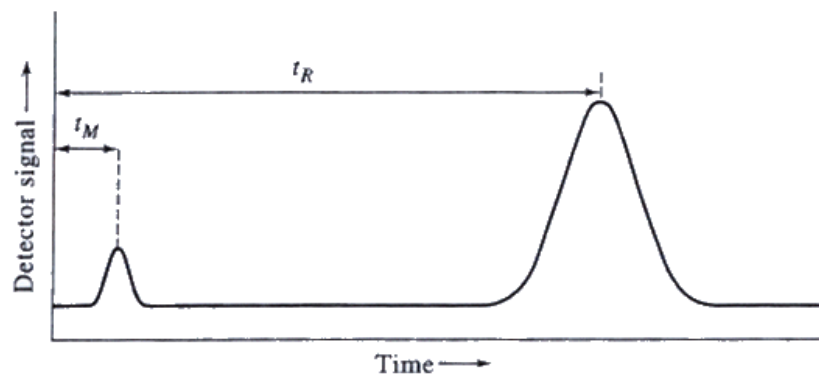


**Figure 1.6** Capacity factor calculation from a sample chromatogram.

$$(1.3) \quad k' = \frac{t_r - t_m}{t_m}$$

All compounds will spend equal time in the mobile phase; therefore, separation of multiple analytes in a matrix will depend upon the amount of time spent in the stationary phase. The ability for the stationary phase to separate two analytes from one another is described by the selectivity, where  $k'_1$  and  $k'_2$  are the capacity factors for the two analytes. Selectivity ( $\alpha$ ) is assessed by equation 1.4.

$$(1.4) \quad \alpha = \frac{k'_1}{k'_2}$$

Column efficiency ( $N$ ) is described by equation 1.5, where  $t_2$  is the retention time and  $w$  is the peak width at the base.

$$(1.5) \quad N = 16 \left( \frac{t_2}{w} \right)^2$$

The resolution between these two analytes is given by equation 1.6. Each term in the equation describes a part of the separation process which leads to resolution between two analytes. The first term ( $N$ ) involves column efficiency, the larger the value for  $N$  the

more narrow the peaks. The second term involves the selectivity ( $\alpha$ ) and how well one analyte is retained over another. The third term involves the capacity factor, which describes the length of time an analyte is on the column. The longer two analytes are on the column, the longer they have to be separated.

$$(1.6) \quad R_s = \frac{1}{4} \sqrt{N} \frac{\alpha - 1}{\alpha} \frac{k'_2}{1 + k'_{avg}}$$

Column efficiency,  $N$ , can be used to calculate the number of theoretical plates,  $H$ . The larger the value of  $H$ , the more efficient the column. Equation 1.7 describes the theoretical plate height in terms of the efficiency,  $N$ , and column length,  $L$ .

$$(1.7) \quad H = \frac{L}{N}$$

Theoretical plate height can be related then to the Van Deemter equation (Equation 1.8), which describes how each type of band broadening determines the total plate height.

$$(1.8) \quad H = Au^{\frac{1}{3}} + \frac{B}{u} + Cu$$

$A$  represents dispersion of the analyte due to Eddy Diffusion, or the multiple paths term.  $B$  is longitudinal diffusion, which is in the direction of flow.  $C$  is the mobile phase transfer term, which is a kinetic term for the mobile phase in the stationary phase.  $u$  represents the mobile phase linear velocity. Diffusion perpendicular to the flow of mobile phase is necessary, because that is what provides the separation, however diffusion parallel to the flow is destructive.

Advances have allowed for the movement towards so-called “ultra” performance liquid chromatography (UPLC). By decreasing particle size ( $<2\mu\text{m}$ ), separations become more efficient and are performed over a shorter period of time. The drive towards UPLC was due to the need for more high throughput methods, as well as the analysis of complex samples. A study by Guillarme et al. showed that by moving from a 4.6 x 150mm column with  $5\mu\text{m}$  particle size to a 2.1 x 50mm column with a  $1.7\mu\text{m}$  particle size, a sample of 12 compounds was separated in 1.6 minutes versus 27 minutes with the larger column [87]. While UPLC utilizes smaller particle sizes that result in higher back pressures, there is no fundamental difference between HPLC and UPLC. UPLC takes advantage of the smaller particle sizes which decreases the Eddy Diffusion term in the Van Deemter equation as described above.

#### *1.6.1.2 Modes of Separation*

There are several different modes of separation in liquid chromatography, including reverse phase, normal phase, ion exchange, and size exclusion. The optimal mode of separation is determined based upon the analytes being separated and which

mode will allow for the best separation. In reverse phase chromatography, the stationary phase is more hydrophobic than the mobile phase. This is by far the most commonly used mode in separations for aqueous samples. The stationary phase in a reverse phase system is silica based and the most common ligands are -C18 (octydecyl) and -C8 (decyl). These carbon chains can be chemically modified for better retention of certain analytes, such as polar endcapping of -C18 chains for better retention of polar compounds. If the analytes of interest are very hydrophobic, they will spend more time in the hydrophobic stationary phase over the more polar mobile phase. This problem can be remedied and thus separation time decreased by adding organic to the mobile phase. This is often why in a gradient separation the second mobile phase has a higher percentage of organic, to help elute hydrophobic compounds from the column. When performing reverse phase chromatography, more hydrophilic compounds might be unretained and elute with the void volume. If there is a mix of hydrophobic and ionic compounds, an ion pairing agent can be added. One such example of an ion pairing agent is 1-octanesulfonic acid (SOS). The charge on the SOS matches up with the charge on the analyte, this decreasing the overall charge on the analyte and allowing it to interact more with the stationary phase, removing it from the void volume.

Normal phase chromatography is another mode of separation. In normal phase, the stationary phase is more polar than the mobile phase. Often times in normal phase chromatography the mobile phase is 100% organic. The stationary phase in normal phase systems are typically silica or alumina based. Silica phases can also be modified to make them more polar, for example by adding hydroxyl groups.



Ion exchange chromatography makes use of an ionic stationary phase and is separated into cationic exchange and anionic exchange depending on the charge of the analyte of interest. Analytes are separated based upon ionic interactions with the stationary phase. The charge of the analytes can be altered by changing the pH of the mobile phase.

Size exclusion chromatography is used for large molecules, greater than around 2,000 amu. The analytes do not interact with the surface of the stationary phase, rather separation is determined by diffusion into the pores of the stationary phase. Small analytes will diffuse into more pores on the stationary phase and thus will elute last, while large molecules that cannot fit into the pores will elute first.

#### *1.6.1.3 Modes of Detection*

The most commonly used detector for LC separations is a UV/Vis absorbance detector. Many compounds absorb UV radiation and a signal is produced. Absorbance (A) is given by equation 1.9, where  $\epsilon$  is the molar absorptivity constant, b is the path length of the detector cell, and c is the concentration.

$$(1.9) \quad A = -\log_{10}\left(\frac{I}{I_0}\right) = \epsilon bc$$

The detector can either be set up for a single wavelength using a monochromator or for multiple wavelengths using a photo-diode array. A monochromator selects one

wavelength (typically near maximum absorptivity) and provides a sharp strong light which will provide the best limits of detection. A diode array detector allows for detection of several different wavelengths at one time and is useful for method development or when several analytes are detected with different absorption maximums. The biggest problem with UV/Vis detection is that it is not very selective. In addition to its relatively poor limits of detection, UV/Vis is a ratio measurement and one is trying to measure a small change in a big signal.

A mode of detection with better limits of detection is fluorescence. Fluorescence occurs when the molecule absorbs a photon at one wavelength and emits the photon at a longer wavelength. The big advantage of fluorescence over UV/Vis is that fluorescence is a direct measurement. While almost all organic molecules absorb UV light, not every molecule fluoresces. The biggest disadvantage to fluorescence detection is that compounds not natively fluorescent must be derivatized, which adds another step to the analysis.

Another detection mode with excellent limits of detection is electrochemical (or amperometric) detection. Electrochemical detection is used when the analytes of interest have moieties that are easily oxidized or reduced. Electrodes can be made of many different materials, the most common being glassy carbon, but also carbon paste, gold, gold/mercury amalgam, and platinum. The selectivity of electrochemical detection is quite good as the applied potential can be changed to maximize the oxidation/reduction of the analyte of interest while remaining below the oxidation/reduction potentials of other compounds in the matrix. The drawback to electrochemical detection is fouling of the electrode surface resulting in the need to polish the electrode on a regular basis.

Recently the most widely used detection scheme is mass spectrometry. Mass spectrometry has been especially useful when coupled with LC, but has been used for decades coupled to gas chromatography. When coupled to LC, mass spectrometry detects analytes based on their mass to charge ratio. One primary problem with using mass spectrometry in conjunction with microdialysis samples is the salt content in aCSF and Ringers solution. Coupling microdialysis with liquid chromatography mass spectrometry has been an issue [88, 89], as the high salt content of microdialysis samples causes signal suppression and decreases ionization efficiency [90]. Since analytes must be in the gas phase for detection, increasing the ionic strength of the solution increases the boiling point and thus results in a significant loss of sample due to poor ionization.

## **1.7 Overview of Research**

The goal of this research was to develop a model for local dosing of 3-Mercaptopropionic acid through an intracerebral microdialysis probe. Microdialysis with an intracerebral microdialysis probe coupled with an internal working electrode for electrophysiological recording of seizure activity at the site of 3-MPA administration was used. The purpose of this research was to develop a seizure model to induce seizures in a specific brain region to model the focal seizures seen in many clinical patients. The microdialysis samples were analyzed for 3-MPA delivered to the brain, as well as to monitor changes in amino acid and catecholamine neurotransmitters and their metabolites.

Chapter three discusses the changes seen in amino acids and catecholamine neurotransmitter levels in three brain regions: the striatum, hippocampus, and *locus coeruleus*, upon administration of 10mM 3-MPA through the microdialysis probe. 3-MPA was administered through one probe while samples were collected in the other two probes concurrently. This allowed for a determination of the local dosing model of 3-MPA, where administering 3-MPA through one probe would not effect the brain region surrounding the other two probes. This also allowed for the investigation of neuronal circuitry where changes can be seen in distant brain regions if neurons project from the region where 3-MPA is administered to a distant brain region where another probe is placed. The delivery of 3-MPA to the brain was also evaluated. The neurochemical changes as well as 3-MPA delivery were correlated to changes in ECoG activity.

Chapter four discusses a multiple dosing approach for 3-MPA in the hippocampus. 3-MPA administration was divided into two equal periods and the changes in amino acids and catecholamine neurotransmitters were monitored to investigate whether neurons lose their plasticity or undergo protective mechanisms in response to subsequent seizure events.

## 1.8 References

1. World Health Organization. July 2009]; Available from: <http://www.who.int/mediacentre/factsheets/fs999/en/index.html>.
2. German, S.-P. and S.-M. German, *Microperfusion of picrotoxin in the hippocampus of chronic freely moving rats through microdialysis probes: A new method to induce partial and secondary generalized seizures*. Journal of Neuroscience Methods, 1996. **67**(2): p. 113-120.
3. French, J.A. and T.A. Pedley, *Initial management of epilepsy*. N. Engl. J. Med., 2008. **359**(2): p. 166-176.
4. Kwan, P. and M.J. Brodie, *Early identification of refractory epilepsy*. N Engl J Med, 2000. **342**(5): p. 314-9.
5. Kossoff Eric, H., A. Zupec-Kania Beth, and M. Rho Jong, *Ketogenic diets: an update for child neurologists*. Journal of child neurology, 2009. **24**(8): p. 979-88.
6. Neal Elizabeth, G., et al., *The ketogenic diet for the treatment of childhood epilepsy: a randomised controlled trial*. Lancet neurology, 2008. **7**(6): p. 500-6.
7. Freeman John, M., H. Kossoff Eric, and L. Hartman Adam, *The ketogenic diet: one decade later*. Pediatrics, 2007. **119**(3): p. 535-43.
8. Bittar Richard, G., et al., *Resective surgery in infants and young children with intractable epilepsy*. Journal of clinical neuroscience official journal of the Neurosurgical Society of Australasia, 2002. **9**(2): p. 142-6.
9. Albensi, B.C., *A comparison of drug treatment versus electrical stimulation for suppressing seizure activity*. Drug News & Perspectives, 2003. **16**(6): p. 347-352.
10. Hodaie, M., et al., *Chronic anterior thalamus stimulation for intractable epilepsy*. 2002, Division of Neurosurgery, University of Toronto, ON, Canada: United States. p. 603-8.
11. Osorio, I., et al., *Automated seizure abatement in humans using electrical stimulation*. Annals of neurology, 2005. **57**(2): p. 258-68.
12. Goddard, G.V., *Development of epileptic seizures through brain stimulation at low intensity*. Nature, 1967. **214**(5092): p. 1020-1.
13. Pinel, J.P. and L.I. Rovner, *Experimental epileptogenesis: kindling-induced epilepsy in rats*. Experimental Neurology, 1978. **58**(2): p. 190-202.

14. Da Silva, L.F., P. Pereira, and E. Elisabetsky, *A neuropharmacological analysis of PTZ-induced kindling in mice*. *General Pharmacology*, 1998. **31**(1): p. 47-50.
15. Diehl, R.G., A. Smialowski, and T. Gotwo, *Development and persistence of kindled seizures after repeated injections of pentylenetetrazol in rats and guinea pigs*. *Epilepsia*, 1984. **25**(4): p. 506-10.
16. Fabisiak, J.P. and W.S. Schwark, *Aspects of the pentylenetetrazol kindling model of epileptogenesis in the rat*. *Experimental Neurology*, 1982. **78**(1): p. 7-14.
17. Crick, E.W., *In vivo Microdialysis Coupled with Electrophysiology for the Neurochemical Analysis of Epileptic Seizures*, in *Chemistry*. 2007, The University of Kansas.
18. Albala, B.J., S.L. Moshe, and R. Okada, *Kainic acid-induced seizures: a developmental study*. *Developmental Brain Research*, 1984. **13**(1): p. 139-48.
19. Cavalheiro, E.A., et al., *Intracortical and intrahippocampal injections of kainic acid in developing rats: an electrographic study*. *Electroencephalography and Clinical Neurophysiology*, 1983. **56**(5): p. 480-6.
20. Veliskova, J., L. Velisek, and P. Mares, *Epileptic phenomena produced by kainic acid in laboratory rats during ontogenesis*. *Physiologia Bohemoslovaca*, 1988. **37**(5): p. 395-405.
21. Chen, X.J., et al., *Detection of the Superoxide Radical Anion Using Various Alkanethiol Monolayers and Immobilized Cytochrome c*. *Anal. Chem.* (Washington, DC, U. S.), 2008. **80**(24): p. 9622-9629.
22. Folbergrova, J., R. Haugvicova, and P. Mares, *Behavioral and metabolic changes in immature rats during seizures induced by homocysteic acid: The protective effect of NMDA and non-NMDA receptor antagonists*. *Experimental Neurology*, 2000. **161**(1): p. 336-345.
23. Folbergrova, J., R. Haugvicova, and P. Mares, *Attenuation of seizures induced by homocysteic acid in immature rats by metabotropic glutamate group II and group III receptor agonists*. *Brain Research*, 2001. **908**(2): p. 120-129.
24. Crick, E.W., et al., *An investigation into the pharmacokinetics of 3-mercaptopropionic acid and development of a steady-state chemical seizure model using in vivo microdialysis and electrophysiological monitoring*. *Epilepsy Res.*, 2007. **74**(2-3): p. 116-125.
25. Fan, S.G., M. Wusteman, and L.L. Iversen, *3-Mercaptopropionic acid inhibits GABA release from rat brain slices in vitro*. *Brain Res.*, 1981. **229**(2): p. 371-7.

26. Horton, R.W. and B.S. Meldrum, *Seizures induced by allylglycine, 3-mercaptopropionic acid and 4-deoxy pyridoxine in mice and photosensitive baboons, and different modes of inhibition of cerebral glutamic acid decarboxylase*. Br J Pharmacol, 1973. **49**(1): p. 52-63.
27. O'Connell, B.K., et al., *Neuronal lesions in mercaptopropionic acid-induced status epilepticus*. Acta Neuropathol, 1988. **77**(1): p. 47-54.
28. Tunnicliff, G., *Action of inhibitors on brain glutamate decarboxylase*. Int. J. Biochem., 1990. **22**(11): p. 1235-41.
29. Bito, L.Z., et al., *Concentration of free amino acids and other electrolytes in cerebrospinal fluid, in vivo dialyzate of brain, and blood plasma of the dog*. Journal of Neurochemistry, 1966. **13**(11): p. 1057-67.
30. Delgado, J.M., et al., *Dialytrode for long term intracerebral perfusion in awake monkeys*. Archives internationales de pharmacodynamie et de therapie, 1972. **198**(1): p. 9-21.
31. Ungerstedt, U., *Measurement of neurotransmitter release by intracranial dialysis*. IBRO Handbook Series, 1984. **6**(Meas. Neurotransm. Release In Vivo): p. 81-105.
32. Castner, S.A., L. Xiao, and J.B. Becker, *Sex differences in striatal dopamine: in vivo microdialysis and behavioral studies*. Brain Research, 1993. **610**(1): p. 127-34.
33. Ungerstedt, U., et al., *Dopamine synaptic mechanisms reflected in studies combining behavioral recordings and brain dialysis*. Advances in the Biosciences (Oxford), 1982. **37**(Adv. Dopamine Res.): p. 219-31.
34. Zetterstrom, T., et al., *In vivo measurement of dopamine and its metabolites by intracerebral dialysis: changes after d-amphetamine*. Journal of Neurochemistry, 1983. **41**(6): p. 1769-73.
35. Zuo, H., M. Ye, and M.I. Davies, *The linear probe: a flexible choice for in vivo microdialysis sampling in soft tissues*. Current Separations, 1995. **14**(2): p. 54-7.
36. Buttler, T., et al., *Membrane characterization and performance of microdialysis probes intended for use as bioprocess sampling units*. Journal of Chromatography, A, 1996. **725**(1): p. 41-56.
37. Scott, D.O., D.S. Bindra, and V.J. Stella, *Plasma pharmacokinetics of lactone and carboxylate forms of 20(S)-camptothecin in anesthetized rats*. Pharmaceutical research, 1993. **10**(10): p. 1451-7.

38. Davies, M.I., *Microdialysis sampling for in vivo hepatic metabolism studies (phenol)*. 1995. p. 163 pp.
39. Chaurasia Chandra, S., et al., *AAPS-FDA workshop white paper: microdialysis principles, application and regulatory perspectives*. Pharmaceutical research, 2007. **24**(5): p. 1014-25.
40. Benveniste, H. and P.C. Huttemeier, *Microdialysis - theory and application*. Progress in Neurobiology (Oxford, United Kingdom), 1990. **35**(3): p. 195-215.
41. Chaurasia, C.S., *In vivo microdialysis sampling: theory and applications*. Biomedical Chromatography, 1999. **13**(5): p. 317-332.
42. Chen, K.C., et al., *Quantitative dual-probe microdialysis: Mathematical model and analysis*. Journal of Neurochemistry, 2002. **81**(1): p. 94-107.
43. Lonroth, P., P.A. Jansson, and U. Smith, *A microdialysis method allowing characterization of intercellular water space in humans*. The American journal of physiology, 1987. **253**(2 Pt 1): p. E228-31.
44. Olson, R.J. and J.B. Justice, Jr., *Quantitative microdialysis under transient conditions*. Analytical Chemistry, 1993. **65**(8): p. 1017-22.
45. Stenken, J.A., et al., *Factors that influence microdialysis recovery. Comparison of experimental and theoretical microdialysis recoveries in rat liver*. Journal of Pharmaceutical Sciences, 1997. **86**(8): p. 958-66.
46. Yokel, R.A., et al., *Antipyrine as a dialyzable reference to correct differences in efficiency among and within sampling devices during in vivo microdialysis*. Journal of Pharmacological and Toxicological Methods, 1992. **27**(3): p. 135-42.
47. Song, Y. and C.E. Lunte, *Comparison of calibration by delivery versus no net flux for quantitative in vivo microdialysis sampling*. Analytica Chimica Acta, 1999. **379**(3): p. 251-262.
48. Menacherry, S., W. Hubert, and J.B. Justice, Jr., *In vivo calibration of microdialysis probes for exogenous compounds*. Analytical Chemistry, 1992. **64**(6): p. 577-83.
49. Lada, M.W. and R.T. Kennedy, *Quantitative in vivo measurements using microdialysis on-line with capillary zone electrophoresis*. Journal of Neuroscience Methods, 1995. **63**(1,2): p. 147-52.
50. Lada, M.W. and R.T. Kennedy, *Quantitative in vivo monitoring of primary amines in rat caudate nucleus using microdialysis coupled by a flow-gated*



- interface to capillary electrophoresis with laser-induced fluorescence detection.* Analytical Chemistry, 1996. **68**(17): p. 2790-7.
51. Pan, Y.-f., et al., *Intracerebral microdialysis technique and its application on brain pharmacokinetic-pharmacodynamic study.* Archives of Pharmacal Research, 2007. **30**(12): p. 1635-1645.
  52. Wei, Y.H., et al., *Microdialysis: a technique for pharmacokinetic-pharmacodynamic studies of oncological drugs.* Current Pharmaceutical Biotechnology, 2009. **10**(6): p. 631-640.
  53. Leenders, A.G.M., et al., *A biochemical approach to study sub-second endogenous release of diverse neurotransmitters from central nerve terminals.* Journal of Neuroscience Methods, 2002. **113**(1): p. 27-36.
  54. Robinson, D.L., et al., *Detecting subsecond dopamine release with fast-scan cyclic voltammetry in vivo.* Clinical Chemistry (Washington, DC, United States), 2003. **49**(10): p. 1763-1773.
  55. Bongiovanni, R., et al., *Relationships between large neutral amino acid levels in plasma, cerebrospinal fluid, brain microdialysate and brain tissue in the rat.* Brain Research. **1334**: p. 45-57.
  56. Buck, K., P. Voehringer, and B. Ferger, *Rapid analysis of GABA and glutamate in microdialysis samples using high performance liquid chromatography and tandem mass spectrometry.* Journal of Neuroscience Methods, 2009. **182**(1): p. 78-84.
  57. Li, H., et al., *Simultaneous monitoring multiple neurotransmitters and neuromodulators during cerebral ischemia/reperfusion in rats by microdialysis and capillary electrophoresis.* Journal of Neuroscience Methods. **189**(2): p. 162-168.
  58. Malanga, C.J., et al., *Augmentation of Cocaine-Sensitized Dopamine Release in the Nucleus Accumbens of Adult Mice following Prenatal Cocaine Exposure.* Developmental Neuroscience (Basel, Switzerland), 2009. **31**(1-2): p. 76-89.
  59. Shou, M., et al., *Monitoring Dopamine in Vivo by Microdialysis Sampling and On-Line CE-Laser-Induced Fluorescence.* Analytical Chemistry, 2006. **78**(19): p. 6717-6725.
  60. Gilinsky, M.A., A.A. Faibushevish, and C.E. Lunte, *Determination of myocardial norepinephrine in freely moving rats using in vivo microdialysis sampling and*

- liquid chromatography with dual-electrode amperometric detection.* Journal of Pharmaceutical and Biomedical Analysis, 2001. **24**(5-6): p. 929-935.
61. Shimizu, S., et al., *In vivo direct monitoring of interstitial norepinephrine levels at the sinoatrial node.* Autonomic Neuroscience. **152**(1-2): p. 115-118.
  62. Fedele, D.E., et al., *Quantitative microdialysis for serotonin in striatum and frontal cortex of genetically altered mice.* Monitoring Molecules in Neuroscience, Proceedings of the International Conference on In Vivo Methods, 9th, Dublin, Ireland, June 16-19, 2001, 2001: p. 97-98.
  63. Kehr, J., et al., *Microdialysis in freely moving mice: determination of acetylcholine, serotonin and noradrenaline release in galanin transgenic mice.* Journal of Neuroscience Methods, 2001. **109**(1): p. 71-80.
  64. Behrens, H.L. and L. Li, *Monitoring neuropeptides in vivo via microdialysis and mass spectrometry.* Methods in Molecular Biology (Totowa, NJ, United States). **615**(Peptidomics): p. 57-73.
  65. Fletcher, H.J., *Enhanced microdialysis sampling of neuropeptides using affinity agents.* 2008. p. 186 pp.
  66. Nandi, P., D.P. Desai, and S.M. Lunte, *Development of a PDMS-based microchip electrophoresis device for continuous online in vivo monitoring of microdialysis samples.* Electrophoresis. **31**(8): p. 1414-1422.
  67. Nicolazzo, J.A., S.A. Charman, and W.N. Charman, *Methods to assess drug permeability across the blood-brain barrier.* Journal of Pharmacy and Pharmacology, 2006. **58**(3): p. 281-293.
  68. Lan, K.-C., et al., *Enhancing effects of morphine on methamphetamine-induced reinforcing behavior and its association with dopamine release and metabolism in mice.* Journal of Neurochemistry, 2009. **109**(2): p. 382-392.
  69. Solinas, M., et al., *Environmental Enrichment During Early Stages of Life Reduces the Behavioral, Neurochemical, and Molecular Effects of Cocaine.* Neuropsychopharmacology, 2009. **34**(5): p. 1102-1111.
  70. Hartmann, J., C. Kiewert, and J. Klein, *Neurotransmitters and energy metabolites in amyloid-bearing APPSWE \* PSEN1dE9 mouse brain.* Journal of Pharmacology and Experimental Therapeutics. **332**(2): p. 364-370.
  71. Miller, B.R., et al., *Up-regulation of GLT1 expression increases glutamate uptake and attenuates the Huntington's disease phenotype in the R6/2 mouse.* Neuroscience (San Diego, CA, United States), 2008. **153**(1): p. 329-337.

72. Rossell, S., L.E. Gonzalez, and L. Hernandez, *One-second time resolution brain microdialysis in fully awake rats. Protocol for the collection, separation and sorting of nanoliter dialyzate volumes*. Journal of Chromatography, B Analytical Technologies in the Biomedical and Life Sciences, 2003. **784**(2): p. 385-393.
73. Kawada, T., et al., *Detection of endogenous acetylcholine release during brief ischemia in the rabbit ventricle: A possible trigger for ischemic preconditioning*. Life Sciences, 2009. **85**(15-16): p. 597-601.
74. Kitagawa, H., et al., *Microdialysis separately monitors myocardial interstitial myoglobin during ischemia and reperfusion*. American Journal of Physiology, 2005. **289**(2, Pt. 2): p. H924-H930.
75. Adams, F., et al., *Influences of levodopa on adipose tissue and skeletal muscle metabolism in patients with idiopathic Parkinson's disease*. European Journal of Clinical Pharmacology, 2008. **64**(9): p. 863-870.
76. Woo, K.L., *Development of multiple probe microdialysis sampling techniques for site-specific monitoring in the stomach*. 2007. p. 189 pp.
77. Woo, K.L. and C.E. Lunte, *The direct comparison of health and ulcerated stomach tissue: A multiple probe microdialysis sampling approach*. Journal of Pharmaceutical and Biomedical Analysis, 2008. **48**(1): p. 85-91.
78. Cibicek, N., et al., *Colon submucosal microdialysis: a novel in vivo approach in barrier function assessment - a pilot study in rats*. Physiological Research (Prague, Czech Republic), 2007. **56**(5): p. 611-617.
79. Holmgaard, R., J.B. Nielsen, and E. Benfeldt, *Microdialysis Sampling for Investigations of Bioavailability and Bioequivalence of Topically Administered Drugs: Current State and Future Perspectives*. Skin Pharmacology and Physiology. **23**(5): p. 225-243.
80. Holovics, H.J., et al., *Investigation of Drug Delivery by Iontophoresis in a Surgical Wound Utilizing Microdialysis*. Pharmaceutical research, 2008. **25**(8): p. 1762-1770.
81. Price, K.E., C.K. Larive, and C.E. Lunte, *Tissue-targeted metabolomics: biological considerations and application to doxorubicin-induced hepatic oxidative stress*. Metabolomics, 2009. **5**(2): p. 219-228.
82. Sun, L., et al., *An in vivo microdialysis coupled with liquid chromatography/tandem mass spectrometry study of cortisol metabolism in monkey adipose tissue*. Analytical Biochemistry, 2008. **381**(2): p. 214-223.

83. Janoria, K.G., et al., *Vitreous pharmacokinetics of peptide-transporter-targeted prodrugs of ganciclovir in conscious animals*. *Journal of Ocular Pharmacology and Therapeutics*. **26**(3): p. 265-271.
84. Herkenne, C., et al., *In Vivo Methods for the Assessment of Topical Drug Bioavailability*. *Pharmaceutical research*, 2008. **25**(1): p. 87-103.
85. Joukhadar, C. and M. Mueller, *Microdialysis: Current applications in clinical pharmacokinetic studies and its potential role in the future*. *Clinical Pharmacokinetics*, 2005. **44**(9): p. 895-913.
86. Waters. July 2010]; Available from: [http://www.waters.com/waters/nav.htm?cid=10049055&locale=en\\_US](http://www.waters.com/waters/nav.htm?cid=10049055&locale=en_US).
87. Guillarme, D., et al., *Method transfer for fast liquid chromatography in pharmaceutical analysis: Application to short columns packed with small particle. Part II: Gradient experiments*. *European Journal of Pharmaceutics and Biopharmaceutics*, 2008. **68**(2): p. 430-440.
88. Canarelli, S., I. Fisch, and R. Freitag, *On-line microdialysis of proteins with high-salt buffers for direct coupling of electrospray ionization mass spectrometry and liquid chromatography*. *Journal of chromatography. A*, 2002. **948**(1-2): p. 139-49.
89. Qiao, J.-p., et al., *Microdialysis combined with liquid chromatography-tandem mass spectrometry for the determination of 6-aminobutylphthalide and its main metabolite in the brains of awake freely-moving rats*. *Journal of Chromatography, B Analytical Technologies in the Biomedical and Life Sciences*, 2004. **805**(1): p. 93-99.
90. Annesley, T.M., *Ion suppression in mass spectrometry*. *Clinical Chemistry (Washington, DC, United States)*, 2003. **49**(7): p. 1041-1044.

## Chapter 2

### Methods

#### 2.1 Introduction

##### 2.1.1 Background and Significance

Previous research in our laboratory involved a pharmacokinetic/pharmacodynamic study of a chemically-induced seizure model with 3-MPA in rats [1]. A steady-state model for 3-MPA dosing was developed where a 60 mg/kg min<sup>-1</sup> bolus dose was followed by a constant intravenous (i.v.) infusion of 50 mg/kg of 3-MPA for 50 minutes. The concentrations of 3-MPA were measured in the blood as well as the striatum and hippocampus. The 3-MPA concentrations in the brain can be seen in Figure 2.1. Steady-state concentrations of 3-MPA were achieved in the brain and the pharmacokinetics of 3-MPA in the blood and brain were studied. This was the first known study of the pharmacokinetics of 3-MPA in a chemically-induced seizure model. By achieving steady-state concentrations of 3-MPA, that variable was held constant when studying the neurochemical changes in the striatum and hippocampus. As expected, 3-MPA inhibited the conversion of glutamic acid to  $\gamma$ -hydroxybutyric acid *in vivo*, resulting in an increase in glutamic acid and a decrease in  $\gamma$ -hydroxybutyric acid. These changes can be seen in both the striatum and hippocampus in Figure 2.2. In addition to measuring the concentrations of 3-MPA and neurochemical changes in the brain, ECoG recordings were made. Thus, seizure number, intensity, and duration were correlated 3-MPA concentrations and neurochemical changes. Table 2.1 outlines the data obtained from the ECoG recordings.

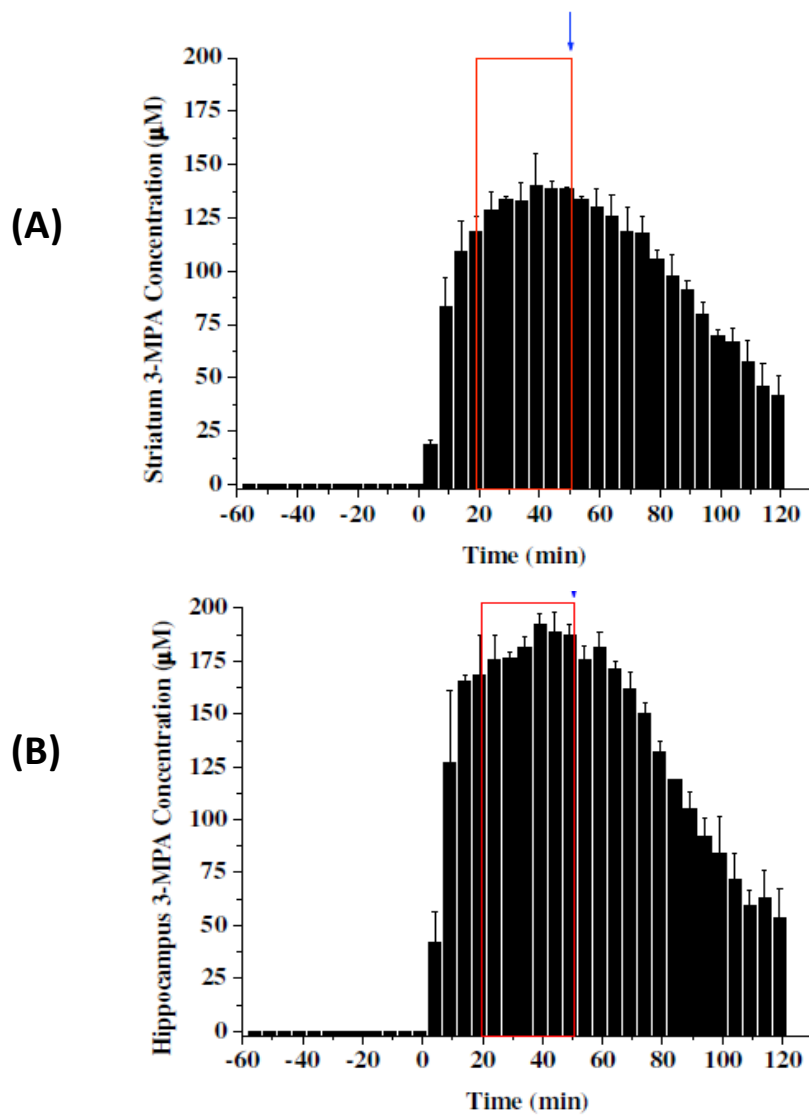


**Figure 2.1.** Average brain 3-MPA concentration-time profiles in the striatum (A) and hippocampus (B) following constant infusion dose of 3-MPA. 3-MPA was dosed at time  $t=0$  minutes. Area in the box denotes steady-state 3-MPA concentrations. The infusion was discontinued at the arrow.  $n=16$  striatum,  $n=3$  hippocampus [1].

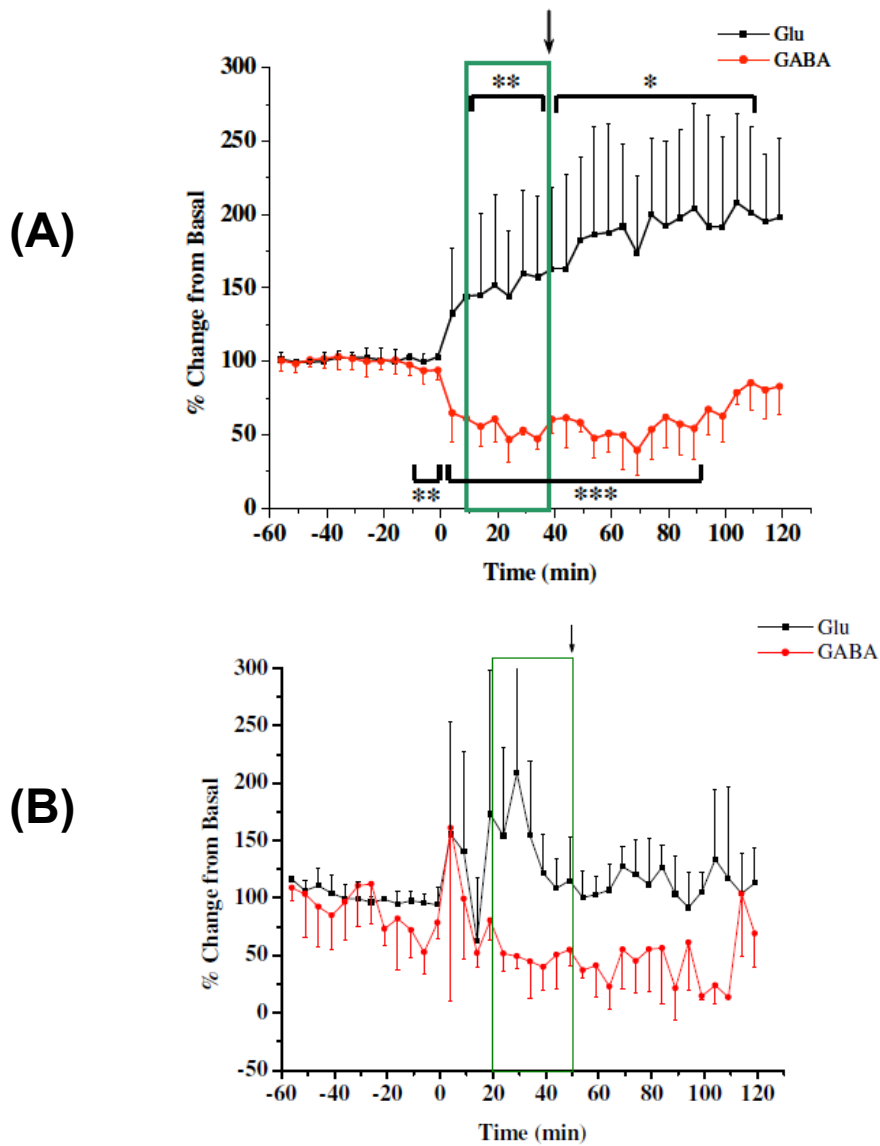


**Figure 2.2** Changes in Glu and GABA in the striatum (A) and hippocampus (B) following systemic dosing of 3-MPA with the constant infusion dosing (60mg/kg bolus + 50mg/kg constant infusion for 50 minutes). (A, n=12 rats), (B, n=3 rats). [ $*=p<0.1$ ,  $**=p<0.05$ ,  $***=p<0.01$ ] [1].

	<b>60 mg/kg Bolus + 50 mg/kg/min Infusion<sup>a</sup></b>
<b>Latency to Seizure Onset (s)</b>	363.2 ± 148.8
<b>Brain [3-MPA] at Seizure Onset (μM)</b>	45.2 ± 19.1
<b>Number of Seizures Detected</b>	592 ± 187
<b>Average of the Average Seizure Duration (s)</b>	0.87 ± 1.78
<b>R<sub>max</sub></b>	71.8 ± 22.2

a: n = 6 rats

**Table 2.1** ECoG data for constant infusion dosing in the striatum [1].



While this constant infusion model was an important first step in the development of 3-MPA epileptic seizure model, was not as clinically relevant. Research has shown that 70% of adult onset epilepsy patients present with partial (focal) seizures [2]. This means that the seizures are localized in a specific brain region. 3-MPA in this constant infusion model is dosed to the brain globally, and thus its physiologic and neurochemical changes are on a global scale as well. The purpose of these studies was to develop a model where 3-MPA is dosed to a specific brain region and the physiological and neurochemical changes could be monitored in a site specific manner while not disturbing the neurochemical balance in the brain as whole. A comparison was made between the local dosing and the constant infusion model, as well as a comparison between awake and anesthetized animals in various brain regions.

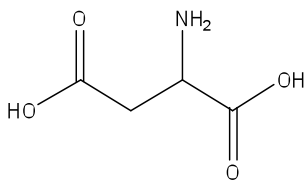
### *2.1.2 Amino acid neurotransmitters*

The structures of the main amino acid neurotransmitters of interest in this research are shown in Figure 2.3. While aspartic acid, arginine, and alanine will be monitored in microdialysis samples, they are not of extra importance since 3-MPA works on the glutamic acid/ $\gamma$ -hydroxybutyric acid system. Glutamic acid is the main excitatory neurotransmitter in the brain;  $\gamma$ -hydroxybutyric acid is the major inhibitory amino acid in the brain. Disruption of this system by administration of 3-MPA, resulting in an increase in glutamic acid and a decrease in  $\gamma$ -hydroxybutyric acid, results in seizures. The Glutamic acid/  $\gamma$ -hydroxybutyric acid ratio will aid in the understanding of seizure

development in the 3-MPA system. The metabolic synthesis of glutamic acid and  $\gamma$ -hydroxybutyric acid can be seen in Figure 2.4.

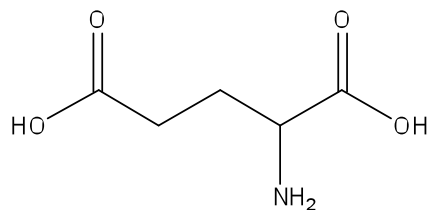
### *2.1.3 Catecholamine neurotransmitters and their metabolites*

The catecholamine neurotransmitters of interest are in Figure 2.5. Figures 2.6 and 2.7 show the biosynthesis and metabolism of the neurotransmitters dopamine (DA), norepinephrine (NE), and serotonin (5-HT) as well as their metabolites 3,4-dihydroxyphenylacetic acid (DOPAC), homovanillic acid (HVA), and 5-hydroxyindoleacetic acid (5-HIAA).



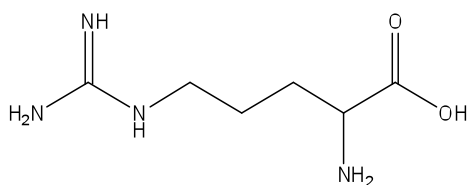
**Aspartic Acid (Asp)**

**pKa ~ 2.28 (most acidic)**



**Glutamic acid (Glu)**

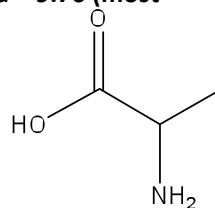
**pKa ~ 2.17 (most acidic)**



**Arginine (Arg)**

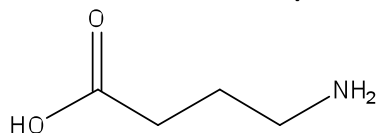
**pKa ~ 2.49 (most acidic)**

**pKa ~ 9.76 (most acidic)**



**Alanine (Ala)**

**pKa ~ 2.31 (most acidic)**



**γ-Hydroxybutyric acid**

**pKa ~ 4.44 (most acidic)**

**Figure 2.3** Structures of the amino acid neurotransmitters of interest. pKa values were obtained from SciFinder© Scholar 2007.

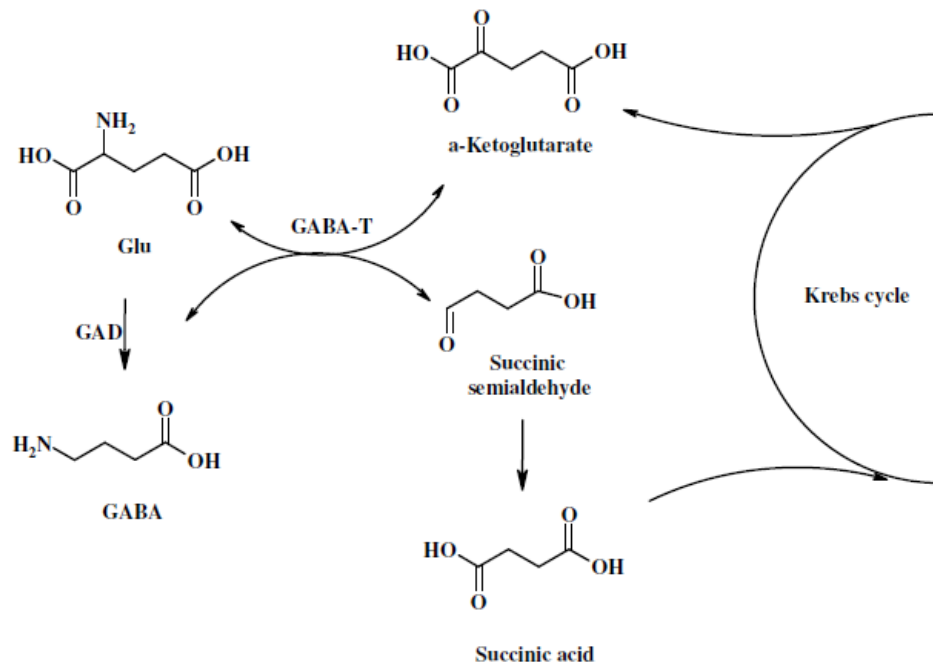
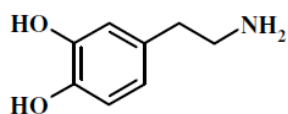
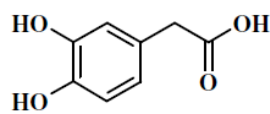


**Figure 2.4** Metabolic synthesis and breakdown of glutamic acid and  $\gamma$ -hydroxybutyric acid [1].



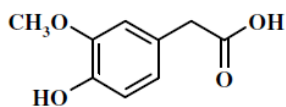
Dopamine (DA)

pKa ~ 9.39 (most acidic)  
pKa ~ 10.11 (most basic)



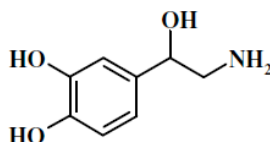
3,4-Dihydroxyphenylacetic acid  
(DOPAC)

pKa ~ 4.42 (most acidic)



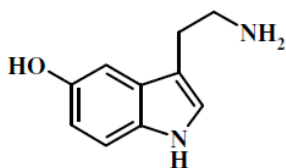
Homovanillic acid (HVA)

pKa ~ 4.39 (most acidic)



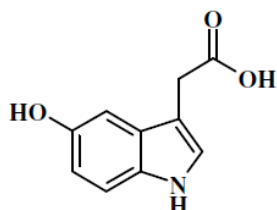
Norepinephrine (NE)

pKa ~ 9.57 (most acidic)  
pKa ~ 8.36 (most basic)



5-Hydroxytryptamine  
(5-HT)

pKa ~ 9.61 (most acidic)  
pKa ~ 10.31 (most basic)



5-Hydroxyindole-3-acetic acid  
(5-HIAA)

pKa ~ 4.54 (most acidic)

**Figure 2.5** Catecholamine neurotransmitters of interest. pKa values were obtained from SciFinder Scholar 2007.

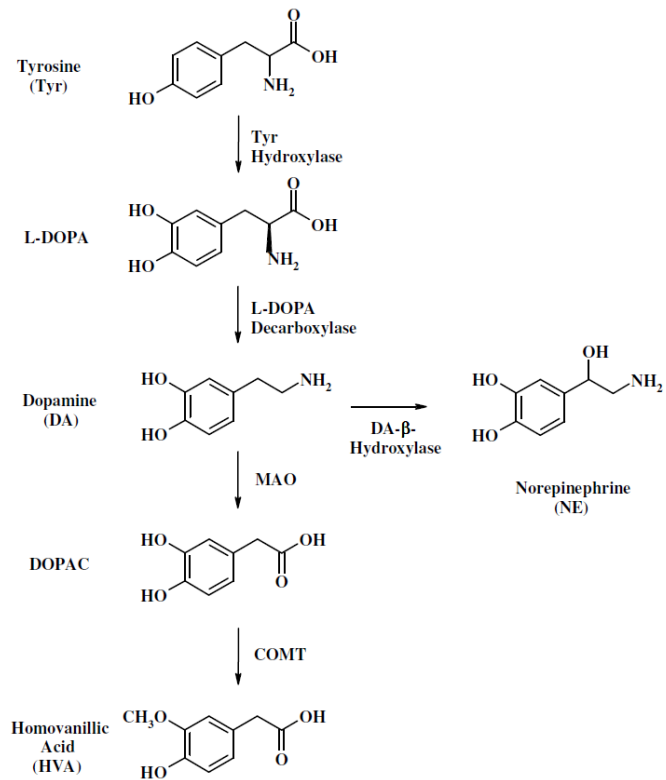


**Figure 2.6** Biosynthesis and metabolism of catecholamine neurotransmitters [1].

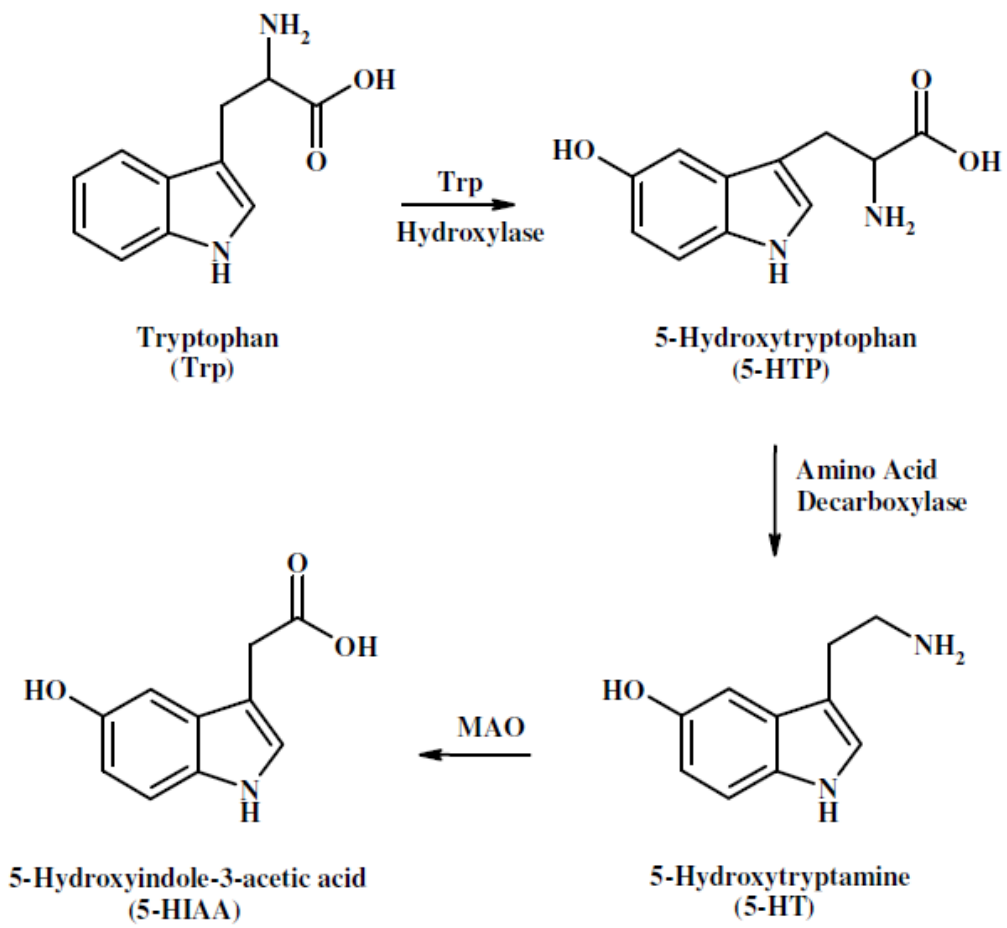


**Figure 2.7** Metabolism of Tryptophan leads to the neurotransmitter 5-Hydroxytryptamine (serotonin) [1].

#### *2.1.4 Methods for the determination of neurotransmitters and their metabolites in biological samples.*

Since the biological samples containing neurotransmitters are often complex, detection is coupled with a separation technique. The two separation techniques used for detection of neurotransmitters are liquid chromatography and capillary electrophoresis. With these two separation techniques, fluorescence and electrochemical detection are most widely used. With an LC separation, fluorescence detection of amino acid transmitters is most often used (see section 2.2.3) [3, 4]. If the neurotransmitters are electroactive, they can be detected by LC coupled with electrochemical detection [5, 6]. When sample size is a consideration, especially with microdialysis samples, capillary electrophoresis is a good separation scheme. As with LC, neurotransmitters are often detected by fluorescence in CE [7, 8] as well as electrochemical detection [9, 10]. Other techniques include biosensors, such as those for glutamate [11], and cyclic voltammetry for dopamine [12, 13].

#### *2.1.5 Mechanisms of action of 3-mercaptopropionic acid*

The mechanism of action of 3-MPA has been well studied. 3-MPA is a competitive inhibitor of the enzyme glutamic acid decarboxylase (GAD) which is responsible for converting glutamic acid to  $\gamma$ -aminobutyric acid [14-17]. This results in an increase in glutamic acid and a decrease in  $\gamma$ -aminobutyric acid [18-22].

3-MPA first produces myoclonic seizures, but over time, tonic-clonic seizures develop [23]. Myoclonic seizures are very brief, 2-3 seconds in duration, and are



characterized by twitches or jerks in the muscle. They usually involve just the forelimbs, nose, and whiskers. Tonic-clonic seizures are more violent and typically last for several minutes. These types of seizures usually involve the entire body.

#### *2.1.6 Current uses for 3-mercaptopropionic acid*

3-MPA has been used as a chemical convulsant for quite some time. 3-MPA has been used to study the pharmacokinetics of the anti-epileptic drug Phenobarbital [24, 25]. Neuronal lesions caused by administration of 3-MPA have been studied by O'Connell [26] and Towfighi [27]. This allows for the study of localized brain damage due to status epilepticus.

While 3-MPA has widespread use as a convulsant, it has many other analytical uses as well. 3-MPA has been used to form a gold monolayer for the detection of catechin, a plant derived polyphenolic antioxidant [28]. Additionally, it has been used as a tag on gold nanoparticles for  $\text{Hg}^{+2}$  detection as well as to form alkanethiol monolayers for the detection of the superoxide radical by immobilized cytochrome c [29, 30].

## **2.2 Materials and Methods**

### *2.2.1 Chemicals and Reagents*

Monobasic sodium phosphate, dibasic sodium phosphate, sodium chloride, potassium chloride, magnesium chloride, calcium chloride, disodium ethylenediamine tetra acetate ( $\text{Na}_2\text{EDTA}$ ), 85% *o*-phosphoric acid, and 0.3  $\mu\text{m}$  alumina powder were

purchased from Fisher Scientific (Pittsburgh, PA). L-aspartic acid, L-glutamic acid, L-arginine, L-alanine, L-gammabutyric acid, DL-2-aminoadipic acid, 3-mercaptopropionic acid, ammonium acetate, 1-octanesulfonic acid, HPLC grade methanol, and HPLC grade tetrahydrofuran were purchased from Sigma-Aldrich (St. Louis, MO). Triple distilled mercury was obtained from Bethlehem Apparatus Company (Hellertown, PA). Ketamine HCl was obtained from Fort Dodge Animal Health (Fort Dodge, IA). Xylazine was obtained from Lloyd Laboratories (Shenandoah, IA). Acepromazine was obtained from Boehringer Ingelheim Vetmedica, Inc. (St. Joseph, MO). All solutions in water were prepared with 18.2 M $\Omega$  distilled, deionized water (Labconco, Kansas City, MO).

### *2.2.2 Microdialysis Sample Considerations*

An appropriate amount of recovery time is needed after microdialysis probe implantation for neurotransmitters to return to basal levels. The trauma induced during microdialysis probe implantation has been well documented. Gliosis occurs from local brain tissue being disturbed during implantation [31, 32]. There is an excess of neurotransmitter release into the extracellular space, as well as increased glucose metabolism and a decrease in blood flow [32].

One key in microdialysis experiments is to maximize the temporal resolution of your sampling so that trends in the extracellular events being explored can be identified. In the experiments described in this thesis, five minute sampling intervals were used. This was the minimum sampling duration that allowed for enough sample to be collected for analysis. An artificial cerebral spinal fluid (aCSF) solution (145mM NaCl, 2.7mM

KCl, 1.0mM MgCl<sub>2</sub>, 1.2mM CaCl<sub>2</sub>, 0.45mM NaH<sub>2</sub>PO<sub>4</sub>, 2.33mM Na<sub>2</sub>HPO<sub>4</sub>) was used that closely mimics the cerebral spinal fluid found in rats, to minimize loss of ions during sampling. aCSF was perfused through the probe at 1.0 μL/min and collected in an outlet vial. During the five minute sampling period, 5 μL of sample was collected. 2.5 μL was used for 3-MPA analysis, while 2.5 μL was reserved for amino acid analysis.

An internal standard in 0.1M perchloric acid was spiked into the microdialysis sample to prevent autooxidation of any compounds in the aCSF sample matrix prior to analysis. Perchloric acid has been shown to increase the stability of these samples [33, 34]. If the microdialysis samples could not be analyzed immediately, the samples were flash frozen in liquid nitrogen and stored in a -20°C laboratory freezer to maintain stability.

### *2.2.3 Sample Derivatization Scheme*

Since many amino acid neurotransmitters are not natively fluorescent (for example glutamate and GABA), they must be derivatized prior to separation by either CE or LC and detection. The two most commonly used reagents are *o*-phthalaldehyde (OPA) and naphthalene-2,3-dicarboxyaldehyde (NDA). OPA selectively reacts with primary amines in the presence of an alkyl thiol (usually β-mercaptoethanol (βME)) to form 1-alkylthio-2-alkyl-substituted isoindoles, as first shown by Simons and Johnson [35]. OPA has been used extensively for the analysis of amino acids by both LC and CE [36, 37]. OPA is non-fluorescent prior to the reaction, thus making it an attractive reagent. The downside to OPA as a derivatization reagent is its poor stability. Jacobs et. al.

showed that the OPA adduct forms within a minute, but then quickly degrades to non-fluorescent by-products [38]. This fact limits the use of OPA for pre-column derivatization schemes.

Naphthalene-2,3-dicarboxyaldehyde is the other most commonly used derivatization reagent, which also reacts selectively with primary amines. NDA was developed by De Montigny et. al. and reacts with a nucleophile, the cyanide ion ( $\text{CN}^-$ ), to form N-substituted-1-cyanobenz[f]isoindole adducts [39]. The N-substituted-1-cyanobenz[f]isoindole adducts are also significantly more stable than those formed with OPA, being stable for 12 hours [39]. NDA adducts with  $\text{CN}^-$  as the nucleophile have an excitation at 440 nm and an emission at 490 nm, with a quantum efficiency of 0.54 in 60% acetonitrile [39]. Like OPA, NDA/ $\text{CN}^-$  has been widely used for the detection of amino acids with both LC and CE [40-42]. The NDA/ $\text{CN}^-$  reaction scheme can be seen in Figure 2.8.

For the analysis of amino acids in microdialysis samples, 2.5  $\mu\text{L}$  of microdialysate was spiked with 1.5  $\mu\text{L}$  of the internal standard (DL-2-aminoadipic acid), 1.0  $\mu\text{L}$  of 500 mM borate : 87 mM  $\text{CN}^-$  (100 : 20 v:v), and 1.0  $\mu\text{L}$  of 3mM NDA in an acetonitrile: water solution (50:50, v:v). Of that 6.0  $\mu\text{L}$  of sample, 5.0  $\mu\text{L}$  was injected for analysis. The reaction was allowed to take place for 30 minutes at room temperature to allow for complete derivitization of the samples. Figure 2.9 shows the change in peak height as a function of reaction time for NDA and the amino acid containing samples.

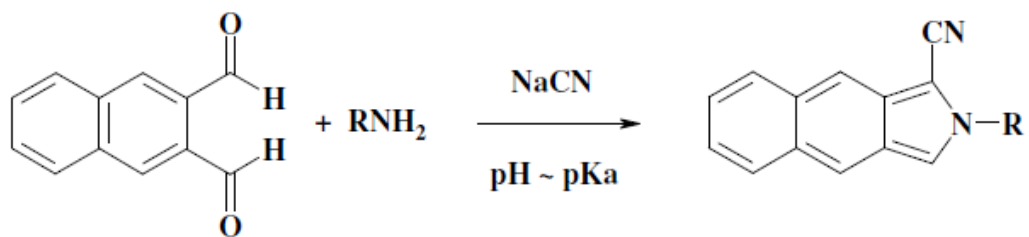


**Figure 2.8** The reaction of NDA/CN<sup>-</sup> with primary amines (RNH<sub>2</sub>).

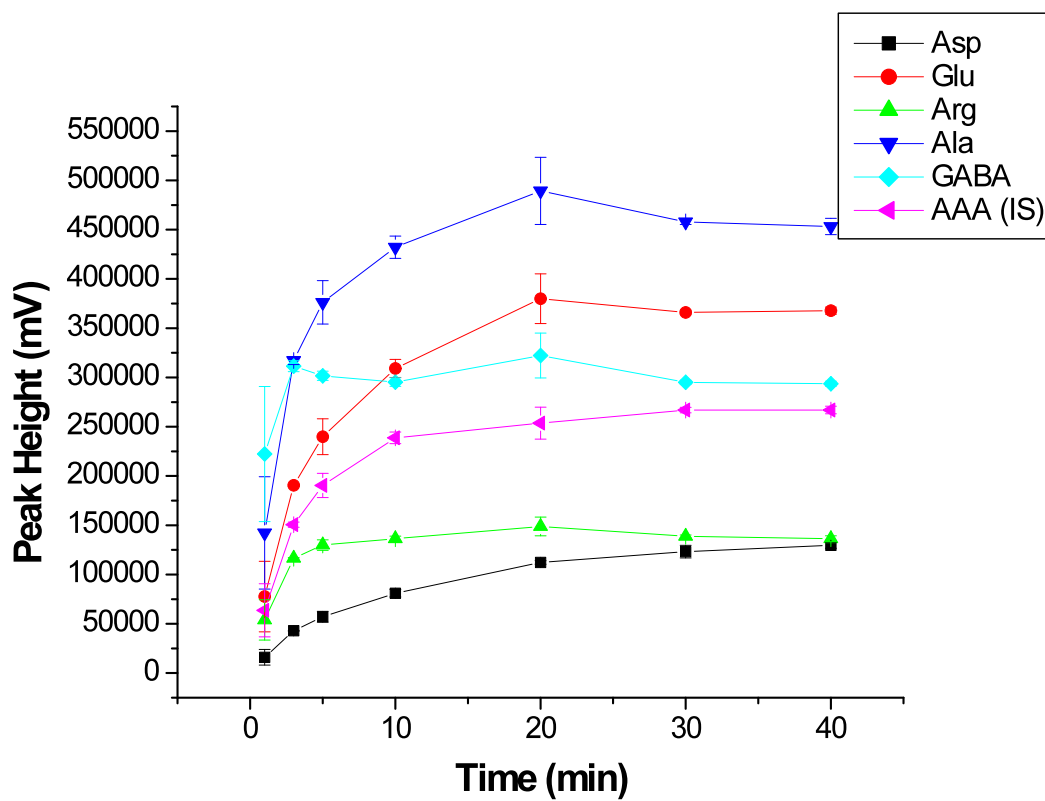


**Figure 2.9** Peak heights for NDA adducts of amino acids as a function of reaction time.

## 2.2.4 Instrumentation

### 2.2.4.1 3-mercaptopropionic acid and catecholamine neurotransmitters

A liquid chromatographic system with electrochemical detection was used for the detection of 3-mercaptopropionic acid and the catecholamines in microdialysis samples. A Shimadzu LC-20AD pump and Rheodyne 9725i PEEK sample injector were connected to an Agilent ZORBAX 3.5 $\mu$ m SB-C18 column (1.0 x 50mm, Agilent Technologies, Santa Clara, CA) with a Phenomenex C18 guard cartridge. The mobile phase was adapted from Stenken et. al. and consisted of a phosphate buffer with methanol (90:10, v:v) [43]. Specifically, 125mM NaH<sub>2</sub>PO<sub>4</sub>, 20.0mM Na<sub>2</sub>EDTA, and 0.75mM 1-octanesulfonic acid was pH adjusted to 3.5 with 85% *o*-phosphoric acid.

Electrochemical detection was performed using a thin layer dual glassy carbon Au/Hg amalgam electrode. Preparation and use of the electrode is described in Allison and Shoup [44]. Briefly, a 3mm glassy carbon/Au electrode embedded in a PEEK block (Bioanalytical Systems, West Lafayette, IN) was polished with 15  $\mu$ m, 6  $\mu$ m, 3  $\mu$ m, 1  $\mu$ m diamond polish (Bioanalytical Systems, West Lafayette, IN) followed by 0.3  $\mu$ m alumina powder. Following polishing, the electrode was rinsed with methanol and water. Triple distilled mercury was placed over the gold electrode and allowed to rest for 5 minutes. Excess mercury was then removed with the edge of a credit card and it was allowed to set overnight. Once the amalgamation process was complete, the electrode was placed into the electrochemical flow cell and was allowed to equilibrate with the mobile phase and dissipate charging current. Figure 2.10 below shows a schematic of the parallel dual electrode setup.

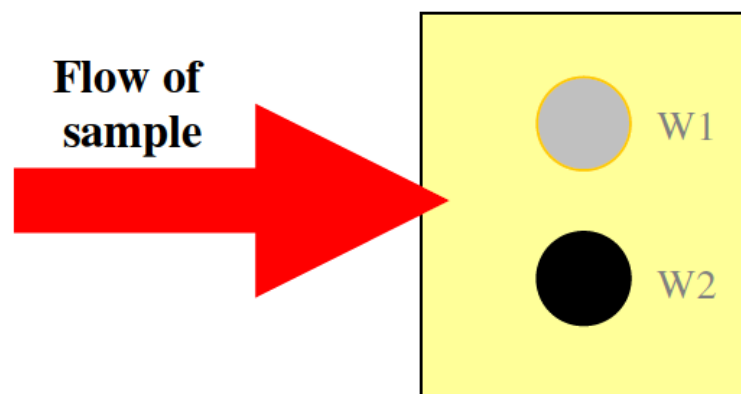
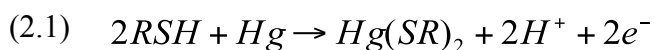


**Figure 2.10** Dual Au/Hg + Glassy carbon working electrode in parallel configuration. Electrochemical operating conditions are identical to those described in 2.2.4.1 [1].



Detection of 3-MPA was done at +100mV versus a Ag/AgCl reference electrode based on a hydrodynamic voltammogram (HDV) [1]. The potential was set using a LC-4C potentiostat (Bioanalytical Systems, West Lafayette, IN). Detection of 3-MPA was done indirectly by the oxidation of mercury as the thiol passes over the electrode surface. 2.5  $\mu$ L of microdialysate was injected for the analysis of 3-MPA. The electrochemical equation can be seen in Equation 2.1.



The data was collected at 10 Hz and processed using a Chrom&Spec Chromatography Data System (Amersand International, Beachwood, OH). The structure of 3-MPA and detection scheme of 3-MPA can be seen in Figure 2.11 below.

Detection of the catecholamines, dopamine (DA) and norepinephrine (NE), and their metabolites, 3,4-dihydroxyphenylacetic acid (DOPAC), homovanillic acid (HVA), and 5-hydroxyindoleacetic acid (5-HIAA), was performed at +750mV at the glassy carbon electrode. A typical chromatogram for detection of the catecholamine neurotransmitters can be seen in Figure 2.12 below.

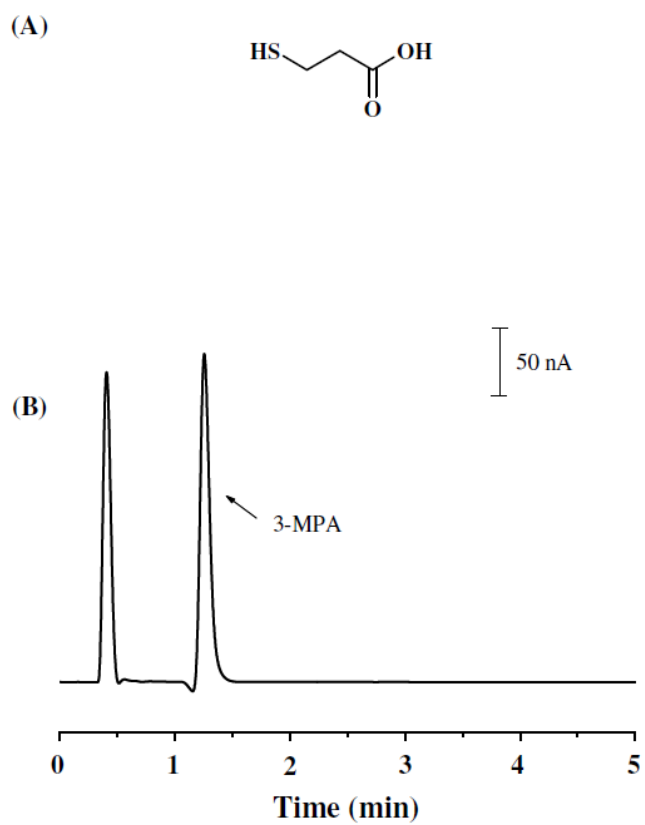


**Figure 2.11** Typical Chromatogram of 3-MPA. (A) Structure of 3-MPA. (B) LC-EC detection of 3-MPA at +100mV versus Ag/AgCl reference electrode [1].

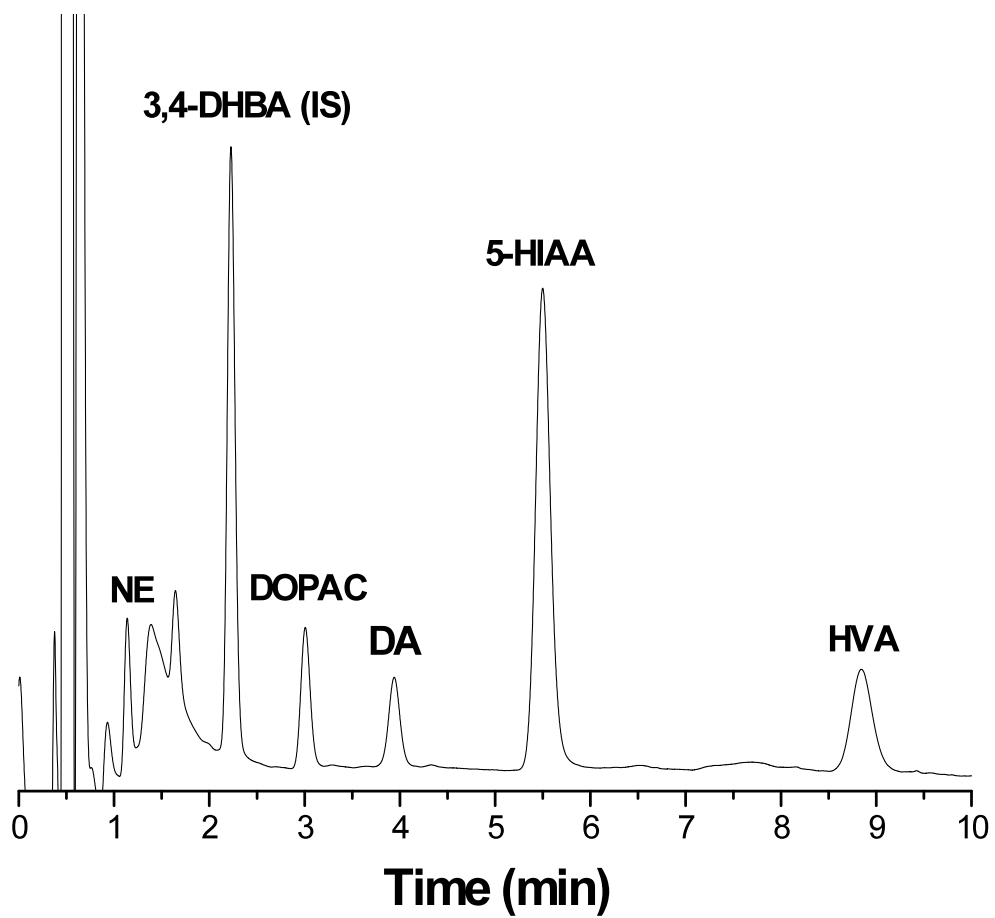


**Figure 2.12** Typical LC-EC chromatogram from brain microdialysate.

#### 2.2.4.2 *Amino acid neurotransmitters*

A liquid chromatographic system with fluorescence detection was used for the analysis of the amino acid neurotransmitters in microdialysis samples. Two Shimadzu LC-10ADvp pumps, a Shimadzu 100  $\mu$ L mixer and Rheodyne 9725i PEEK sample injector were connected to a Phenomenex Synergi 4 $\mu$ m Hydro-RP column (150 x 2.0mm, Phenomenex, Torrance, CA) with a Phenomenex C18 guard cartridge. The binary gradient was controlled by a Shimadzu SCL-10vp System Controller. Mobile Phase A consisted of 50mM ammonium acetate pH adjusted to 6.8 with glacial acetic acid. 5% Tetrahydrofuran (THF) was added making the final concentration 95% acetate : 5% THF (v:v). Mobile phase B consisted of 100% methanol. The method was adapted from Shah et. al. [45]. A Shimadzu 10AXL fluorescence detector was operated at an excitation wavelength of 442nm and an emission wavelength of 490nm [46]. A typical chromatogram for the detection of the amino acids can be seen below is Figure 2.13.

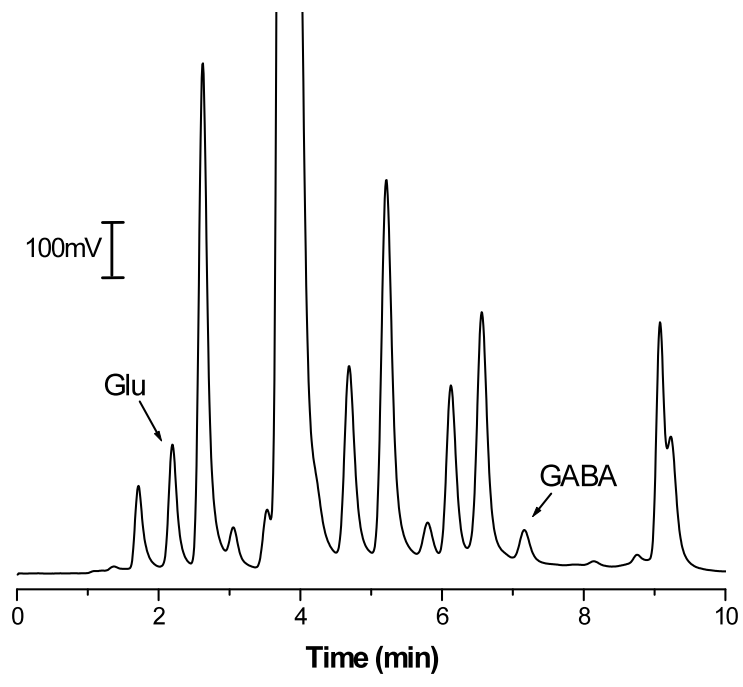


**Figure 2.13** Typical LC-FL chromatogram from brain microdialysate.

## *2.2.5 Surgical Procedures*

### *2.2.5.1 Animal and Instrumentation Preparation*

Male Wistar Rats (Charles River, Charles River Laboratories, Wilmington, MA) weighing between 300-450g were used. The animals were kept on a 12 hour light/dark cycle and had free access to food and water prior to surgery. The research described follows the principles stated in the Guide for the Care and Use of Laboratory Animals, NIH publication 86-23, 1996 edition. Experimental animals were initially anesthetized by inhalation of isoflurane followed by an i.p. injection of a ketamine (67.5 mg/kg)/ xylazine (3.4 mg/kg)/ acepromazine (0.67 mg/kg) mixture. The animals were closely monitored during all procedures. Booster doses of one-fourth or one-half of the original dose of ketamine was used as needed to maintain adequate anesthesia. The animal's body temperature was kept at 37°C using a Homeothermic Blanket Control Unit (Harvard Apparatus, Holliston, MA). The incision sites were prepared by shaving away as much hair as possible and then disinfecting with three alternate scrubs each of Prodine Scrub (0.75% aqueous iodine, Phoenix Pharmaceutical, Inc. St. Joseph, MO. USA) and a 70% (v:v) solution of aqueous ethanol. The incisions were closed with sutures or surgical staples. All solutions injected into the animal were filtered using a disposable 0.2 µm nylon syringe filter (Acrodisc filters, Fisher Scientific). Surgical tools, drapes, sutures, cannulas, and rinsing water used for survival procedures were sterilized by ethylene oxide.

#### 2.2.5.2 Microdialysis Brain Probe Implantation

Rats were anesthetized as described above. The hair on the top of the rat skull was shaved and the skin and scalp cleansed via betadine/alcohol rub. The animal was then securely positioned in a stereotaxic apparatus with incisor bar set at 3.3 mm from the interaural saggital suture. Adventitious tissue covering the skull was removed using cotton swabs. Two 1 mm diameter holes were drilled approximately 2 mm anterior and posterior to the insertion site of the guide cannula through the skull. Two stainless steel anchor screws (1 mm diameter, 2 mm length) were inserted into these holes. Next, a 1 mm diameter hole was drilled through the skull at the insertion site and an intracerebral guide cannula (CMA Microdialysis Inc., North Chelmsford, MA) was lowered into the cerebral cortex using a micromanipulator attached to the stereotaxic apparatus. The guide cannula was positioned 2 mm above the hippocampus, 4mm above the striatum, and 0.5mm above the *locus coeruleus*, then affixed to the skull with dental cement. The dummy probe in the guide cannula was then replaced with an Applied Neuroscience (Applied Neuroscience, London, UK) microdialysis probe with an internal Ag/AgCl working electrode. A 4mm Applied Neuroscience microdialysis probe with a Polyarylethersulphone (PAES) membrane was used in the striatum with coordinates: posterior +0.2 mm, lateral +3.2 mm, ventral -7.5 mm, a 2mm probe was used in the hippocampus (CA1) with the coordinates: anterior -3.3 mm, lateral +1.7 mm, ventral -3.7 mm, and a 0.5mm probe was used in the *locus coeruleus* with the coordinates: anterior -9.8mm, lateral +1.2mm, ventral -7.2mm.

### *2.2.6 ECoG recording*

ECoG recordings were made using a SynAmps RT system (Compumedics Neuroscan, Charlotte, NC). Microdialysis probes with an internal Ag/AgCl working electrode were connected to the headbox and Ag/AgCl wires were placed under the scalp as the reference and ground. Data was collected using SCAN software. A 20000Hz sampling rate was reduced to a 200Hz sampling rate by computing mean values of the signals within adjacent time windows with the volume 100 samples. Seizures were detected based upon their score from the algorithm output.



## 2.3 References

1. Crick, E.W., *In vivo Microdialysis Coupled with Electrophysiology for the Neurochemical Analysis of Epileptic Seizures*, in *Chemistry*. 2007, The University of Kansas.
2. French, J.A. and T.A. Pedley, *Initial management of epilepsy*. *N. Engl. J. Med.*, 2008. **359**(2): p. 166-176.
3. Clarke, G., et al., *An isocratic high performance liquid chromatography method for the determination of GABA and glutamate in discrete regions of the rodent brain*. *Journal of Neuroscience Methods*, 2007. **160**(2): p. 223-30.
4. Gui, L., et al., *Simultaneously determining 4 amino acid neurotransmitters in mice brain by high-performance liquid chromatography with fluorescence detector*. *Di-San Junyi Daxue Xuebao*, 2009. **31**(8): p. 675-678.
5. Hubbard, K.E., et al., *Determination of dopamine, serotonin, and their metabolites in pediatric cerebrospinal fluid by isocratic high performance liquid chromatography coupled with electrochemical detection*. *Biomedical Chromatography*. **24**(6): p. 626-631.
6. Riggin, R.M. and P.T. Kissinger, *Determination of catecholamines in urine by reverse-phase liquid chromatography with electrochemical detection*. *Analytical Chemistry*, 1977. **49**(13): p. 2109-11.
7. Li, H., et al., *Simultaneous monitoring multiple neurotransmitters and neuromodulators during cerebral ischemia/reperfusion in rats by microdialysis and capillary electrophoresis*. *Journal of Neuroscience Methods*. **189**(2): p. 162-168.
8. Parrot, S., et al., *High temporal resolution for in vivo monitoring of neurotransmitters in awake epileptic rats using brain microdialysis and capillary electrophoresis with laser-induced fluorescence detection*. *Journal of Neuroscience Methods*, 2004. **140**(1-2): p. 29-38.
9. Chen, G., J.N. Ye, and J.S. Cheng, *Determination of monoamine transmitters and tyrosine in biological samples by capillary electrophoresis with electrochemical detection*. *Chromatographia*, 2000. **52**(3/4): p. 137-141.
10. Kuklinski Nicholas, J., E.C. Berglund, and G. Ewing Andrew, *Micellar capillary electrophoresis--electrochemical detection of neurochemicals from Drosophila*. *Journal of separation science*. **33**(3): p. 388-93.

11. McLamore, E.S., et al., *A self-referencing glutamate biosensor for measuring real time neuronal glutamate flux*. Journal of Neuroscience Methods. **189**(1): p. 14-22.
12. Zachek, M.K., et al., *Microfabricated FSCV-compatible microelectrode array for real-time monitoring of heterogeneous dopamine release*. Analyst (Cambridge, United Kingdom). **135**(7): p. 1556-1563.
13. Zachek, M.K., et al., *Simultaneous monitoring of dopamine concentration at spatially different brain locations in vivo*. Biosensors & Bioelectronics. **25**(5): p. 1179-1185.
14. Horton, R.W. and B.S. Meldrum, *Seizures induced by allylglycine, 3-mercaptopropionic acid and 4-deoxypyridoxine in mice and photosensitive baboons, and different modes of inhibition of cerebral glutamic acid decarboxylase*. Br J Pharmacol, 1973. **49**(1): p. 52-63.
15. Netopilova, M., et al., *Inhibition of glutamate decarboxylase activity by 3-mercaptopropionic acid has different time course in the immature and adult rat brains*. Neurosci. Lett., 1997. **226**(1): p. 68-70.
16. Netopilova, M., et al., *Differences between immature and adult rats in brain glutamate decarboxylase inhibition by 3-mercaptopropionic acid*. Epilepsy Res., 1995. **20**(3): p. 179-84.
17. Sarhan, S. and N. Seiler, *Metabolic inhibitors and subcellular distribution of GABA*. J Neurosci Res, 1979. **4**(5-6): p. 399-421.
18. Fan, S.G., M. Wusteman, and L.L. Iversen, *3-Mercaptopropionic acid inhibits GABA release from rat brain slices in vitro*. Brain Res., 1981. **229**(2): p. 371-7.
19. Herbison, A.E., R.P. Heavens, and R.G. Dyer, *Endogenous release of gamma -aminobutyric acid from the medial preoptic area measured by microdialysis in the anesthetised rat*. J. Neurochem., 1990. **55**(5): p. 1617-23.
20. Ma, D., et al., *Simultaneous determination of gamma -aminobutyric acid and glutamic acid in the brain of 3-mercaptopropionic acid-treated rats using liquid chromatography-atmospheric pressure chemical ionization mass spectrometry*. J. Chromatogr., B: Biomed. Sci. Appl., 1999. **726**(1 + 2): p. 285-290.
21. Timmerman, W., J. Zwaveling, and B.H.C. Westerink, *Characterization of extracellular GABA in the substantia nigra reticulata by means of brain microdialysis*. Naunyn-Schmiedeberg's Arch. Pharmacol., 1992. **345**(6): p. 661-5.
22. Tunnicliff, G., *Action of inhibitors on brain glutamate decarboxylase*. Int. J. Biochem., 1990. **22**(11): p. 1235-41.

23. Mares, P., et al., *Motor and electrocorticographic epileptic activity induced by 3-mercaptopropionic acid in immature rats*. *Epilepsy Res.*, 1993. **16**(1): p. 11-18.
24. Hoecht, C., et al., *Differential hippocampal pharmacokinetics of phenobarbital and carbamazepine in repetitive seizures induced by 3-mercaptopropionic acid*. *Neurosci. Lett.*, 2009. **453**(1): p. 54-57.
25. De Deyn, P.P., et al., *Chemical models of epilepsy with some reference to their applicability in the development of anticonvulsants*. *Epilepsy Res.*, 1992. **12**(2): p. 87-110.
26. O'Connell, B.K., et al., *Neuronal lesions in mercaptopropionic acid-induced status epilepticus*. *Acta Neuropathol*, 1988. **77**(1): p. 47-54.
27. Towfighi, J., et al., *Substantia nigra lesions in mercaptopropionic acid induced status epilepticus: a light and electron microscopic study*. *Acta Neuropathol*, 1989. **77**(6): p. 612-20.
28. Moccelini, S.K., et al., *Self-assembled monolayer of nickel(II) complex and thiol on gold electrode for the determination of catechin*. *Talanta*, 2009. **78**(3): p. 1063-1068.
29. Chen, X.J., et al., *Detection of the Superoxide Radical Anion Using Various Alkanethiol Monolayers and Immobilized Cytochrome c*. *Anal. Chem.* (Washington, DC, U. S.), 2008. **80**(24): p. 9622-9629.
30. Yu, C.-J. and W.-L. Tseng, *Colorimetric Detection of Mercury(II) in a High-Salinity Solution Using Gold Nanoparticles Capped with 3-Mercaptopropionate Acid and Adenosine Monophosphate*. *Langmuir*, 2008. **24**(21): p. 12717-12722.
31. Plock, N. and C. Kloft, *Microdialysis - theoretical background and recent implementation in applied life-sciences*. *Eur. J. Pharm. Sci.*, 2005. **25**(1): p. 1-24.
32. Robinson, T.E., Justice Jr., J.B. , *Microdialysis in the Neurosciences* 1991, Amsterdam: Elsevier.
33. Thorre, K., et al., *New antioxidant mixture for long term stability of serotonin, dopamine and their metabolites in automated microbore liquid chromatography with dual electrochemical detection*. *J. Chromatogr., B: Biomed. Sci. Appl.*, 1997. **694**(2): p. 297-303.
34. Zhang, X., et al., *Neurotransmitter sampling and storage for capillary electrophoresis analysis*. *Fresenius' J. Anal. Chem.*, 2001. **369**(3-4): p. 206-211.

35. Simons, S.S., Jr. and D.F. Johnson, *The structure of the fluorescent adduct formed in the reaction of o-phthalaldehyde and thiols with amines*. J. Am. Chem. Soc., 1976. **98**(22): p. 7098-9.
36. Bowser, M.T. and R.T. Kennedy, *In vivo monitoring of amine neurotransmitters using microdialysis with on-line capillary electrophoresis*. Electrophoresis, 2001. **22**(17): p. 3668-3676.
37. Farrant, M., F. Zia-Gharib, and R.A. Webster, *Automated pre-column derivatization with o-phthalaldehyde for the determination of neurotransmitter amino acids using reversed-phase liquid chromatography*. J. Chromatogr., Biomed. Appl., 1987. **417**(2): p. 385-90.
38. Jacobs, W.A., M.W. Leburg, and E.J. Madaj, *Stability of o-phthalaldehyde-derived isoindoles*. Anal. Biochem., 1986. **156**(2): p. 334-40.
39. De Montigny, P., et al., *Naphthalene-2,3-dicarboxyaldehyde/cyanide ion: a rationally designed fluorogenic reagent for primary amines*. Anal. Chem., 1987. **59**(8): p. 1096-101.
40. Denoroy, L., et al., *In-capillary derivatization and capillary electrophoresis separation of amino acid neurotransmitters from brain microdialysis samples*. J. Chromatogr., A, 2008. **1205**(1-2): p. 144-149.
41. Lunte, S.M., et al., *Determination of desmosine, isodesmosine, and other amino acids by liquid chromatography with electrochemical detection following precolumn derivatization with naphthalenedialdehyde/cyanide*. Anal Biochem, 1989. **178**(1): p. 202-7.
42. Zhou, S.Y., et al., *Continuous in Vivo Monitoring of Amino Acid Neurotransmitters by Microdialysis Sampling with Online Derivatization and Capillary Electrophoresis Separation*. Anal. Chem., 1995. **67**(3): p. 594-9.
43. Stenken, J.A., et al., *Detection of N-acetylcysteine, cysteine and their disulfides in urine by liquid chromatography with a dual-electrode amperometric detector*. J. Pharm. Biomed. Anal., 1990. **8**(1): p. 85-9.
44. Allison, L.A. and R.E. Shoup, *Dual electrode liquid chromatography detector for thiols and disulfides*. Anal. Chem., 1983. **55**(1): p. 8-12.
45. Shah, A.J., F. Crespi, and C. Heidebreder, *Amino acid neurotransmitters: separation approaches and diagnostic value*. J. Chromatogr., B: Anal. Technol. Biomed. Life Sci., 2002. **781**(1-2): p. 151-163.

46. Robert, F., et al., *Coupling on-line brain microdialysis, precolumn derivatization and capillary electrophoresis for routine minute sampling of O-phosphoethanolamine and excitatory amino acids*. J Chromatogr A, 1998. **817**(1-2): p. 195-203.

## Chapter 3

### 3-MPA Local Dosing in the striatum, hippocampus, and *locus coeruleus*

#### 3.1 Introduction

##### 3.1.1 Background and Significance

The major reasons for modifying the existing method for systemic dosing of 3-MPA [1, 2] were to achieve true local administration and minimal systemic toxicity of 3-MPA to generate seizures in a defined local brain region. This was important since many clinical cases present with local seizures, defined to a brain region [3]. One way to determine whether local administration of 3-MPA is being achieved is to place microdialysis probes in different brain regions and collect samples while dosing 3-MPA through the probe in another region. The circuitry of the brain is quite complex. The brain is such a heterogeneous tissue with neuronal projections between many regions reaching far and wide. The expectations are that concentrations of amino acids and catecholamine neurotransmitters will remain at basal levels in the surround tissue, unless the region where 3-MPA is being administered has afferent or efferent pathways connecting it with the region where a control probe is placed. Afferent pathways carry nerve impulses toward the central nervous system (CNS), while efferent pathways carry nerve impulses away from the CNS. In these sets of experiments, three probes were placed in the brain, in the striatum (putamen), the hippocampus (CA1), and the locus

coeruleus and samples were collected simultaneously in all three probes while 3-MPA was administered through only one probe, to see if excitation in one region is transmitted to another.

### *3.1.2 Striatum*

The striatum is one of four regions making up the basal ganglia, as can be seen in Figure 3.1. The striatum can be broken up into two regions, the caudate and the putamen. In rodents the caudate and the putamen are one single structure, but they are divided by an internal capsule in carnivores and primates [4]. The other three regions in the basal ganglia are the subthalamic nucleus, globus pallidus (including the internal and external segments), and the substantia nigra (composing both the pars compacta and pars reticulata). The putamen region of the striatum contains substantial neurons which release both glutamate and GABA, making this region a good choice for study of the 3-MPA model [5]. Widely studied, Figure 3.2 shows a schematic of circuitry within the basal ganglia. Studies have shown the connections between regions of the basal ganglia and other reaches of the brain. Carpenter et al. demonstrated, using horseradish peroxidase and isotopically labeled amino acids, that the subthalamic nucleus has connections with the globus pallidus pars external within the basal ganglia, but there were no connections with the striatum or substantia nigra [6]. Research has shown that there are three major types of neurons in the striatum: medium spiny neurons, large aspiny neurons, and medium aspiny neurons [4, 7-9]. 95% of the striatum consists of medium spiny neurons, which project to the substantia nigra and the globus pallidus (both internal and external)

[4, 9]. The striatum receives excitatory inputs from the substantial part of the cortex with the exception of primary auditory and visual cortex [4, 10]. Importantly, for this research project, these inputs from the cortex utilize glutamate as their neurotransmitter [11, 12]. Additional inputs via medium spiny neurons project in the form of glutamate from the centromedian and parafascicular nuclei of the thalamus [13, 14], adjacent medium spiny neurons project GABA from within the striatum [15], and dopamine from the substantia nigra pars compacta [6]. There are no indications of projections either from the striatum to the hippocampus (CA1) and *locus coeruleus* or from the hippocampus or *locus coeruleus* to the striatum. Therefore, administering 3-MPA into the striatum probe should not result in changes in amino acids and catecholamine neurotransmitters in the other brain regions. The same can be said when dosing in either the hippocampus or *locus coeruleus* and collecting in the striatum.

### 3.1.3 Hippocampus

The hippocampus is part of the cerebral hemisphere and plays an important role in memory and learning. The hippocampus is one of the most studied brain regions in epilepsy, due to its ability to be easily excited, in addition to evident tissue damage in the hippocampus following temporal lobe epilepsy [16-18]. Seizures in the hippocampus are better understood than any other brain region. Seizures in the hippocampus most closely resemble human limbic and temporal lobe epilepsy, which comprises 40% of all human cases, and provides the reason this region is so well studied [19, 20]. There are three major pathways in the hippocampus which have been detailed by Andersen et al.: the



*preforant pathway* extends from the entorhinal cortex to the granule cells of the dentate gyrus, the *mossy fiber pathway*, which consists of the axons on the granule cells, extends to the CA3 pyramidal cells, and the *Schaffer collateral pathway*, which projects from the CA3 to the CA1 neurons [21, 22]. This can be seen in Figure 3.3. Output from the hippocampus stretches to the prefrontal cortex and lateral septal area of the hypothalamus [23]. Inputs containing serotonin, norepinephrine, and dopamine are received from the nucleus reuniens of the thalamus [23]. GABAergic inputs also come from the medial septal area to all of the hippocampus [23]. Based upon these biochemical processes, there is no expectation for amino acids and catecholamine neurotransmitters to deviate from basal levels while dosing in the striatum or the *locus coeruleus*. Additionally, when dosing in the hippocampus, there should not be any changes in either the striatum or the *locus coeruleus*.

#### 3.1.4 *locus coeruleus*

The *locus coeruleus* (LC) is the main synthesis site of norepinephrine (NE) in the brain [24]. Studies have shown the norepinephrine content in the LC to be between 15 and 53 ng/mg protein [25, 26]. Norepinephrine has been shown to be anti-epileptic [27, 28]. This has been supported by the fact that NE has resulted in a delayed onset of amygdala kindling [29] and depletion of NE has resulted in shorter seizure onset time [30]. Projections from the *locus coeruleus* stretch to almost every region of the brain, with the exception of the striatum. Regions innervated include the amygdala, thalamus, hippocampus, neocortex, pallidum, and the cerebellum [31-33]. Inputs to the *locus*

*coeruleus* are received from the central nucleus of the amygdala as well as the frontal cortex [34]. Figure 3.4 shows the inputs and outputs of the *locus coeruleus*. The study of the *locus coeruleus* is interesting not just because of the role of norepinephrine in this region and its effect on the rest of the brain, but also due to the ability to see the effect of projections from this region. While dosing in the *locus coeruleus*, no changes should be seen in the striatum; however changes should be seen in the hippocampus while dosing in the *locus coeruleus*, due to the projections within these two regions.

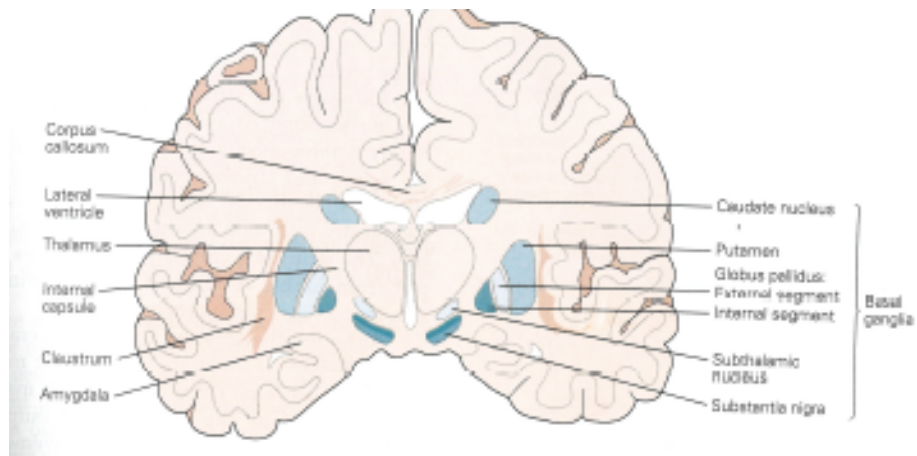


**Figure 3.1** Coronal slice showing the basal ganglia components, including the putamen, where probes are placed in these experiments [22].

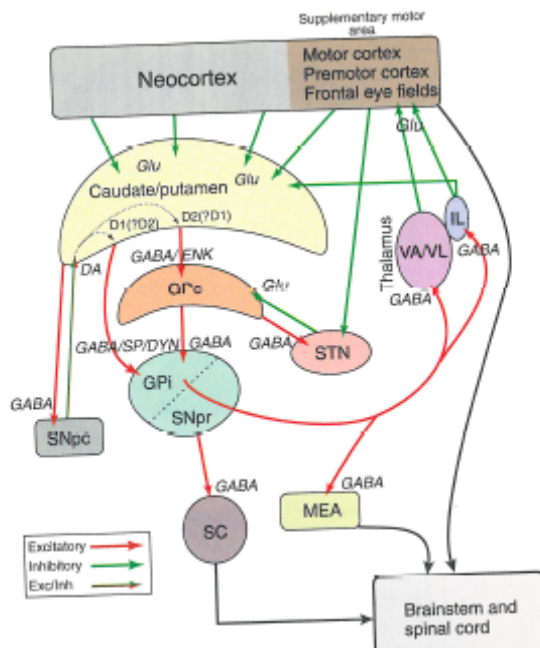


**Figure 3.2** Circuitry of the basal ganglia. Excitatory neurons are in red, inhibitory neurons are in green, and excitatory/inhibitory circuits are in red and green. Substantia nigra pars compacta (SNpc); globus pallidus pars externa (GPe); globus pallidus pars interna (GPI); intralaminar thalamic nucleus (IL); mid-brain extrapyramidal area (MEA); superior colliculus (SC); substantia nigra pars reticulata (SNpr); subthalamic nucleus (STN) [4].

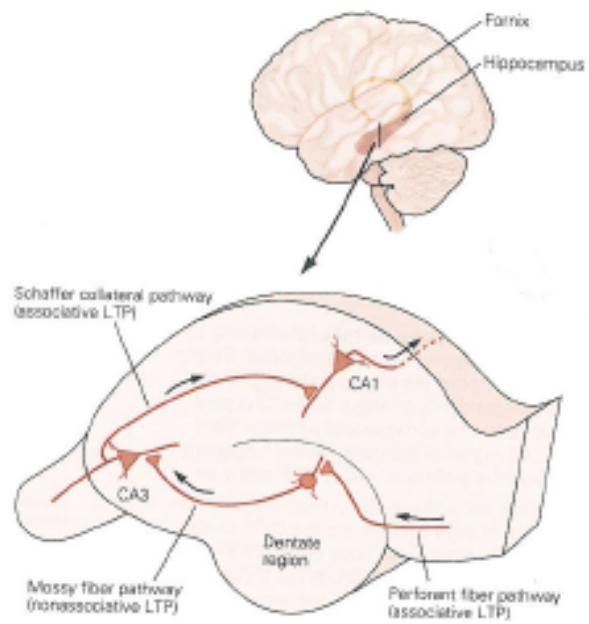
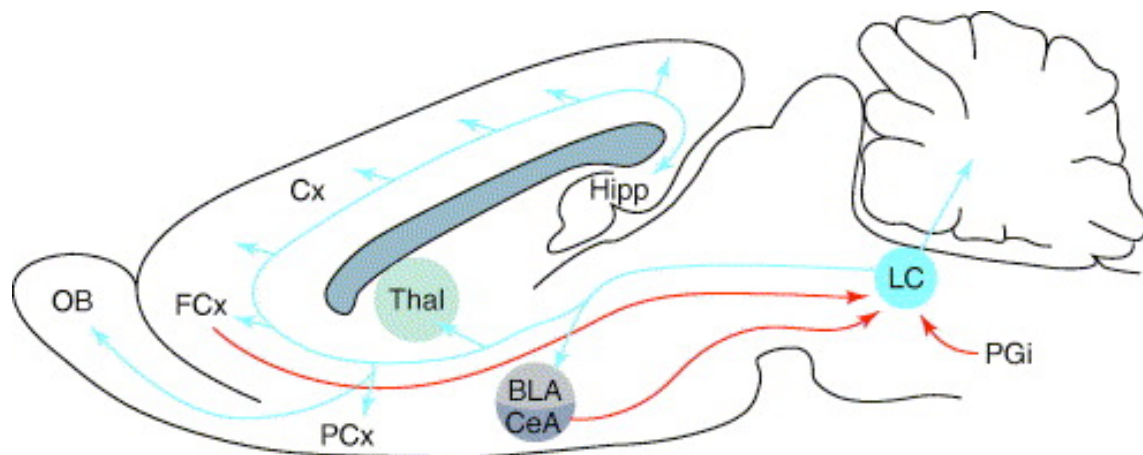


**Figure 3.3** Pathways within the hippocampus. Probes in these experiments are placed in the CA1 region [22].



TRENDS in Neurosciences

**Figure 3.4** Projections into and from the *locus coeruleus*. *Locus coeruleus* (LC); hippocampus (Hipp); thalamus (Thal); olfactory bulb (OB); piriform cortex (PCx); neocortex (Cx); frontal cortex (FCx); paragigantocellularis brainstem nucleus (PGi); amygdala central nucleus (CeA); basolateral nucleus of the amygdala (BLA) [34].

### 3.1.5 Neuronal projections

While microdialysis has been used in the past to determine the underlying neuronal projections within the brain [35-37], these studies were usually done using radiolabeled substrates and neurotransmitters [6, 38]. By using a radiolabeled neurotransmitter, one can follow the efferent pathways by monitoring the radiolabeled neurotransmitter in brain regions where projections are made. One of the disadvantages to using microdialysis for these studies is that you cannot determine if neurotransmitter release in one region is of the same origin as what was released in another region. Also, the time scale for these projections, on the order of milliseconds, is overshadowed by the longer sampling rate.

### 3.1.6 Experimental

In these sets of experiments for the anesthetized rats, three probes were placed in the brain, one in each of the three brain regions: striatum (putamen), hippocampus (CA1), and the *locus coeruleus*. Following probe implantation the rat was allowed to recover, while maintaining anesthesia, while aCSF was perfused through the probe (1.0  $\mu$ l/min) for four hours. This was to allow time for the amino acids and catecholamine neurotransmitters to return to basal levels. Following the four hour recover period, six background samples were collected every ten minutes. Following background collection, 10mM 3-MPA prepared in artificial cerebral spinal fluid (aCSF), was perfused through one of the probes for 50 minutes, while aCSF was perfused through the other two probes.

Following the 50 minutes of 3-MPA administration, the 3-MPA perfusion was terminated and aCSF was perfused through that probe the remaining 70 minutes of the experiment. During these two hours samples were collected every 5 minutes. A three probe approach was not implemented in the awake animal experiments, thus only one probe was implanted. During the awake animal experiments the rats were allowed to come out from under anesthesia and recover for 24 hours. Following these 24 hours, background and dosing samples were collected in the same fashion as for the anesthetized animals.

## 3.2 Results and Discussion

### 3.2.1 3-MPA delivery in the striatum, hippocampus, and locus coeruleus

Multiple 10mM 3-MPA standards were injected on the LC-EC system (Method described in 2.2.4.1) and averaged to obtain the value for a 10mM 3-MPA standard. Dialysate samples were injected and the amount of 3-MPA delivered to the brain (in  $\mu\text{g}/\text{min}$ ) was determined based on the calculated extraction efficiency ( $EE_D$ ) of 3-MPA. Extraction efficiency of 3-MPA was calculated using equation 3.1.

$$(3.1) \quad EE_D = \frac{(C_{perfusate} - C_{dialysate})}{C_{perfusate}}$$

The amount of 3-MPA delivered to the brain was calculated by subtracting the amount of 3-MPA in the dialysate from the perfusate and then converted to mass per unit time ( $\mu\text{g}/\text{min}$ ) using the density of 3-MPA and flow rate of the syringe pump. Figures 3.5 and



3.6 show the delivery of 10mM 3-MPA in the striatum and hippocampus of both anesthetized and awake rats. Figure 3.7 shows the delivery of 10mM 3-MPA in the *locus coeruleus* of anesthetized rats.

Steady-state delivery of 3-MPA is reached in all rats. This steady-state delivery is consistent across all three brain regions and in both awake and anesthetized rats. This steady-state delivery of 3-MPA is advantageous, similar to the steady-state systemic dosing of 3-MPA, as the delivery of 3-MPA during steady-state can be held constant allowing for fewer variables when analyzing neurotransmission. Following termination of the 3-MPA perfusion, there is an exponential clearance of 3-MPA from the probe. The percent delivery of 3-MPA was on average  $19.7 \pm 8.4\%$  across all three brain regions. Based upon the delivery of 3-MPA, on average the concentration of 3-MPA delivered to the brain was 2mM. This is only a semi-quantitative concentration of 3-MPA, as there is a concentration gradient of 3-MPA down the length of the probe as well as out into the brain. The concentrations of 3-MPA in the striatum and hippocampus during systemic dosing of 3-MPA were 125 and 175  $\mu\text{M}$  respectively.

In the three probe experiments, when 3-MPA was administered through one probe, it was not detected in either of the other two probes. This was important, as it shows that any changes that were seen in the other brain regions were not due to 3-MPA directly, but rather projections from one region to another. This also supports the local dosing regime of 3-MPA. 3-MPA would be detected at all three probes during systemic dosing. By administering 3-MPA through the probe, one can generate neurochemical changes in a defined region.

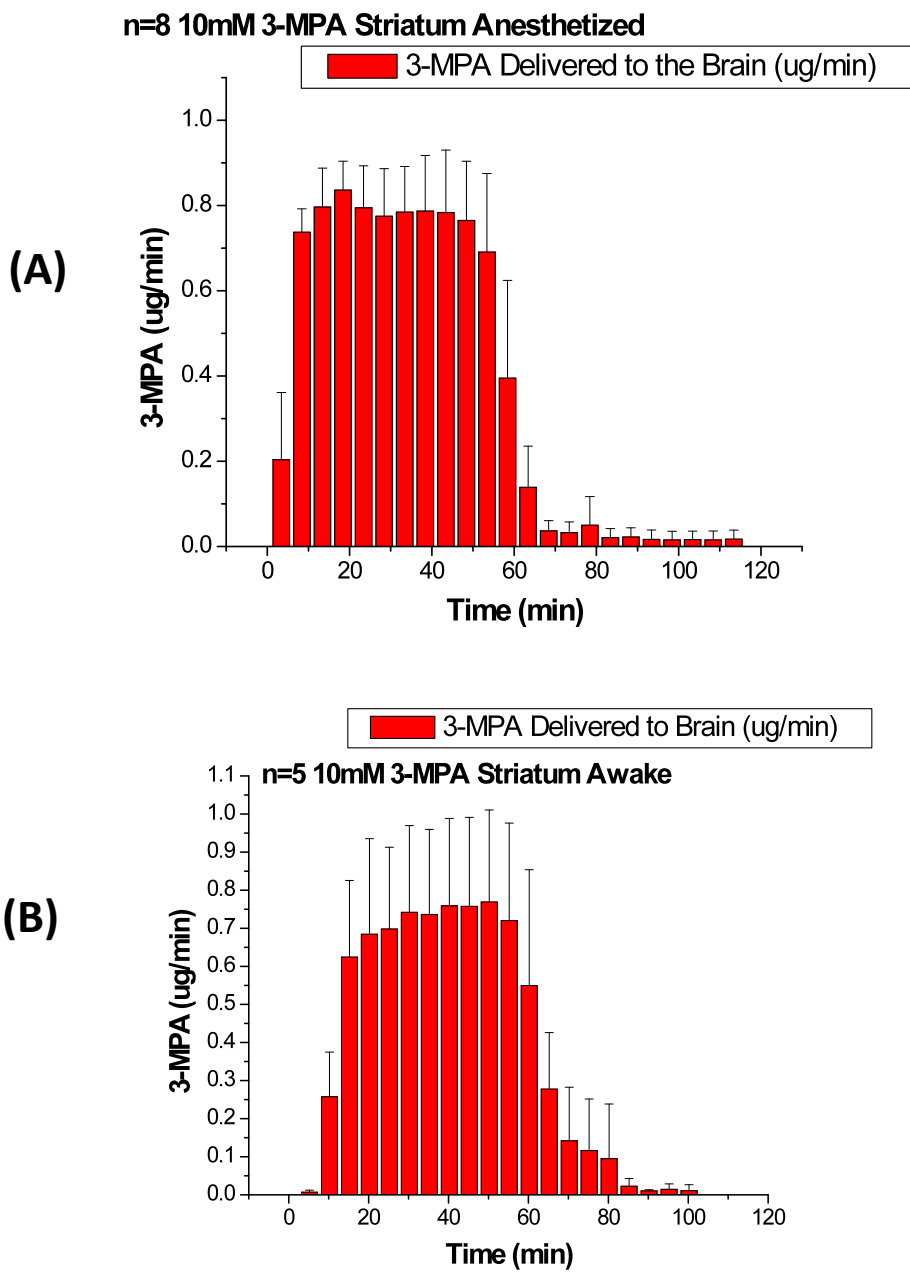


**Figure 3.5** Delivery of 10mM 3-MPA ( $\mu\text{g}/\text{min}$ ) to the striatum of anesthetized (A) and awake (B) rats.

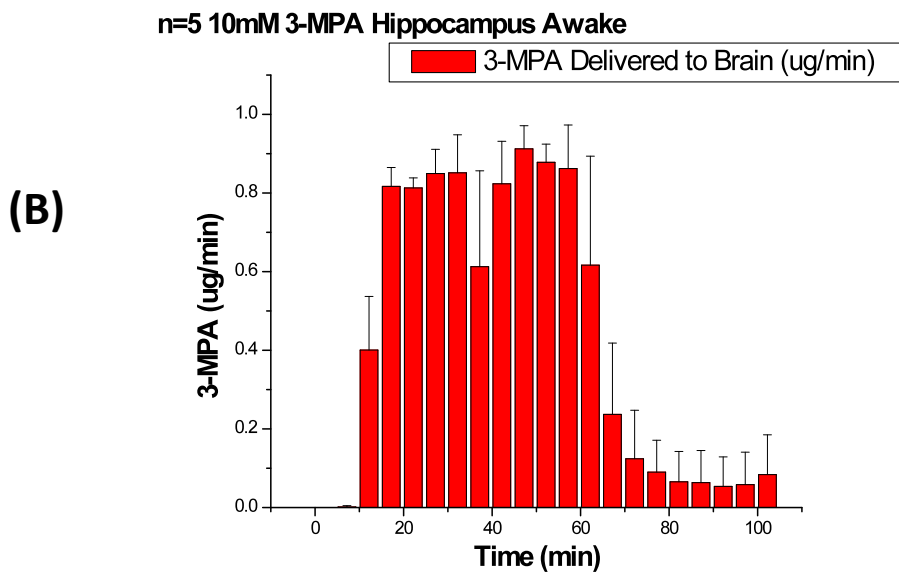
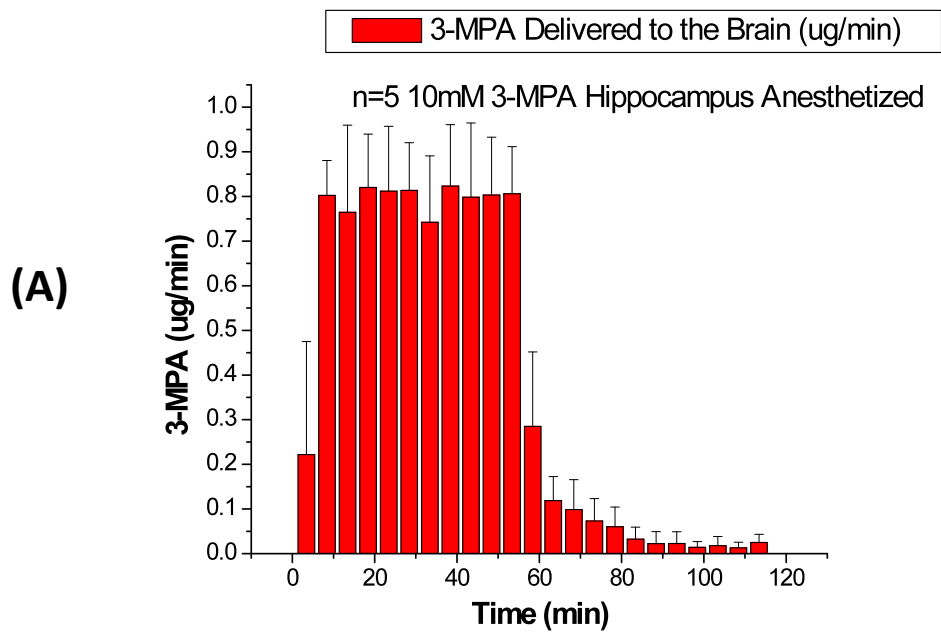


Figure 3.6 Delivery of 10mM 3-MPA ( $\mu\text{g}/\text{min}$ ) to the hippocampus of anesthetized (A) and awake (B) rats.

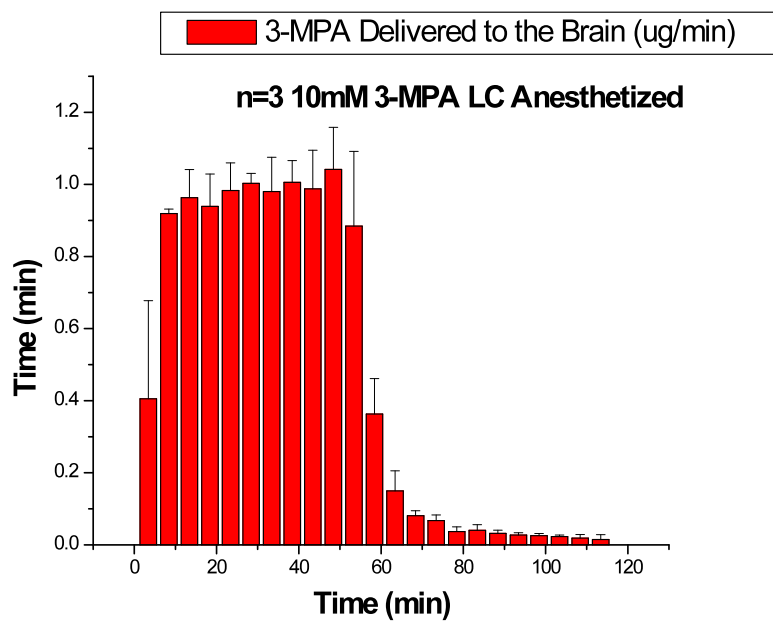


Figure 3.7 Delivery of 10mM 3-MPA ( $\mu\text{g}/\text{min}$ ) to the locus coeruleus of anesthetized rats.

### 3.2.2 *Striatum Amino Acids*

#### 3.2.2.1 *Striatum Amino Acids in Anesthetized Rats*

Due to trauma from probe implantation during surgery, neurotransmitter levels need to be allowed to return to basal levels before dosing [39, 40]. Therefore, one of the first studies monitored changes in amino acid and catecholamine neurotransmitter levels immediately after probe implantation. Figure 3.8 shows the levels of amino acids and neurotransmitters returning to baseline following probe implantation. From these data it was concluded that, following probe implantation, the probe will be perfused with aCSF for four hours prior to collection of background samples.

Figure 3.9 shows a control experiment in the striatum (n=3 rats), where aCSF was perfused through the probe for four hours following probe implantation, and aCSF continued to be perfused while collecting six 10 minute background samples followed by two hours of collections in five minute increments. There are slight increases in aspartate during the third hour of collecting samples, which would correspond to the second hour of perfusing 3-MPA, however this increase is due mainly to one rat. The changes in amino acids are expected to occur during the fifty minutes of dosing, and during this time period in the control experiment there are no large changes in the amino acids. In addition, while there are small changes, the changes that are expected to be seen in test animals will be much larger than anything observed in the control rats.

Figure 3.10 shows the changes in amino acids during perfusion of 10mM 3-MPA through the microdialysis probe. There was a 15-fold increase in glutamate following perfusion of 10mM 3-MPA.

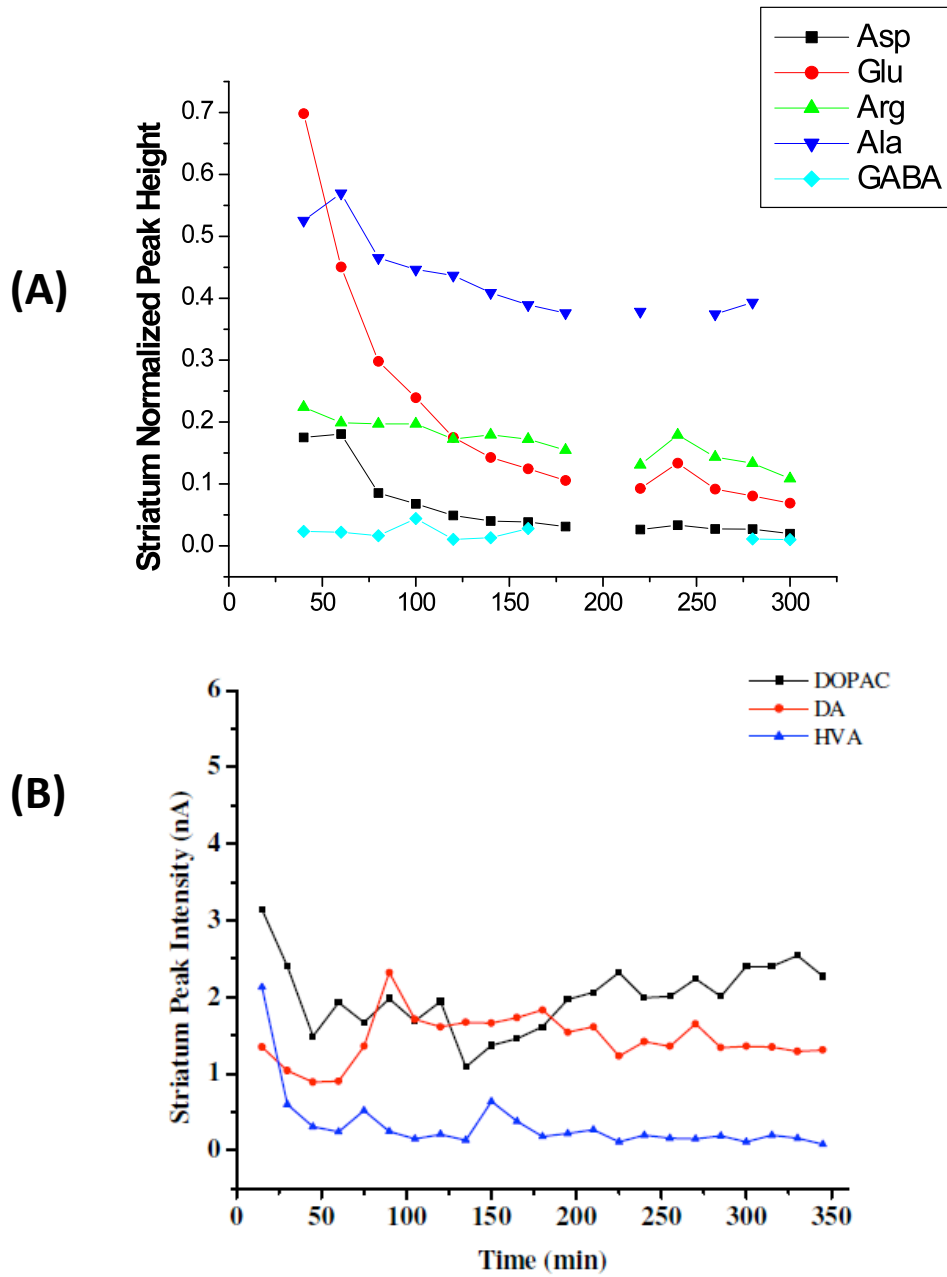


**Figure 3.8** (A) striatum amino acids return to basal and (B) striatum catecholamines return to basal following probe implantation [1].

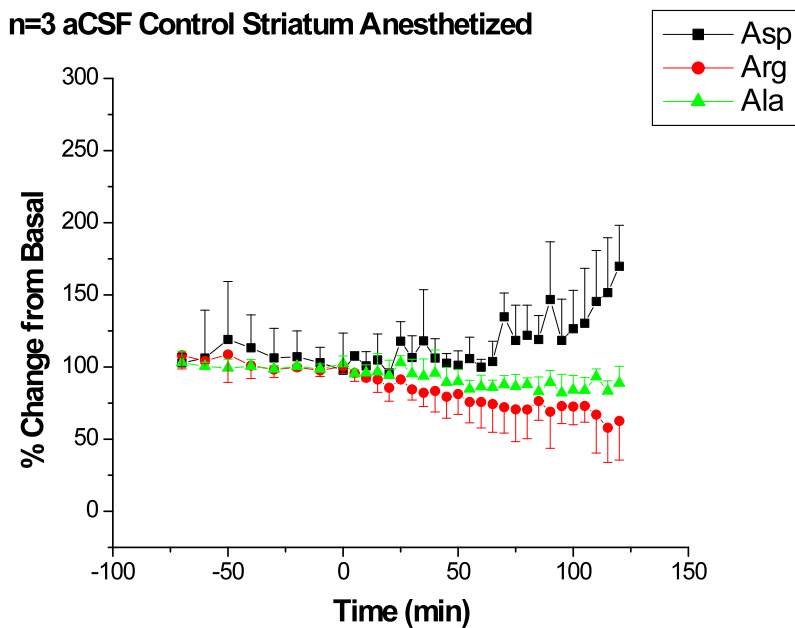
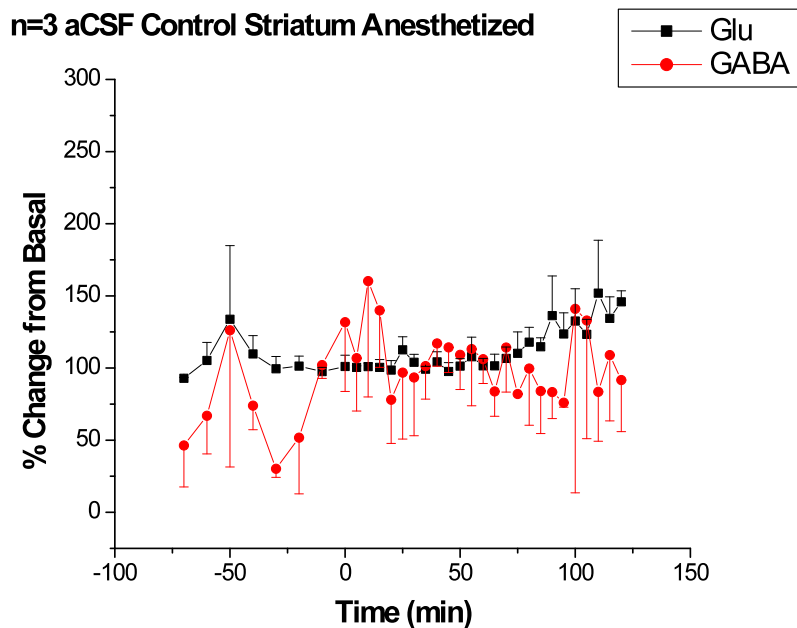


Figure 3.9 aCSF control assessments in the striatum of anesthetized rats (n=3).

The changes in glutamate were significant from basal at both  $p < 0.05$  and  $p < 0.01$ . There was also a 5-fold increase in GABA following 3-MPA perfusion. This increase in GABA was unexpected considering the mechanism of action of 3-MPA on GAD; 3-MPA is an inhibitor of the GAD enzyme. Some of the GABA data points were significant from basal at  $p < 0.05$ . Unlike glutamate, GABA levels remain elevated, after the perfusion of 3-MPA was terminated. Aspartate, an excitatory amino acid, similar to glutamate, increased 10-fold. Most aspartate data points are significant from basal at  $p < 0.01$ . Arginine and alanine are neither excitatory or inhibitory amino acids. As would be expected there are no significant changes in either arginine or alanine.

#### *3.2.2.2 Striatum Amino Acids in Awake Rats*

Figure 3.11 shows the changes in amino acids in the striatum of awake rats. There was a 250-fold increase in glutamate accompanied by a 50-fold increase in GABA. There was also a 20-fold increase in aspartate. Alanine remained around basal levels. Due to the large changes, the arginine peak could not be integrated as there were large peaks co-eluting. Glutamate, GABA, and aspartate were significant from basal at  $p < 0.05$  and  $p < 0.01$ .



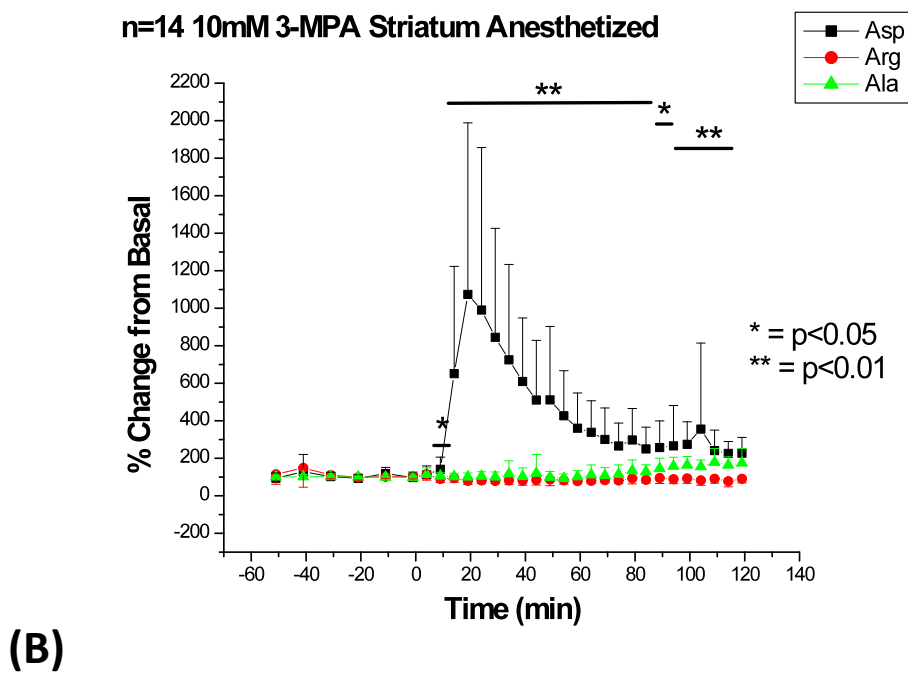
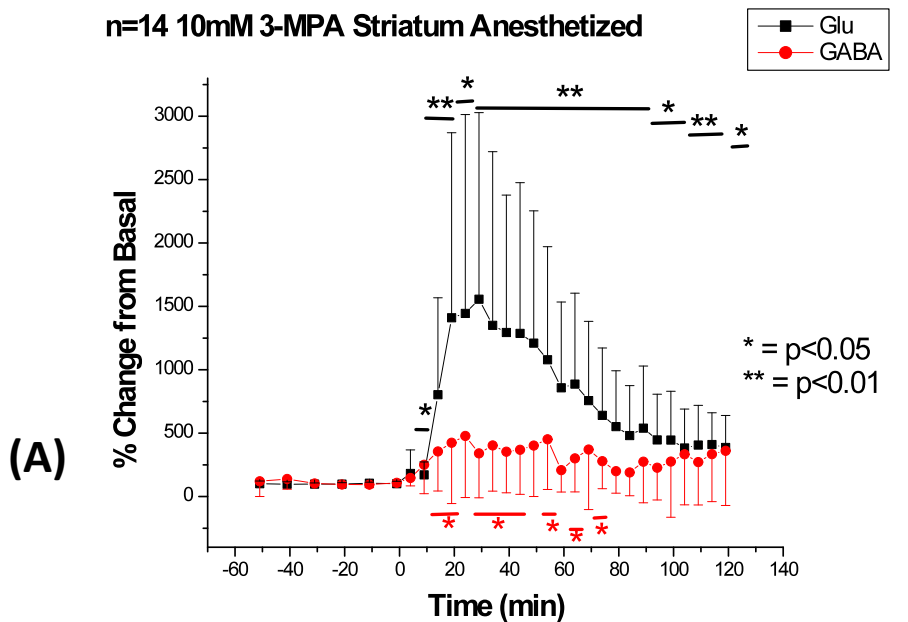
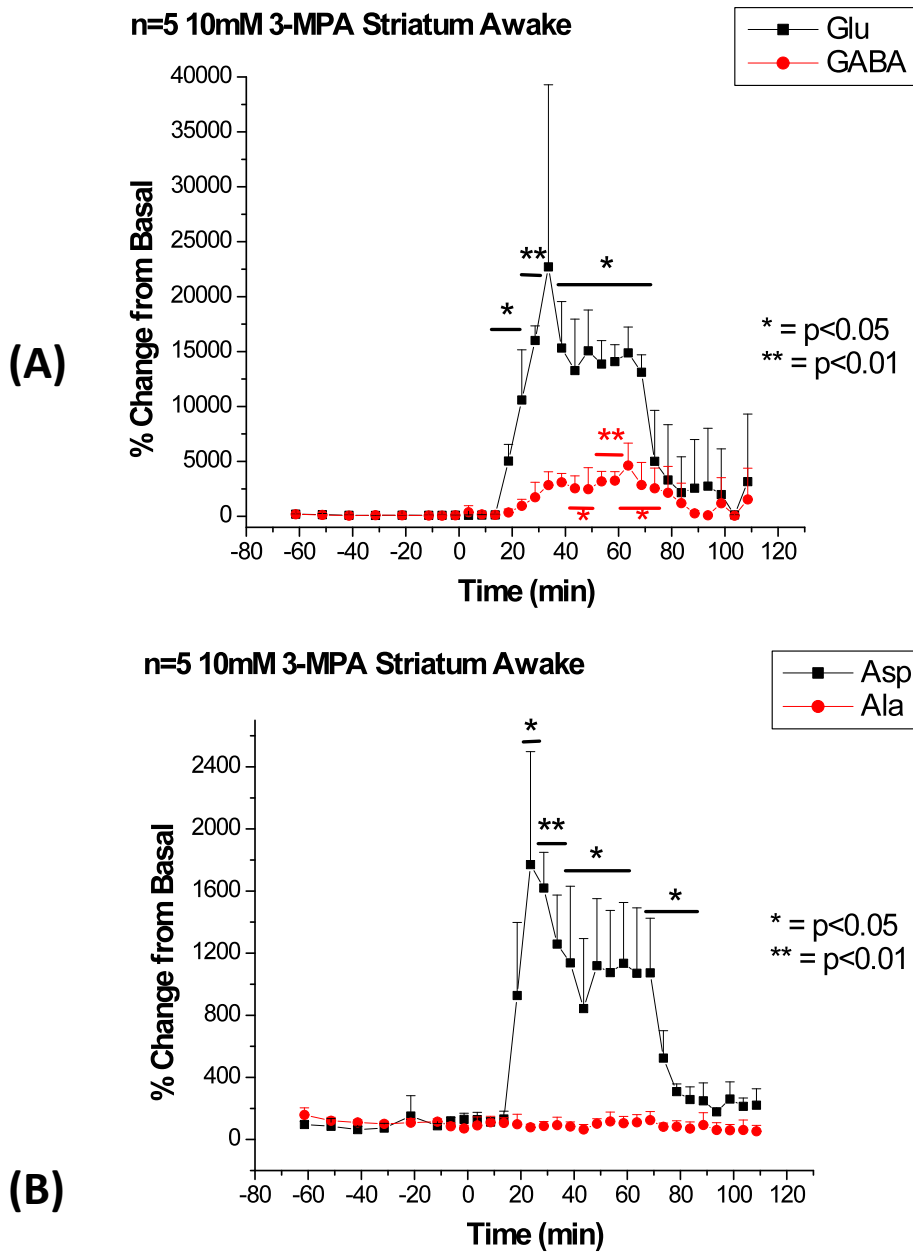


Figure 3.10 10mM 3-MPA perfusion in the striatum of anesthetized rats. (A) Changes in Glu and GABA and (B) changes in aspartate, arginine, and alanine (n=14 rats). 10mM 3-MPA was perfused beginning at t = 0 minutes and the perfusion was stopped at t = 50 minutes.



**Figure 3.11** 10mM 3-MPA perfusion in the striatum of awake rats. (A) Changes in Glu and GABA and (B) changes in aspartate, arginine, and alanine (n=14 rats). 10mM 3-MPA was perfused beginning at t = 0 minutes and the perfusion was stopped at t = 50 minutes.

### 3.2.2.3 Striatum amino acid projections into the hippocampus

As predicted, there were no significant changes in the amino acids in the hippocampus while dosing in the striatum. Figure 3.12 shows changes in the hippocampus while dosing in the striatum. While GABA does increase roughly 2-fold, these changes were variable from rat to rat and the increases are mostly due to only two of the five rats studied. In the other three rats, GABA decreased slightly. The large error bars seen in several of the aspartate data points were due to one rat. Alanine was very stable, ranging from 94-108% of baseline over the course of the experiment.

### 3.2.2.4 Striatum amino acid projections into the *locus coeruleus*

Figure 3.13 shows the changes in amino acids in the *locus coeruleus* while dosing in the striatum. Glutamate remained around basal levels with the exception of roughly 3 data points corresponding to the 69, 74, and 79 minute samples. This increase was only seen in one rat and was seen in aspartate and alanine as well. GABA actually decreased in all 3 rats to under half of basal. This decrease was not expected; as was stated before, there are few projections into the *locus coeruleus* and the striatum is not one of them. There have been a few studies indicating that norepinephrine has a role in decreasing the synthesis of GABA [41]. Studies looking into the interaction of GABAergic and noradrenergic receptors suggest there is a link between the two [42-45], where GABA<sub>A</sub> receptor agonists act to increase the release of norepinephrine and GABA<sub>B</sub> receptor agonists decrease the release of norepinephrine [44, 46]. GABA<sub>A</sub> and GABA<sub>B</sub> receptors may interact with both the presynaptic and postsynaptic noradrenergic terminals [47].

Other studies have been shown an inverse relationship between GABA and norepinephrine. Increases in GABA have been shown to decrease norepinephrine release, while decreases in GABA result in an increase in norepinephrine [48, 49]. This relationship between GABA and norepinephrine could explain the decrease of GABA in the *locus coeruleus*. Since the *locus coeruleus* is the main synthesis site of norepinephrine in the brain and contains a high number of noradrenergic neurons compared with other types of neurons, the decrease in GABA might be due to this relationship.

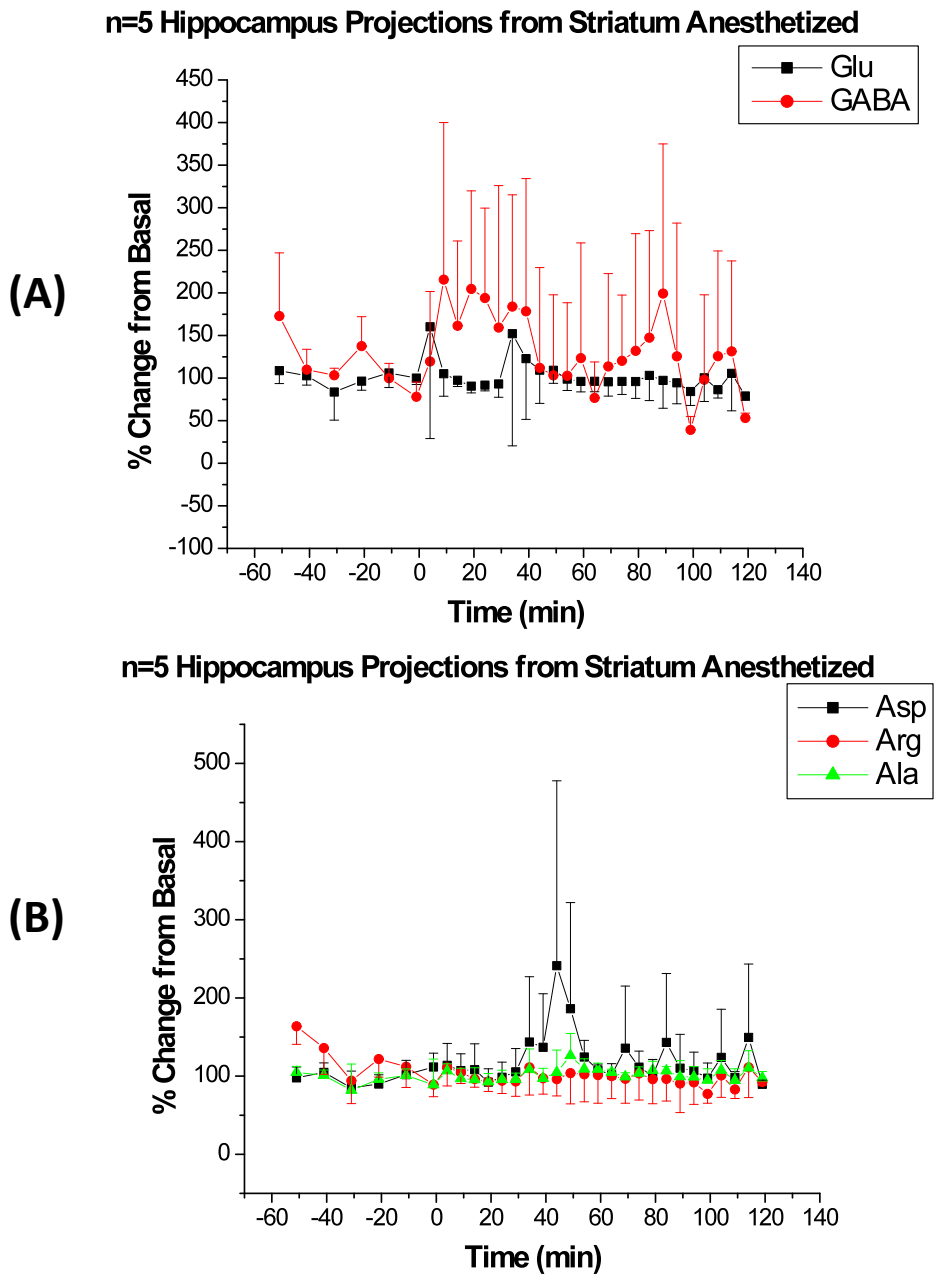


Figure 3.12 Striatum projections into the hippocampus. (A) Glutamate and GABA. (B) Aspartate, arginine, and alanine.

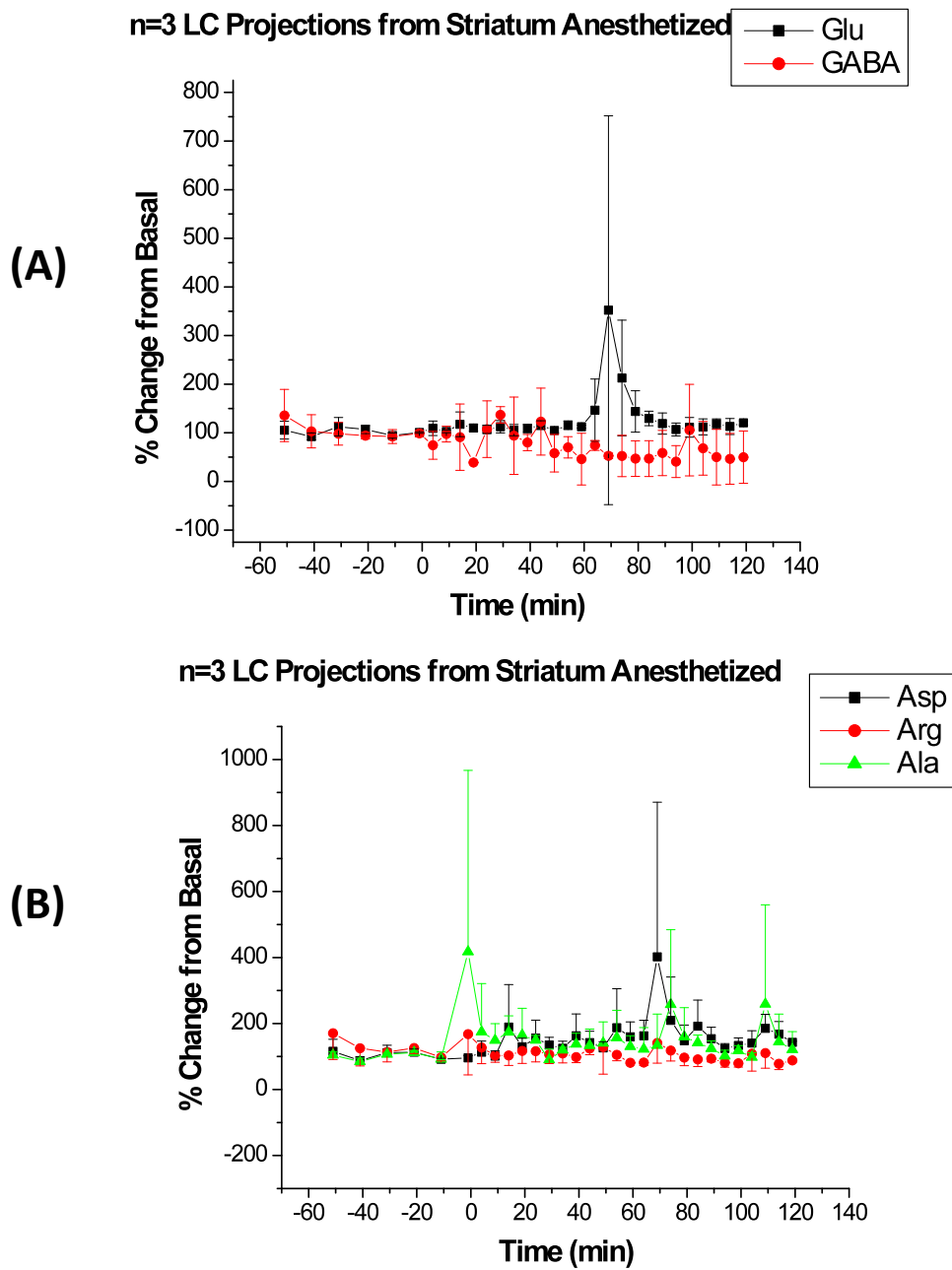


Figure 3.13 Striatum projections into the locus coeruleus. (A) Glutamate and GABA. (B) Aspartate, arginine, and alanine.

### 3.2.3 Hippocampus Amino Acids

#### 3.2.3.1 Hippocampus Amino Acids in Anesthetized Rats

The same experimental procedure was followed in the hippocampus as in the striatum. Figure 3.14 shows the control experiment where aCSF was perfused through the probe for entire length of the experiment. Changes in the amino acids during perfusion of aCSF are small and random; no trends are observed across all 3 rats. As with the striatum, changes in the amino acids in these control experiments are negligible compared to what is seen in the dosed animals.

Figure 3.15 shows the changes in amino acids during dosing of 10mM 3-MPA in the hippocampus. The 7-fold increase in glutamate is smaller than what was seen in the striatum, but glutamate remains elevated during the extent of 3-MPA dosing, while in the striatum glutamate peaks and levels begin to fall before the perfusion of 3-MPA is stopped. Glutamate levels are significant from basal at both  $p < 0.05$  and  $p < 0.01$ . GABA levels are elevated roughly 2-fold, again smaller than the 5-fold changes seen in the striatum. GABA is only significantly different from basal levels ( $p < 0.05$ ) at one time point. Additionally, GABA returns to baseline, and even goes below 100% towards the end of collection, while in the striatum GABA levels remain elevated the length of the experiment. There is a nearly 6-fold increase in aspartate in the hippocampus of anesthetized rats. These changes are significant at both  $p < 0.05$  and  $p < 0.01$ . In general the changes in amino acids levels in the hippocampus are half of what was seen in the striatum. As with the striatum, the changes in glutamate and aspartate were expected.

Again, the increase in GABA was not expected, however it was much smaller in the hippocampus.

### *3.2.3.2 Hippocampus Amino Acids in Awake Rats*

As with the hippocampus in anesthetized rats, as well as the striatum in anesthetized and awake rats, glutamate, GABA, and aspartate all increased. Figure 3.14 shows the data for the hippocampus in awake rats. Glutamate and GABA levels remained elevated for the length of 3-MPA perfusion. However, the error bars are large and glutamate and GABA were only significant at  $p < 0.05$  for a couple of time points. Interestingly, unlike any other brain region, there are large increases in arginine and alanine, which are neither excitatory nor inhibitory amino acids. Arginine increases 15-fold while alanine increases 20-fold. These increases could point towards excitotoxicity for the neurons, where they are dumping all their intracellular components, hence the increase in all amino acids, even those that have no effect on excitation/inhibition in the neuron.

### *3.2.3.3 Hippocampus amino acid projections into the striatum*

Figure 3.17 shows the change in amino acids in the striatum while dosing 3-MPA in the hippocampus. As expected there are no significant changes in the striatum. Glutamate remains around basal, between 84-111% of baseline throughout the experiment. There is an increase in GABA at the end of the experiment, but this is due to one rat. Also, these



increases in GABA do not correspond to the time points where 3-MPA is administered in the hippocampus. Aspartate, arginine, and alanine remain close to basal levels throughout the experiment.

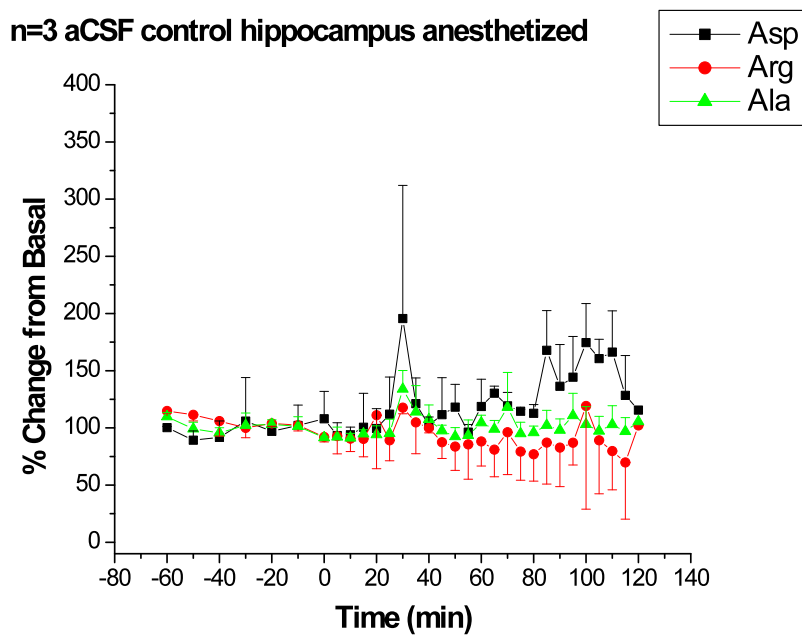
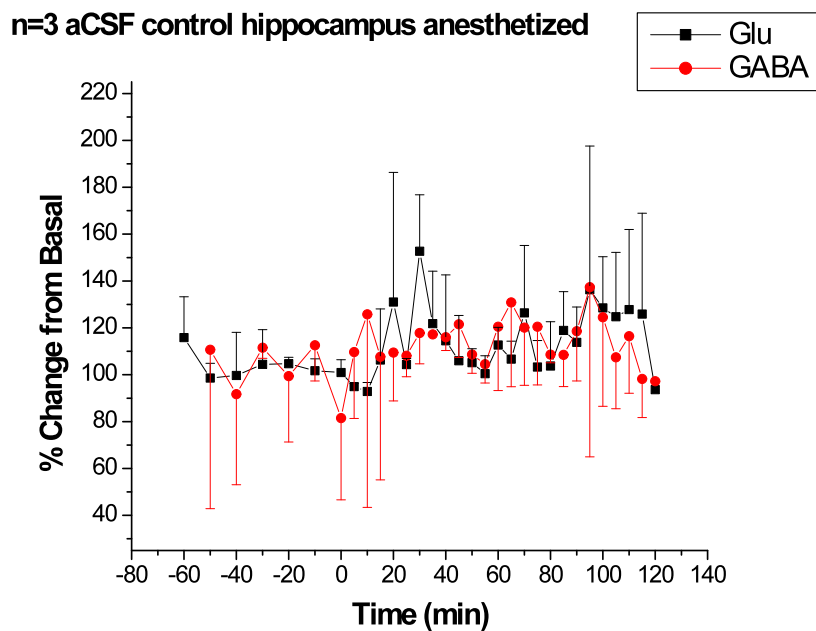


**Figure 3.14** aCSF control experiment in the hippocampus of anesthetized rats (n=3).

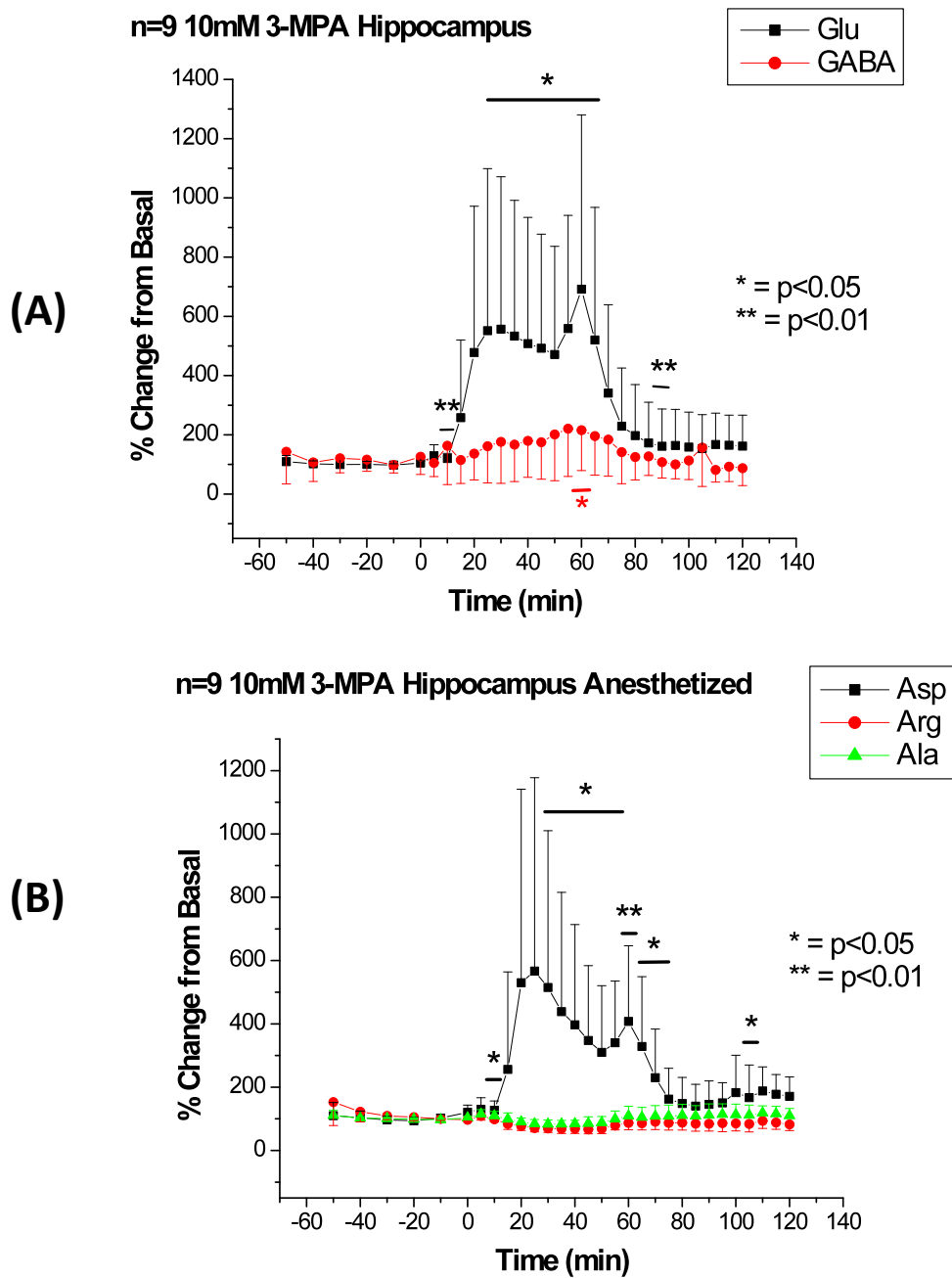


Figure 3.15 10mM 3-MPA perfusion in the hippocampus of anesthetized rats. (A) Changes in Glu and GABA and (B) changes in aspartate, arginine, and alanine (n=9 rats). 10mM 3-MPA was perfused beginning at t = 0 minutes and the perfusion was stopped at t = 50 minutes.

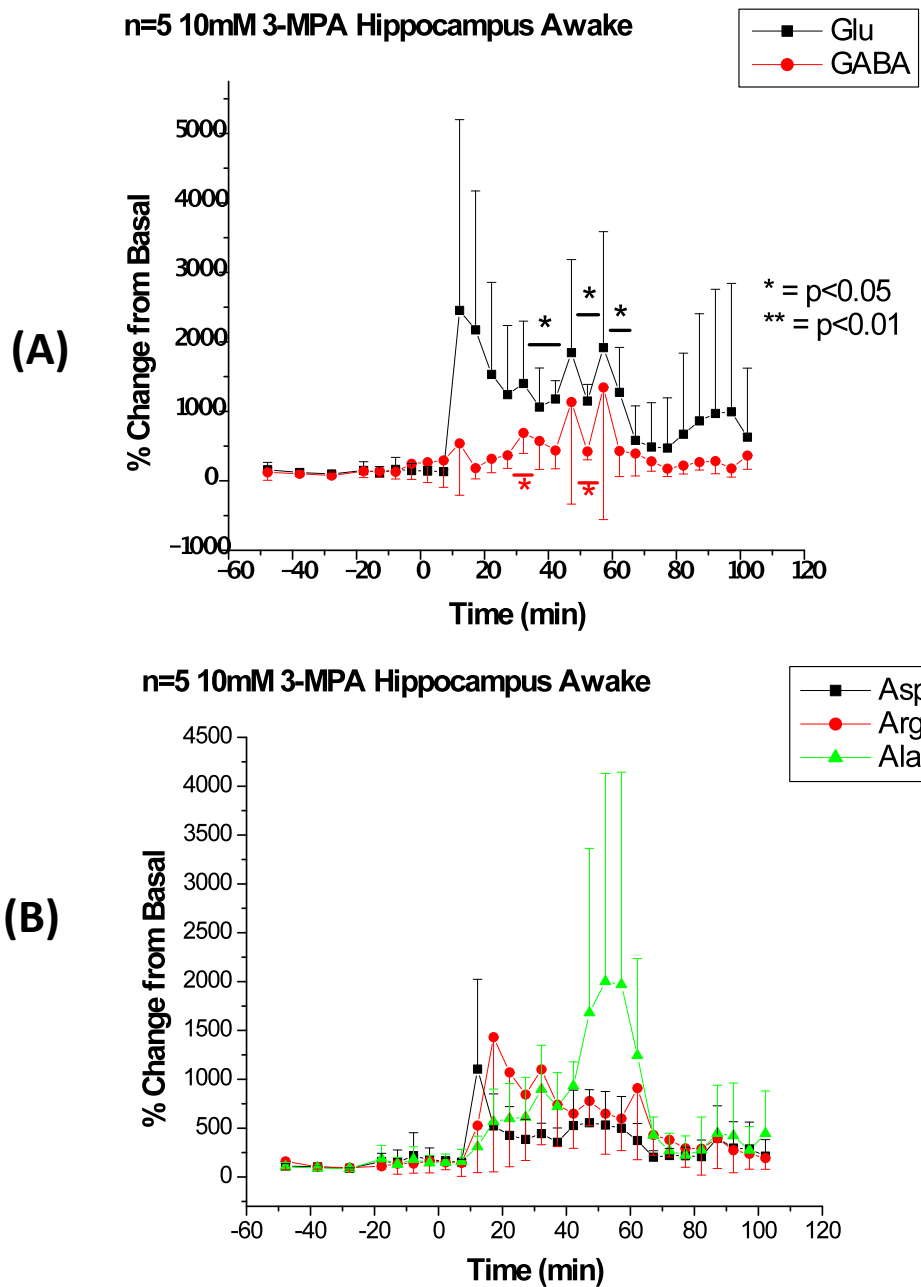


Figure 3.16 10mM 3-MPA perfusion in the hippocampus of awake rats. (A) Changes in Glu and GABA and (B) changes in aspartate, arginine, and alanine (n=5 rats). 10mM 3-MPA was perfused beginning at t = 0 minutes and the perfusion was stopped at t = 50 minutes.

#### 3.2.3.4 Hippocampus amino acid projections into the locus coeruleus

Figure 3.18 shows the changes in amino acids in the *locus coeruleus* while administering 3-MPA in the hippocampus. Glutamate remains around basal levels, as does arginine. Alanine and aspartate increase slightly, however the increase in aspartate is due mostly to one rat, and a spike in aspartate for one time point in another rat. Alanine increases to around 150% of basal. The most interesting finding is the decrease in GABA. This is the same magnitude decrease (down as low as 50% of basal) that was seen in the *locus coeruleus* when dosing 3-MPA in the striatum (See section 4.2.1.2 for discussion). Again, this decrease was not expected, as there have been no pathways discovered from the hippocampus to the *locus coeruleus*.

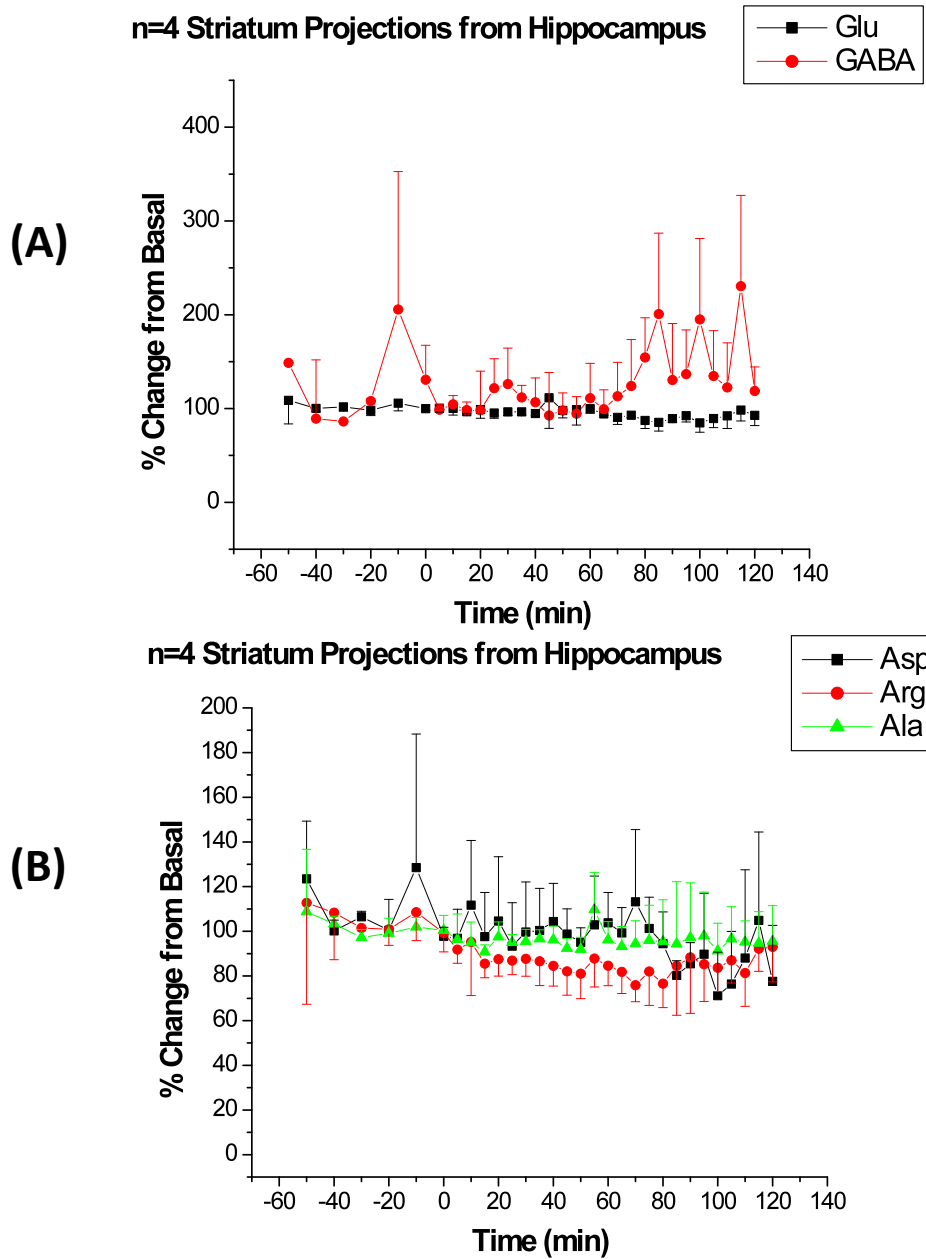
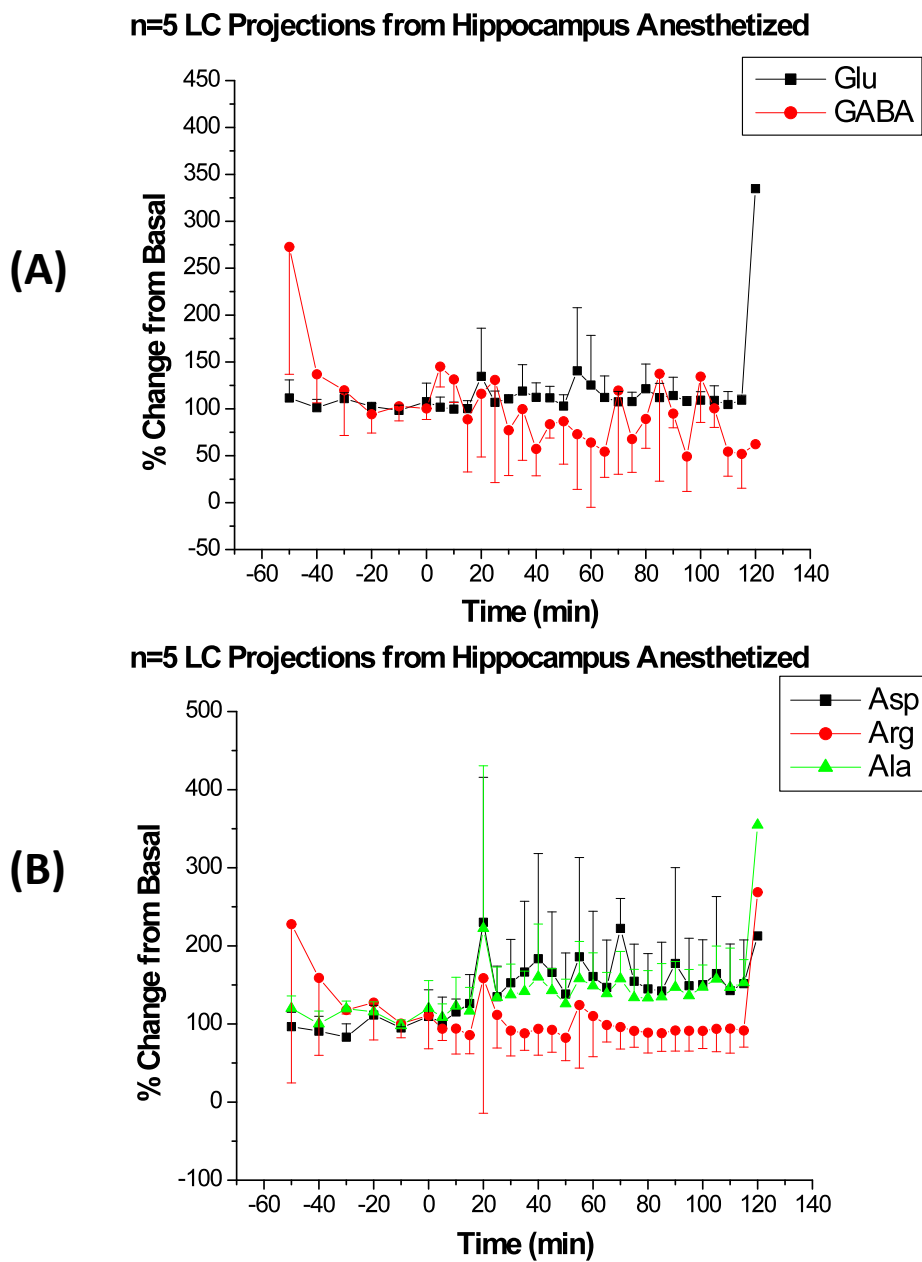


Figure 3.17 Hippocampus projections into the striatum. (A) Glutamate and GABA. (B) Aspartate, arginine, and alanine.



**Figure 3.18** Hippocampus projections into the *locus coeruleus*. (A) Glutamate and GABA. (B) Aspartate, arginine, and alanine.

### 3.2.4 *locus coeruleus* Amino Acids

#### 3.2.4.1 *locus coeruleus* Amino Acids in Anesthetized Rats

Figure 3.19 shows the amino acids in the *locus coeruleus* of anesthetized rats. The results in the LC were surprising. The 4-fold increase in GABA was similar to that which was seen in the striatum and hippocampus. However, the changes in glutamate were not expected, based upon the action of 3-MPA on GAD, but also based upon what was seen in the striatum and hippocampus. Glutamate increased in all 5 rats; however, the extent to which it increased varied widely. In two rats, glutamate increased to 315% and 260% of basal. In the other three rats, increases in glutamate were modest, a less than 1.5-fold increase. In all five rats following perfusion of 3-MPA (from the 85 minute sample on), glutamate decreased to below 100%. Glutamate went as low as 60% of basal by the end of the experiment in one rat. While the average increase of glutamate for all 5 rats reached 171% of basal, these changes were substantially smaller than the 15 and 7-fold increases seen in the striatum and hippocampus. There was a 2-fold increase in aspartate in the LC, but again this was much smaller than the 10 and 6-fold changes seen in the striatum and hippocampus.

On average, the concentrations of glutamate in the *locus coeruleus* are not significantly different from the concentrations in both the striatum and the hippocampus. Studies have found that glutamate concentrations, measured by microdialysis, in the *locus coeruleus* are as low as  $0.90 \pm 0.20$   $\mu\text{M}$ , more than 3-times less than the concentrations in the striatum and hippocampus [50]. It would seem from these reports that data that there is plenty of glutamate for neurons in the LC to release, however the



are under the curve (AUC) for the increase in glutamate in the *locus coeruleus* is so much less than for the striatum and the hippocampus might mean this is not the case. Studies have been done to determine the content of GAD in the striatum, hippocampus, and LC. The content of GAD is relatively the same in the striatum and hippocampus [51]. There is also

significant expression of GAD in the LC; it has been quantified by Majumdar et al. [52, 53].

Therefore, it seems that lack of glutamate or GAD expression in the LC cannot explain the small increase in glutamate seen in the LC upon perfusion of 3-MPA.

#### *3.2.4.2 locus coeruleus amino acid projections into the striatum*

Figure 3.20 shows the changes in the striatum while dosing 3-MPA in the *locus coeruleus*. There are no changes in glutamate, arginine, and alanine. There is an increase in aspartate, however, this increase is mostly due to one rat and it does not follow the time course of 3-MPA administration. As was seen in the *locus coeruleus*, there is a decrease in GABA; however this decrease would not be statistically different from basal levels.

#### *3.2.4.3 locus coeruleus amino acid projections into the hippocampus*

Figure 3.21 shows the changes in amino acids in the hippocampus while dosing 3-MPA in the *locus coeruleus*. Glutamate remains at basal levels throughout the

experiment. Arginine and alanine remain around basal levels as well. Aspartate increases, though the increase in aspartate during the second hour (60-120 minutes) is due to an increase in one rat. Also, the increase in aspartate shortly after starting to administer 3-MPA is due to an increase in aspartate in one rat.

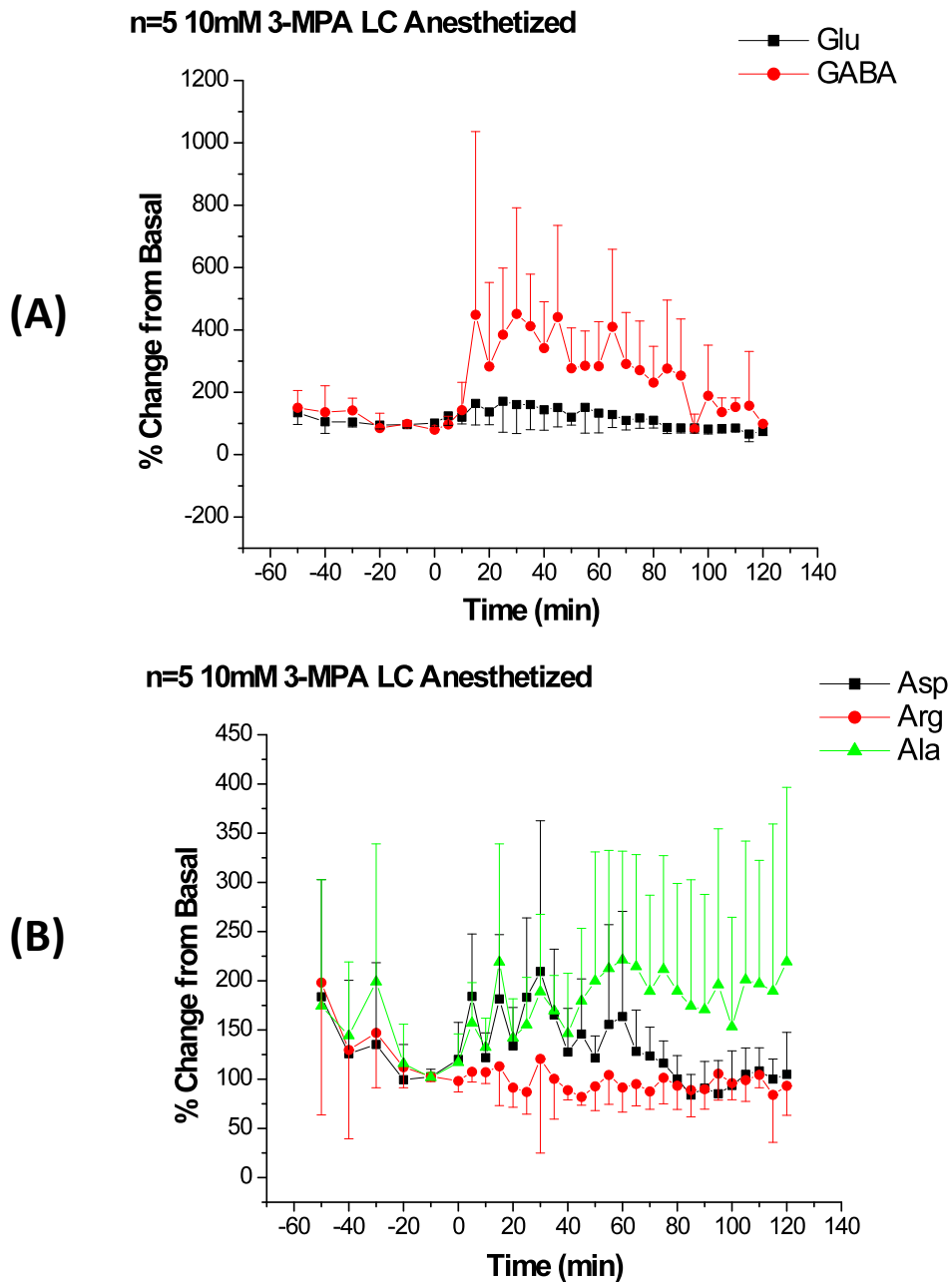


Figure 3.19 10mM 3-MPA perfusion in the locus coeruleus of anesthetized rats. (A) Changes in Glu and GABA and (B) changes in aspartate, arginine, and alanine (n=14 rats). 10mM 3-MPA was perfused beginning at t = 0 minutes and the perfusion was stopped at t = 50 minutes.

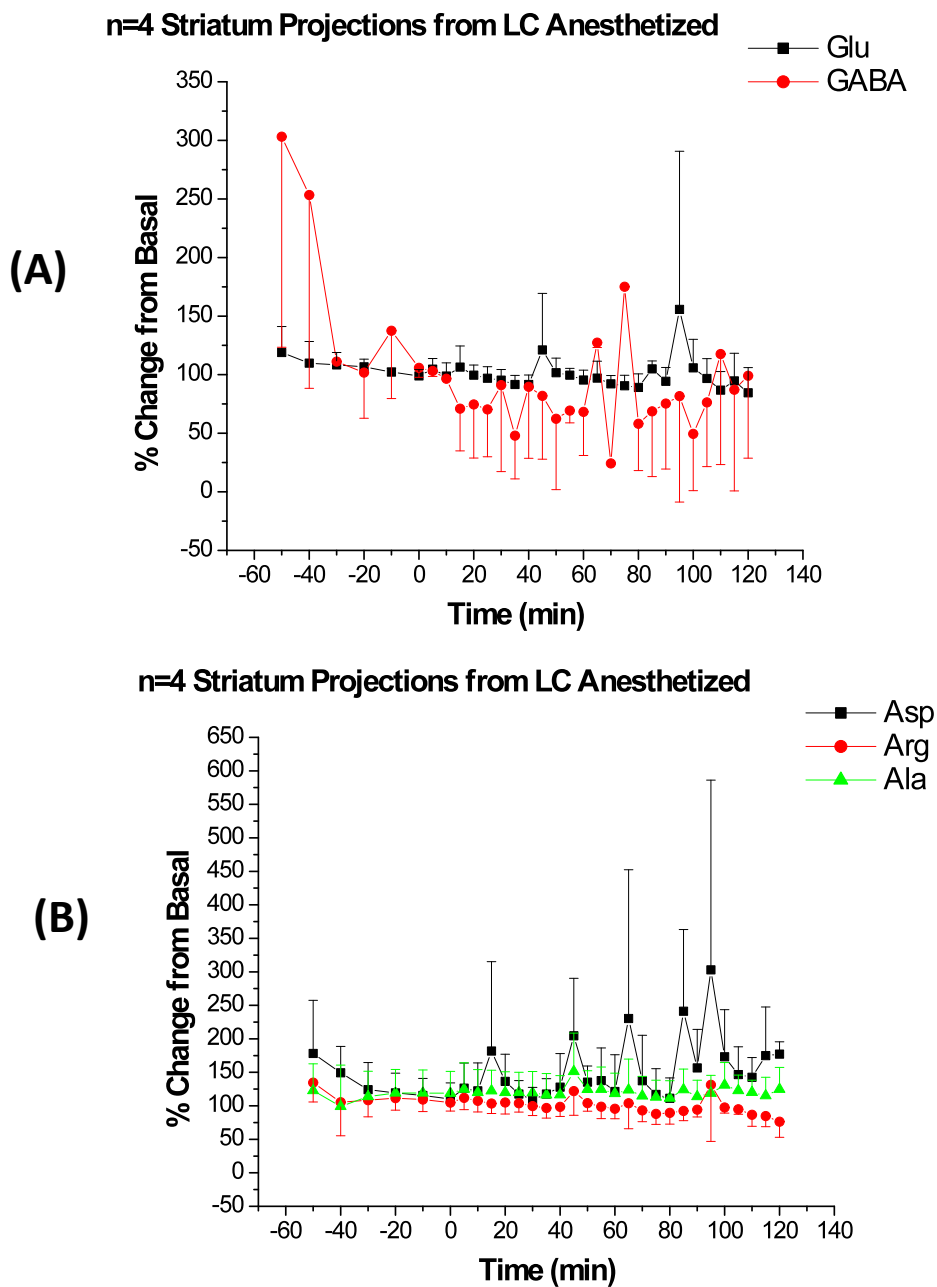


Figure 3.20 locus coeruleus projections into the striatum. (A) Glutamate and GABA. (B) Aspartate, arginine, and alanine.

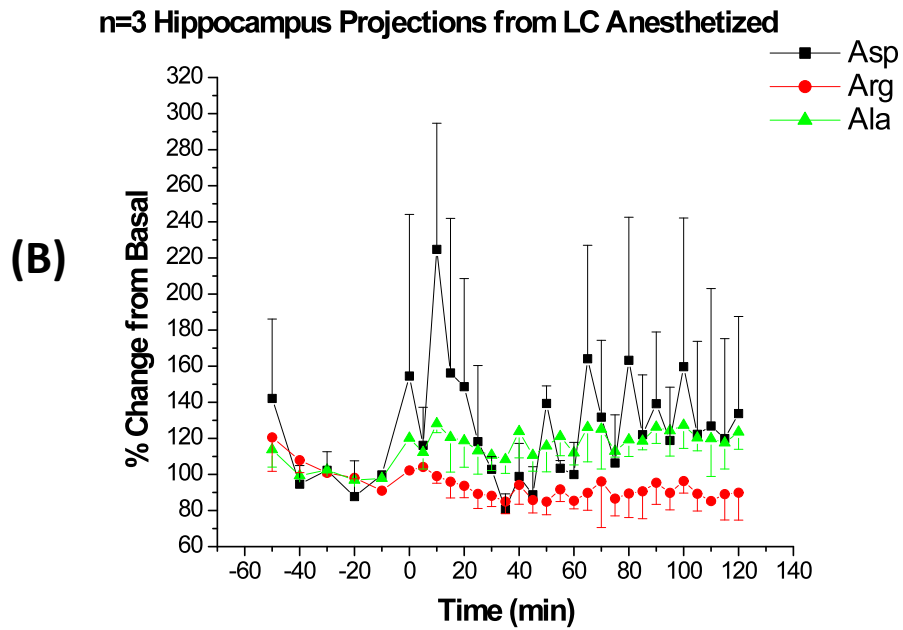
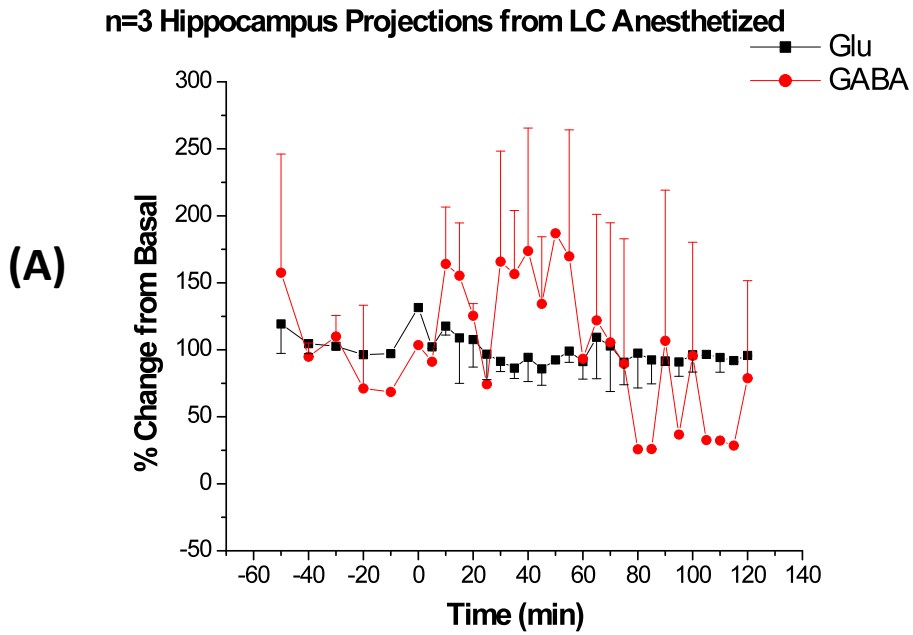


Figure 3.21 locus coeruleus projections into the hippocampus. (A) Glutamate and GABA. (B) Aspartate, arginine, and alanine.

### 3.2.5 Amino Acids in Anesthetized Versus Awake Rats

The increases in glutamate, GABA, and aspartate were much larger in awake compared with anesthetized rats. Differences in amino acids release in awake versus anesthetized rats is most likely due to the action of ketamine, the anesthetic used in anesthetized experiments. Glutamate receptors can be categorized into two groups, ionotropic and metabotropic receptors. Ionotropic receptors directly gate channels and allow the passage of ions and metabotropic receptors are gated by secondary messengers. There are three major types of ionotropic receptors: NMDA (*N*-methyl-D-aspartate), AMPA ( $\alpha$ -amino-3-hydroxy-5-methylisoxazole-4-propionic acid), and kainate (kainic acid), all named after the ligands which activate them [4, 22, 54]. AMPA and kainite receptors are often referred to as non-NMDA receptors. Glutamate binds to NMDA receptors allowing the passage of  $\text{Na}^+$ ,  $\text{K}^+$ , and  $\text{Ca}^{+2}$  ions. This leads to depolarization and an excitatory effect. Blockage of NMDA receptor glutamate binding has been shown to result in decreased excitatory transmission [55, 56]. Ketamine, an NMDA antagonist, is the anesthetic used in the anesthetized experiments. It has been characterized as an uncompetitive NMDA channel blocker [57]. Ketamine has also been shown to inhibit voltage-sensitive  $\text{Ca}^{+2}$  channels, which also suppresses excitatory transmission [58, 59]. Ketamine has been shown in many studies to decrease glutamate release [60, 61]. Kitayama et al. showed that in the presence of excess  $\text{K}^+$  (40mM) to evoke release of glutamate, ketamine blocked this release in a dose-dependent manner.

In rat experiments with ketamine as the anesthetic, this could explain the decreased release of glutamate. It should be noted that in both the anesthetized and awake experiments, the basal levels of glutamate are on average the same. This would

point to the fact that basal levels of glutamate have not been altered by the use of ketamine, but rather it is any subsequent release that is inhibited. From these data it can be concluded that, if at all possible, experiments should be performed in awake rats, as the use of ketamine in anesthetized rats masks the effect of 3-MPA.

### *3.2.6 Inhibitory surround*

The data show an increase in excitation, via the increase in glutamate, as can be seen in Figure 3.20. However, looking at the amino acids individually there is also an increase in inhibition from release of GABA. The idea of an inhibitory surround, which surrounds the seizure focus, has received widespread acceptance, while there may be an increase in excitation in the seizure focus, there is a corresponding inhibition in the inhibitory surround [62-65]. Figure 3.21 illustrates the seizure focus and the inhibitory surround [22]. Inhibition in the inhibitory surround is thought to be a mechanism in stopping the spread of seizures from one brain region to surrounding tissue, as studies have shown that blockage of inhibition in the inhibitory surround is needed for the spread of epileptiform activity [64, 66]. Newer studies seem to support the concept that long range inhibition appears to limit excitability of neurons outside the focus [67, 68]. When excitation begins to break down the inhibition from the inhibitory surround, seizures can propagate from the focus to surrounding tissue [22, 69].

The idea that there could be inhibition within epileptogenic areas is not new [70-73] and it occurs due to neuronal organization around a region of hyperexcitability [74-76]. Studies in the cat cortex have shown that stimulation at a single point can lead to

inhibition throughout all cell layers up to 10mm away [77, 78]. While there appears to be recurrent excitation in the hippocampus [21, 79, 80], and presumably in other regions, recurrent inhibition is widespread in the hippocampus and appears to override excitation [81-84].

The best explanation for the increases in GABA seen upon perfusion of 3-MPA has to do with the presence of the inhibitory surround. When administering drugs through the microdialysis probe, the area surrounding the probe that is affected is very small. If the excitatory effect of 3-MPA on the neurons surrounding the probe is large, but the number of total neurons being affected is considerably small, the surrounding neurons might overcompensate by releasing excess GABA to counteract the large increases in glutamate seen in the seizure focus. While there have been studies looking at the inhibitory surround, most of these have involved excitatory postsynaptic potentials (EPSPs) and inhibitory postsynaptic potentials (IPSPs) [65, 85, 86]. While some work has been done investigating metabolic changes in the inhibitory surround [62], few studies have been done looking at inhibitory neurotransmission in the surround. The diffusion coefficient of GABA has been reported to be  $0.3 \times 10^{-6} \text{cm}^2/\text{s}$  [87]. Based upon this diffusion coefficient it is plausible that GABA released in the inhibitory surround to diffuse to the probe and account for the increase in GABA seen in these data. GABA begins to increase in the 10 minute sample during local administration of 3-MPA in the striatum. Based upon the above diffusion coefficient for GABA, it would diffuse 0.2mm during that time. As stated above, point excitation can lead to inhibition 10mm away [77, 78]. An interesting study would be to place probes at different distances from the dosing probe and measure changes in GABA.



n=14 Glu/GABA Ratio Striatum Anesthetized

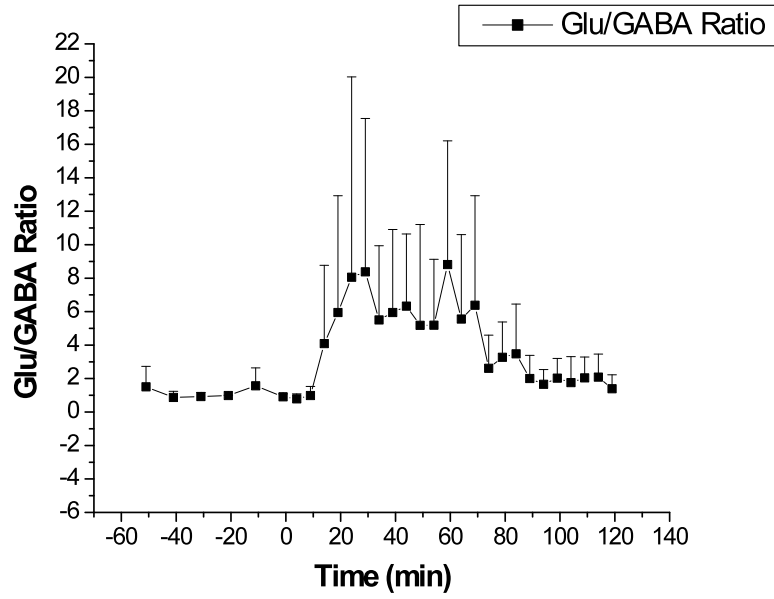
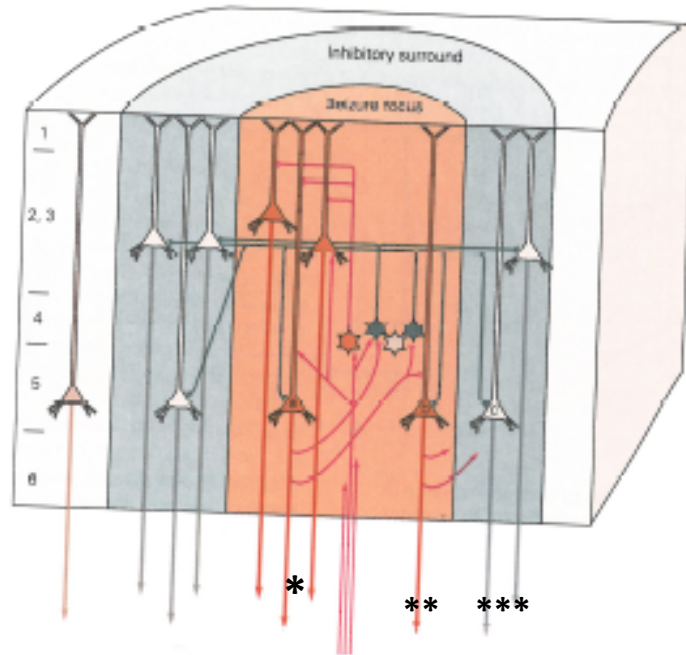


Figure 3.22 Glutamate/GABA ratio in the striatum of anesthetized rats (n=14 rats).



**Figure 3.23** Illustration of the inhibitory surround. Neuron labeled (\*) in the seizure focus has electrical discharges which can also activate neuron other neurons (\*\*). The first neuron in the seizure focus (\*) can activate inhibitory GABA-ergic cells (\*\*\*) in the inhibitory surround which through feedback mechanisms, can

### 3.2.7 *Source of extracellular glutamate and GABA*

There has been much debate regarding the source of glutamate and GABA collected with microdialysis. There have been conflicting results regarding whether glutamate and GABA collected with microdialysis is due to neuronal release of the neurotransmitters or from glial cells. Tetrodotoxin (TTX) is a compound often used to differentiate between neuronal or glial release. TTX blocks voltage gated  $\text{Na}^+$  channels, thus preventing neuronal release of neurotransmitters. While some studies using microdialysis have shown a decrease in GABA upon probe perfusion of TTX [88, 89], others have shown no net change [90-92], begging the question as to whether the GABA seen is from glial origin. Glutamate and GABA reside in two separate transmitter and metabolic pools. GABA is synthesized from glutamate via GAD in the neurons. Glutamate and GABA can be released by the neurons and then are taken back up by glial cells [93, 94]. Compartmental analysis of glutamate has shown that glial cells contain 15% of glutamate, while 50% resides in the neuronal metabolic pools and only 20-30% in the neurons ready for release [95]. However, it is hard to pinpoint whether the measured glutamate and GABA is due directly to neuronal release, slow reuptake, or what compartment it is coming from. There are also many nonneurotransmitter uses for glutamate, as it is used as a precursor for protein and peptide synthesis, in fatty-acid synthesis, to regulate ammonia levels, and in the metabolism of carbohydrates [96].

### *3.2.8 GAD isoform compartmentalization*

Prior research has shown that GAD is upregulated following seizures, likely a response to an increase in the amount of synthesized GABA [97, 98]. An increase in GAD expression would result in more turnover of glutamate to GABA, even in the presence of 3-MPA. The function of GABA is also quite complicated. GABA exists in two separate pools intracellularly, as metabolic GABA in the cytosol and as neurotransmitter GABA in the synaptic vesicles. This picture is complicated further because there are two different isoforms of GAD, GAD<sub>65</sub> and GAD<sub>67</sub> [99]. GAD<sub>65</sub> comprises around 70% of total GAD in the rat cortex and is predominantly found in the neuron terminals where it is used for vesicular GABA synthesis [100]. The less abundant GAD<sub>67</sub> isoform is involved in metabolic GABA synthesis from glutamate [101]. Therefore, the effect of 3-MPA dosing on GABA might depend on which cellular GABA component 3-MPA works on. Finally, GAD<sub>65</sub> is mostly in its inactive form under anesthesia in this 3-MPA model [102]. Since GAD<sub>65</sub> is the isoform mostly found in neuronal terminals, this again raises the question as to whether the increases in GABA are due to the metabolic compartment.

### *3.2.9 Striatum catecholamine neurotransmitters*

#### *3.2.9.1 Striatum catecholamines in anesthetized rats*

There is an increase in both dopamine and norepinephrine in the striatum during perfusion of 3-MPA. The relationship between dopamine and norepinephrine are well known, as norepinephrine is converted to dopamine via the enzyme dopamine  $\beta$ -

hydroxylase. It is not surprising therefore, to see an increase in both dopamine and norepinephrine. Figure 3.22 shows these data. However, during systemic dosing of 3-MPA there has been an increase in dopamine, but a decrease in norepinephrine [1, 103], while other microdialysis experiments have shown an increase release of norepinephrine [104-106].

Norepinephrine has been shown to play an important role in seizures. *Fos* induction, a gene used as a marker for neuronal activation, has been shown to be upregulated in the *locus coeruleus* following seizures [107-111]. Treatment with reserpine, a monoamine depleting agent, lowered seizure threshold to several convulsants [112-115]. Selective depletion of norepinephrine and dopamine show that animals with depleted dopaminergic and noradrenergic neurons are more susceptible to seizures [30, 112, 116, 117].

The role of dopamine in seizures has been less defined. Unlike norepinephrine, there is not an increase in *fos* expression in dopaminergic neurons following seizures [111, 118, 119]. Some studies have shown modification to dopaminergic neurons following seizures, such as an increase in firing [120], an increase in tyrosine hydroxylase (TH, responsible for the synthesis of L-DOPA, the dopamine precursor) and dopamine active transporter (DAT) [111], as well as an increase in D<sub>2</sub> dopamine receptors and D<sub>2</sub> receptor mRNA [121-123].

There has been a substantial amount of research investigating the connection between glutamate and dopamine. The striatum receives glutamatergic projections from the cortex via the corticostriatal pathway and receives dopaminergic inputs from the

substantia nigra pars compacta via the nigro-striatal pathway [124]. Figure 3.23 illustrates the neuronal circuitry and projections in the basal ganglia involving glutamate and dopamine [1, 125]. While most studies have demonstrated this relationship between dopamine and glutamate modulation [126-132], this is not universally accepted [133, 134]. One crucial piece of evidence for glutamate modulating dopamine was the finding that dopamine synapses contain both AMPA and NMDA receptors, both binding sites for glutamate [135]. While the biochemical activity of 3-MPA is on the glutamate-GABA system, the increase in glutamate has a role in dopamine regulation. Therefore, the increase in dopamine upon 3-MPA perfusion is not surprising.

There is a small decrease in the dopamine metabolites, DOPAC and HVA, which supports findings elsewhere, where a decrease in these metabolites was seen following excitation of glutamate with NMDA [136].

#### *3.2.9.2 Striatum catecholamine projections into the hippocampus*

All the catecholamines remain near basal levels in the hippocampus during 3-MPA administration in the striatum. An increase in norepinephrine and HVA around the 20 minute mark is due to a spike in one rat. Figure 3.24 show these changes

#### *3.2.9.3 Striatum catecholamine projections into the locus coeruleus*

As in the hippocampus, there are no significant changes in the catecholamine neurotransmitters in the *locus coeruleus* while dosing in the hippocampus. The one

increase seen in DOPAC is due to one high point in one of the rats. Figure 3.25 shows these changes

### *3.2.10 Hippocampus catecholamines neurotransmitters*

#### *3.2.10.1 Hippocampus catecholamine in anesthetized rats*

Like the striatum, there was an increase in norepinephrine and dopamine in the hippocampus (Figure 3.26). The metabolites DOPAC, 5-HIAA, and HVA remain around basal levels. During systemic dosing of 3-MPA there was no increase in NE, an increase in DA, and also an increase in the metabolites [1].

#### *3.2.10.2 Hippocampus catecholamine projections into the striatum*

Figure 3.27 shows the changes in catecholamine neurotransmitters in the striatum while perfusing 3-MPA in the hippocampus. The catecholamines remain around basal levels and there are no trends seen in any of the 3 rats.

#### *3.2.10.3 Hippocampus catecholamine projections into the locus coeruleus*

Figure 3.28 illustrates the changes in the catecholamines in the *locus coeruleus* while dosing in the hippocampus. There are several peaks in norepinephrine that are seen in the *locus coeruleus*, however these are due again to larger increases in one rat and there were no trends in the data that suggest these changes are due to the 3-MPA administration.

n=4 10mM 3-MPA Striatum Anesthetized

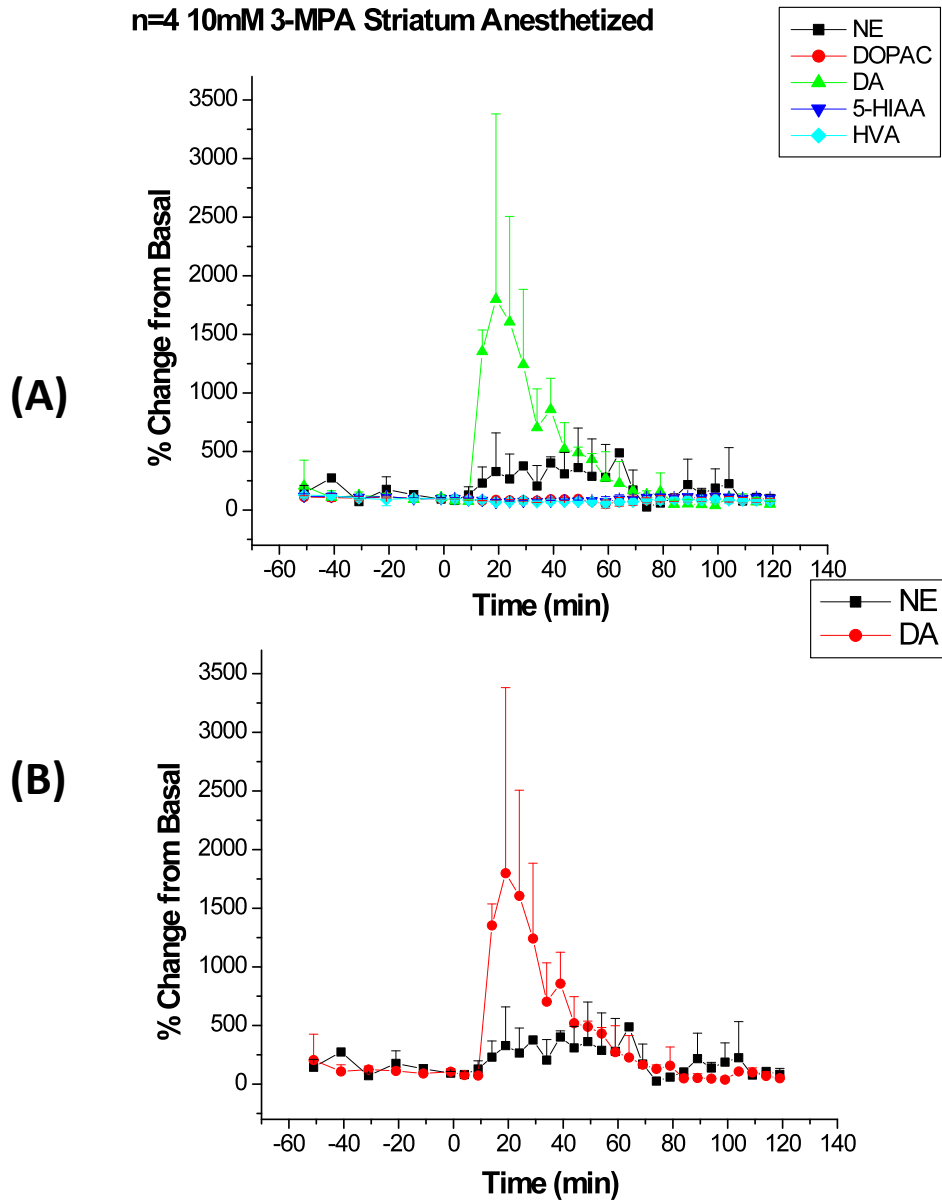
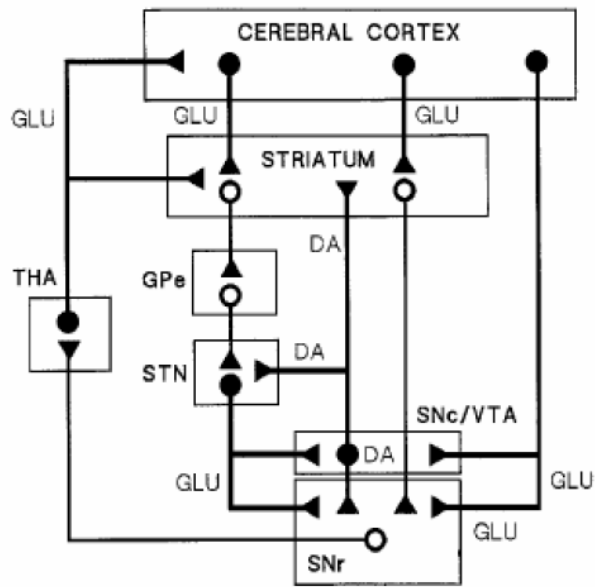


Figure 3.24 10mM 3-MPA perfusion in the striatum of anesthetized rats. (A) Catecholamines NE, DA, and metabolites 5-HIAA, DOPAC, and HVA. (B) NE and DA (n=4 rats).





**Figure 3.25** Glutamate and dopamine projections within the basal ganglia. GPe (pars externa of globus pallidus); SNc (pars compacta substantia nigra); SNr (pars reticula substantia nigra); STN (subthalamic nucleus); THA (thalamus); VTA (ventral tegmental area).

n=3 Hippocampus Projections from Striatum Anesthetized

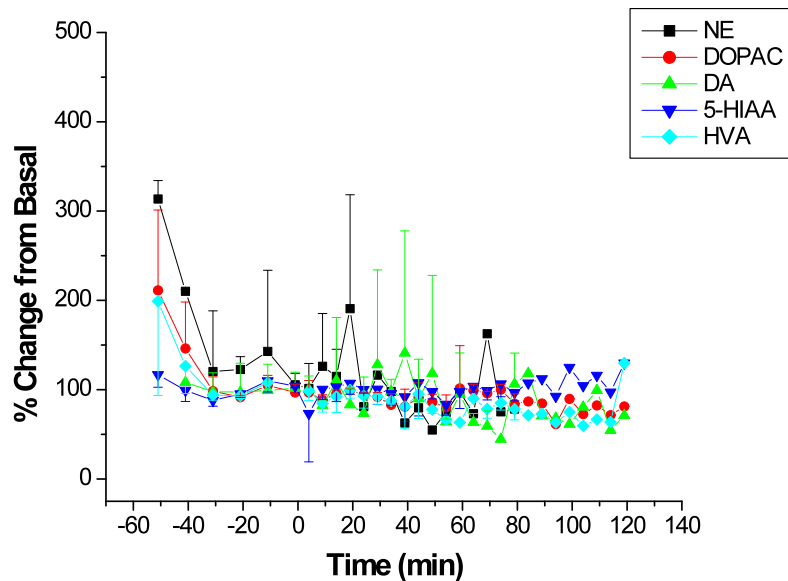


Figure 3.26 Striatum catecholamine neurotransmitter projections into the hippocampus.

n=3 locus coeruleus projections from the striatum

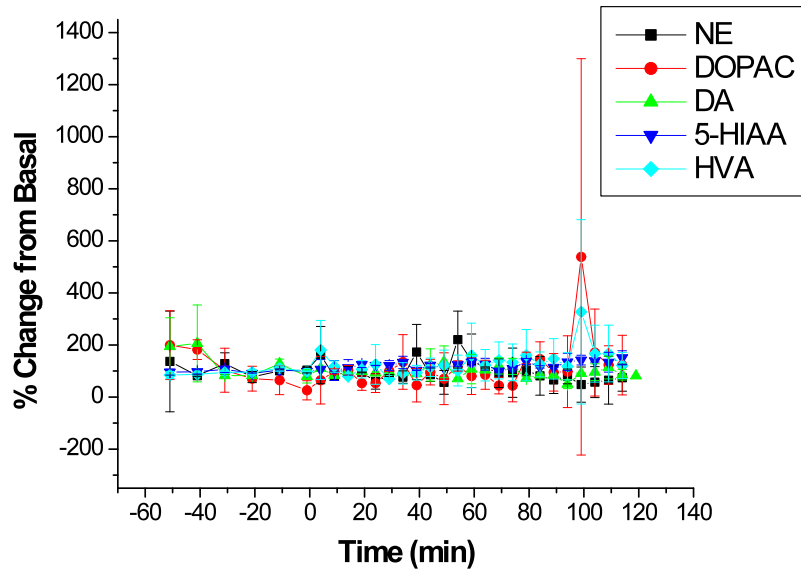


Figure 3.27 Striatum catecholamine neurotransmitter projections into the locus coeruleus.

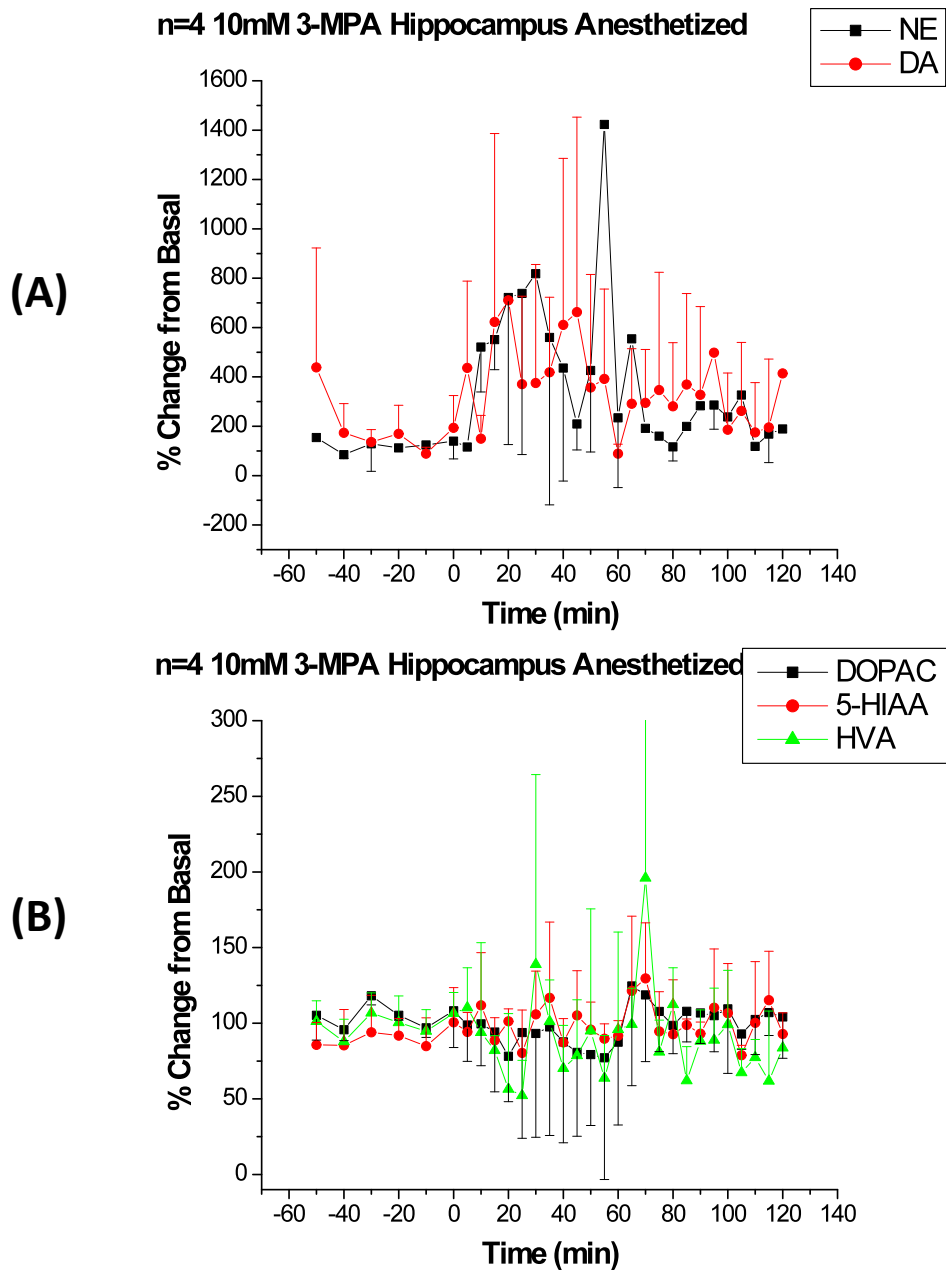


Figure 3.28 10mM 3-MPA perfusion in the hippocampus of anesthetized rats. (A) Catecholamines NE and DA. (B) Metabolites 5-HIAA, DOPAC, and HVA (n=4 rats).

n=3 Striatum NTs Projections from Hippocampus

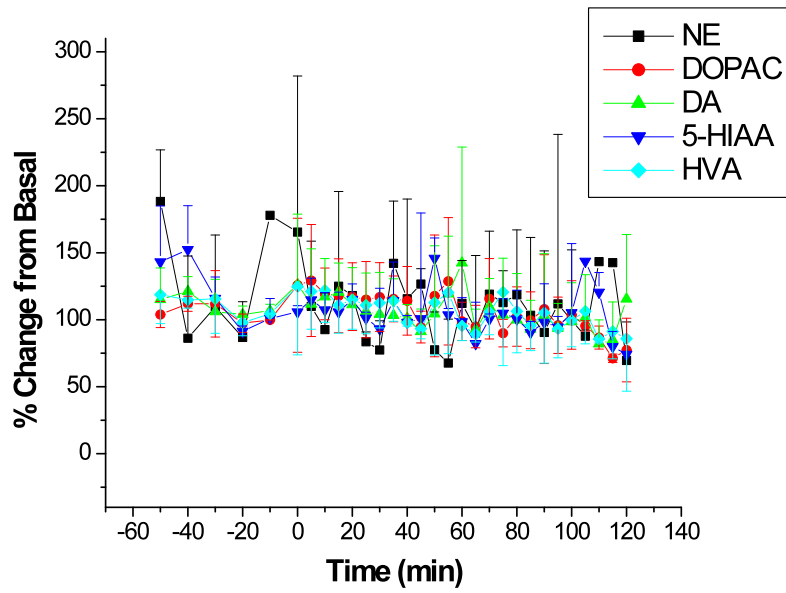
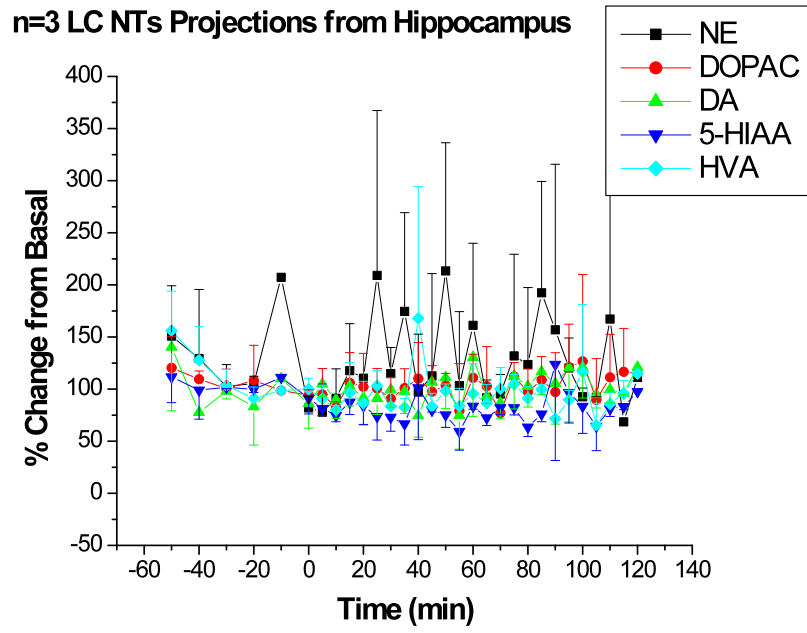


Figure 3.29 Hippocampus catecholamine neurotransmitter projections into the striatum.



**Figure 3.30** Hippocampus catecholamine neurotransmitter projections into the *locus coeruleus*.

### 3.2.11 *locus coeruleus catecholamine neurotransmitters*

#### 3.2.11.1 *locus coeruleus catecholamines in anesthetized rats*

Figure 3.29 show the changes in catecholamine neurotransmitters in the *locus coeruleus*. The *locus coeruleus* was studied because it is the main synthesis site for norepinephrine in the brain. Levels of norepinephrine collected in the brain region were substantially higher than in the striatum and hippocampus. Upon perfusion of 3-MPA, there was an approximately 3-fold increase in norepinephrine concentrations.

Quantitation of dopamine in the *locus coeruleus* has not been widely reported. It is thought this is due to the low concentrations of dopamine in this brain region [26]. Dopamine was only detected in three of the five rats.

The metabolites remained around basal levels throughout the experiment. The two spikes in DOPAC at 40 and 115 minutes were mainly due to large increases in one rat and are not considered significant events.

#### 3.2.11.2 *locus coeruleus projections into the striatum*

Figure 3.30 shows the changes in the catecholamine neurotransmitters in the striatum while administering 3-MPA in the hippocampus. Dopamine remains at basal levels throughout; however there is an increase in norepinephrine. This increase was seen across all the rats, around the same time point. This was unexpected, as an increase in norepinephrine was not expected in the striatum. Additionally, it was expected that increases in norepinephrine due to projections from the *locus coeruleus* should have been

seen during the administration of 3-MPA and not after the perfusion was pulled. Previous studies have employed a dual-probe microdialysis setup, where one probe was placed in the *locus coeruleus* and another in the prefrontal cortex to examine noradrenaline release [36]. In these studies there was no distinction in the time course of norepinephrine changes in either of the two regions. Pudovkina et al. sampled at a rate of 15 minutes and the changes in norepinephrine in the *locus coeruleus* and prefrontal cortex mirrored one another. It is thus surprising to see an increase in norepinephrine in the striatum well after the perfusion of 3-MPA in the *locus coeruleus* has been stopped. However, there have been other studies that have shown that the GABAergic and noradrenergic relationship may have an effect here as well. Intraventricular injections of GABA have shown that there is an initial decrease in norepinephrine, followed by a subsequent increase [137].

### 3.2.11.3 *locus coeruleus* projections into the hippocampus

Figure 3.31 shows changes in catecholamines in the hippocampus while administering 3-MPA in the *locus coeruleus*. This was the brain region that had inputs from the *locus coeruleus*, and thus an increase in norepinephrine was expected in this region; however, there were no increases in norepinephrine in the hippocampus while dosing 3-MPA in the *locus coeruleus*.



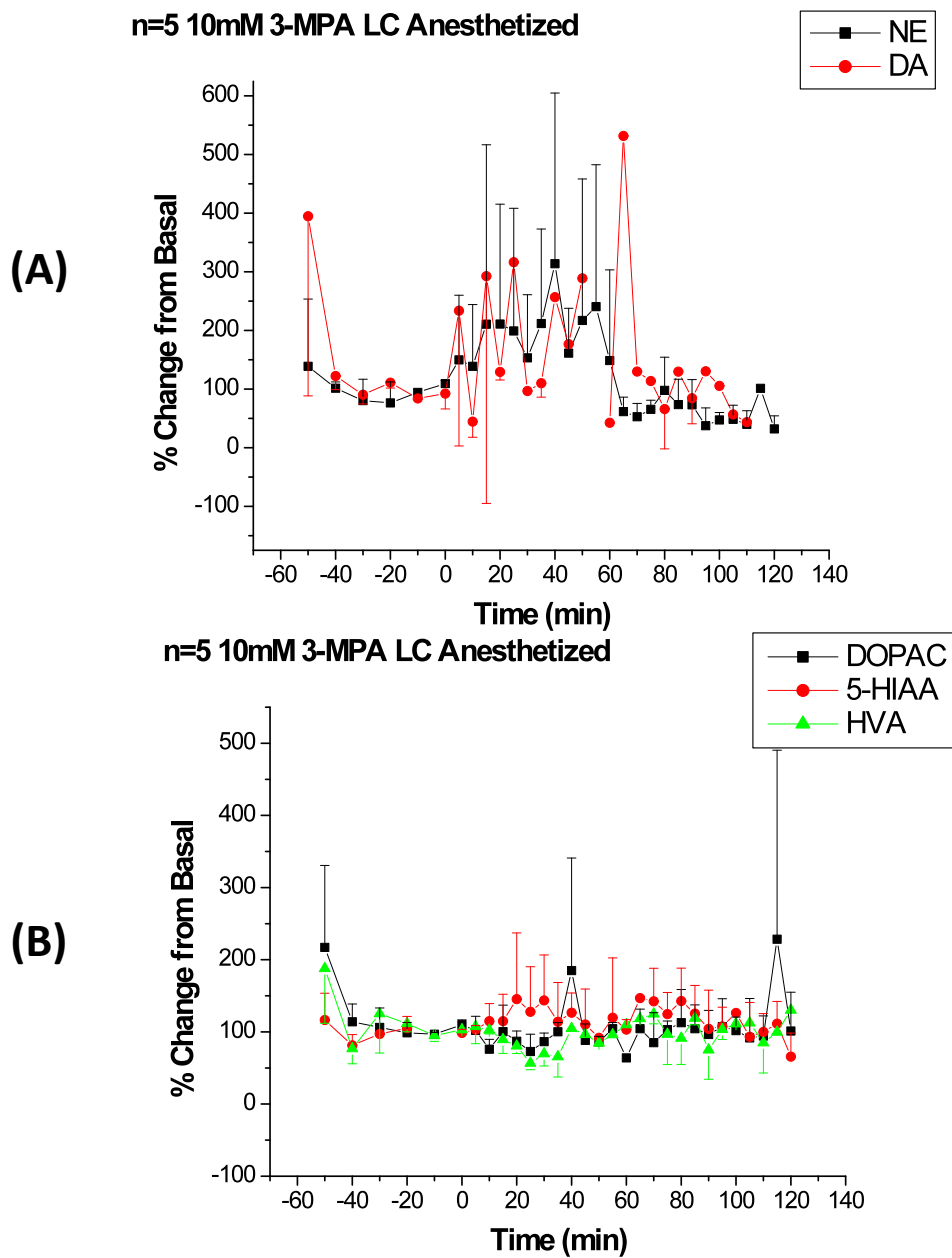


Figure 3.31 10mM 3-MPA perfusion in the locus coeruleus of anesthetized rats. (A) Catecholamines NE and DA. (B) NE, DA, and metabolites 5-HIAA, DOPAC, and HVA (n=5 rats).

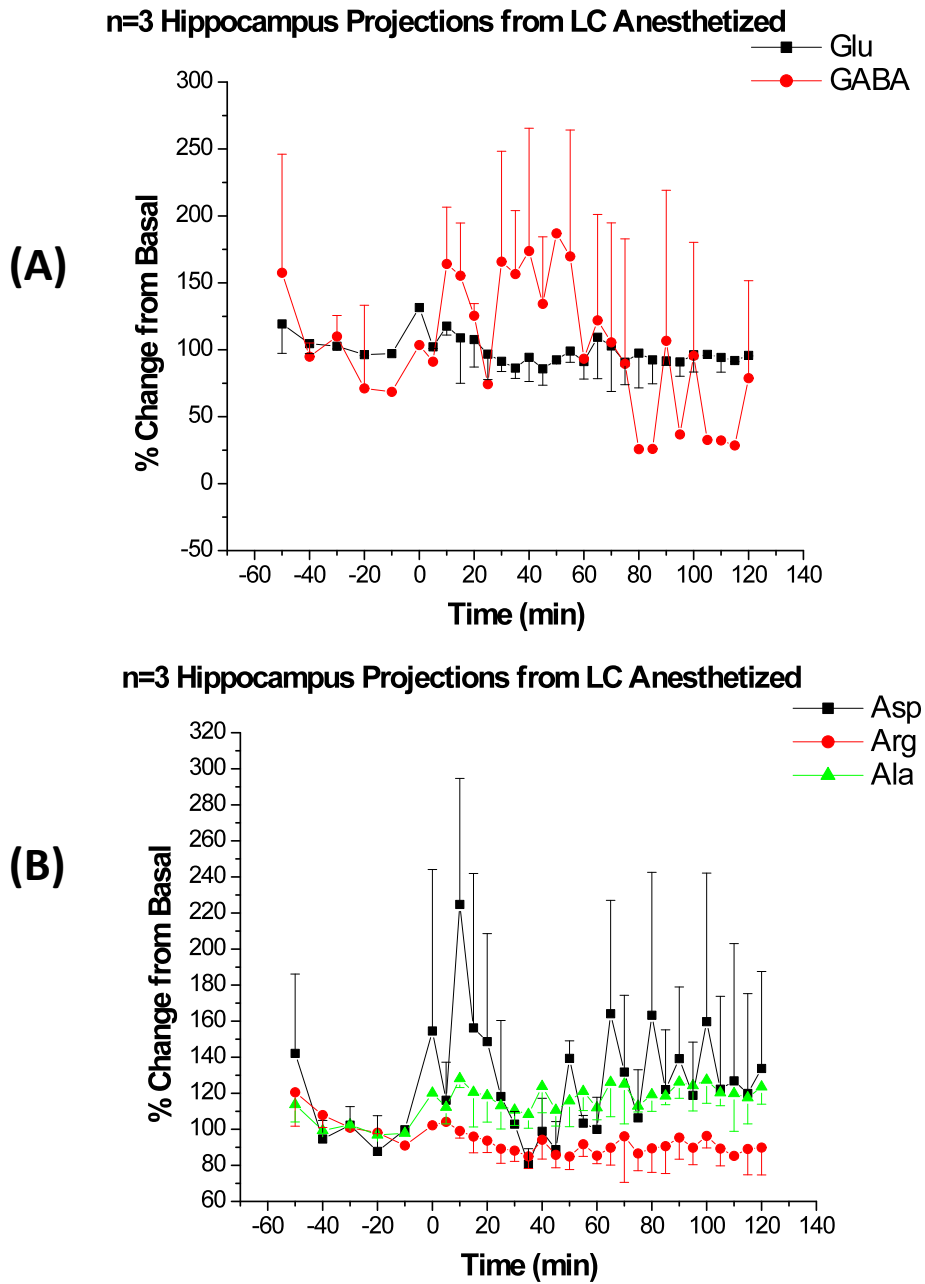


Figure 3.32 locus coeruleus catecholamine neurotransmitter projections into the striatum. (A) norepinephrine and dopamine. (B) DOPAC, 5-HIAA, and HVA.

n=3 Hippocampus projections from LC anesthetized

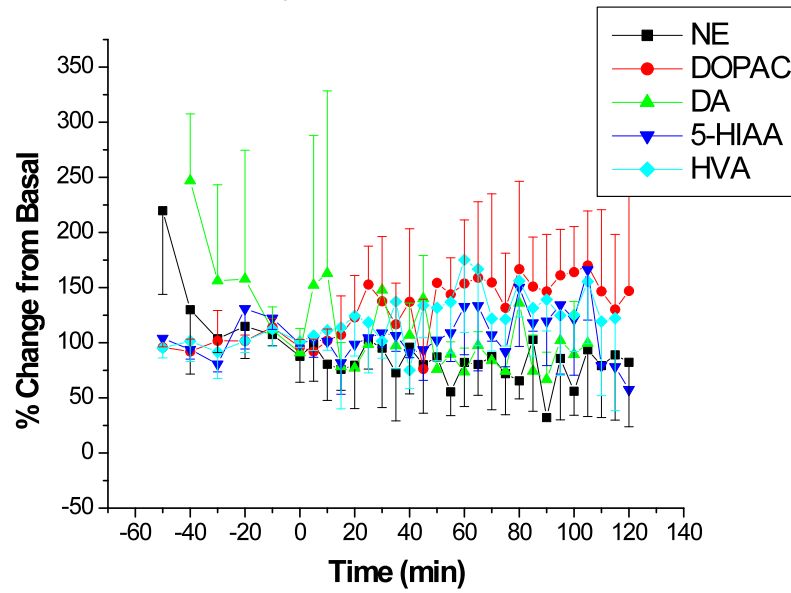


Figure 3.33 locus coeruleus catecholamine neurotransmitter projections into the hippocampus.

### 3.2.12 ECoG results

One of the advantages of the systemic dosing of 3-MPA is the large electrical signal that is produced. In the systemic dosing model of 3-MPA screws were placed on the cortex. This works because 3-MPA affects the brain globally and all the neurons are firing, so the signal is large enough to be detected in this manner. However, with the local dosing of 3-MPA the signal is so small, even in the tissue surrounding the probe, that changes in electrical activity due to local perfusion of 3-MPA cannot be detected on the cortex. The first experiment was to place individual wires down into the brain alongside the microdialysis probe to detect electrical activity as close to the probe as possible, with the idea that the only neurons that are firing are those immediately surrounding the probe. Seizures were detected ( $25.3 \pm 29.3$  seizures) in 3 rats (2 awake and 1 anesthetized) in the striatum. Seizures were detected in such a small number of rats that it was thought maybe this was due to placement of the wires. Since the wires were not stereotaxically placed in the brain, it was unknown the final proximity of the wires to the probe itself. With such a small area being affected by the 3-MPA, placement of the wires with respect to the probe was crucial in detecting seizures. In addition, the role of the inhibitory surround could be a contributing factor as well. If wires were placed in the surround as opposed to the seizure focus, no seizures would be detected.

Specially designed microdialysis probes with internal Ag/AgCl electrodes were then used with the potential to obtain electrical activity at the site of dosing. Figure 3.32 shows the design of the probes. Figure 3.33 is raw ECoG data obtained from a the systemic dosing model of 3-MPA. Two screws were placed on the cortex and a

microdialysis probe with an internal Ag/AgCl electrode was placed in the striatum. The top two traces in Figure 3.33 are from the two screws on the cortex, while the bottom trace is from the probe electrode. This trace was from after dosing of 3-MPA and seizures can be seen in all three traces. Figures 3.34 and 3.35 shows the seizure detection algorithm output. Figure 3.34 is from screws on the cortex, while Figure 3.35 is for the microdialysis probe electrode. The systemic injection of 3-MPA was given at 30 minutes (1800 seconds). The top graph in Figures 3.34 and 3.35 are the time-frequency maps for the power spectral density logarithm. The bottom graph in these two figures is the 2-D time-frequency map. The existence of seizures manifests itself in strip-like structure of spectral evolution time-frequency map because seizure is an abrupt increasing of oscillation power in some frequency bands. From this it was determined that these probes are functional and can detect electrical seizure activity. From here these probes were used with the local dosing of 10mM 3-MPA. However, as can be seen in Figure 3.36 upon local dosing of 10mM 3-MPA in the *locus coeruleus* no seizures were detected. This same result holds true for recording ECoG activity in one of the control probes, no seizures were detected. There was also a large band at 60 Hz, which is indicative of the large noise accompanying these samples. Seizures were not detected in any of the rats where local dosing of 3-MPA was used. This was most likely due in part to the significant amount of noise, as well as the small number of neurons that would be firing due to the local administration of 3-MPA. Because of the large noise seen using the microdialysis probe electrodes in anesthetized animals, these probes were not used in awake and freely moving rats, as the noise component would be even more significant.

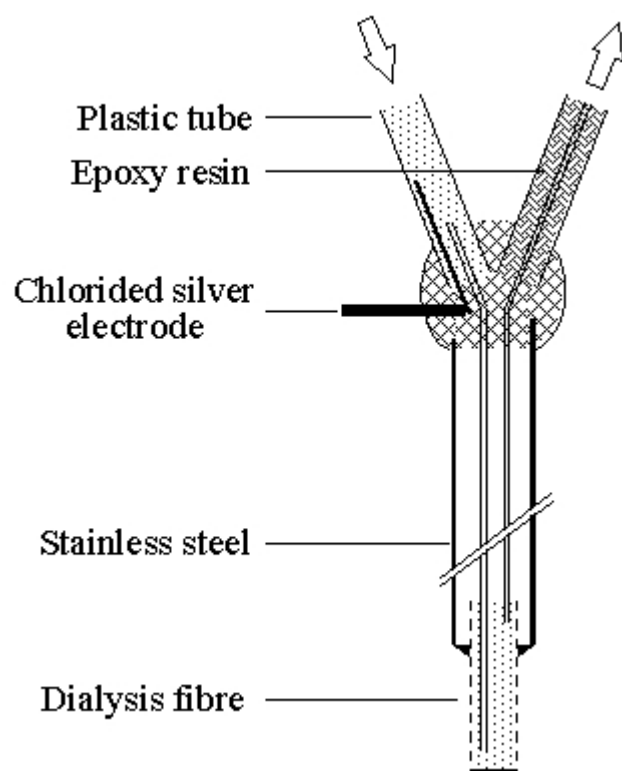


**Figure 3.34** Diagram of microdialysis probe with internal Ag/AgCl working electrode [138].

Subject:  
EEG file: Rat01152010.cnt Recorded : 18:02:19 15-Jan-2010  
Rate - 20000 Hz, HPF - 0 Hz, LPF - 3500 Hz, Notch - off, Montage - None

Neuroscan  
SCAN 4.3  
Printed : 17:10:14 08-Mar-2010

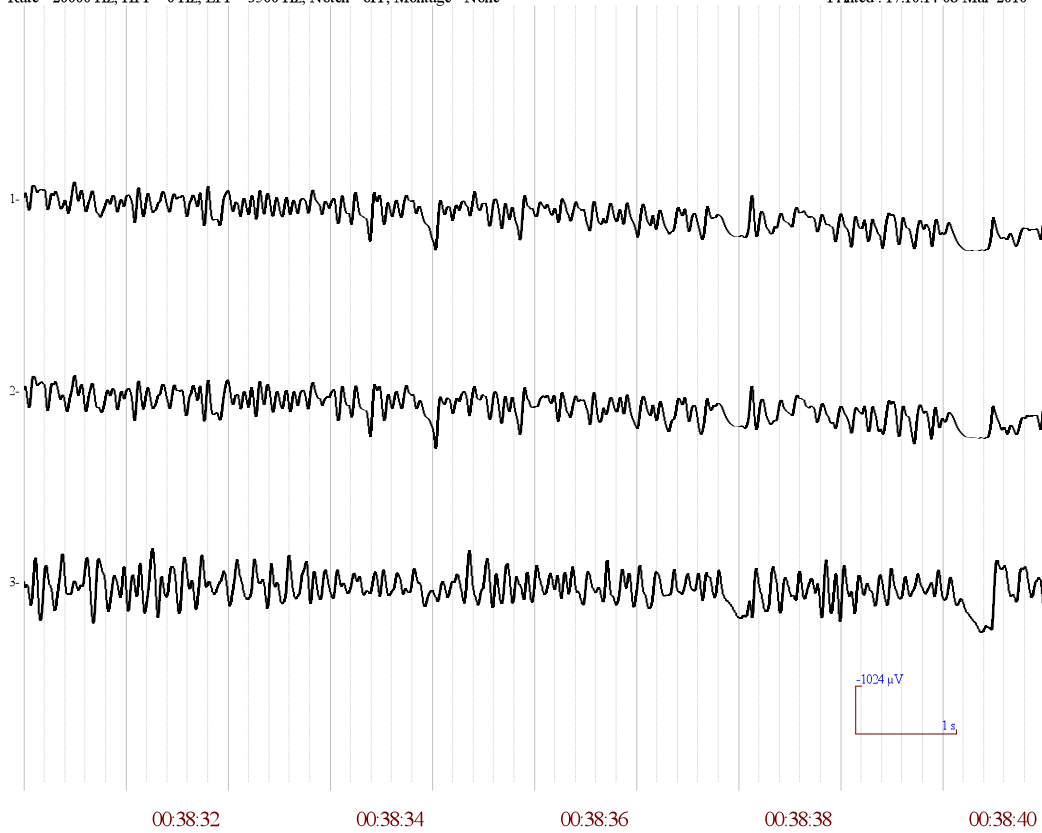
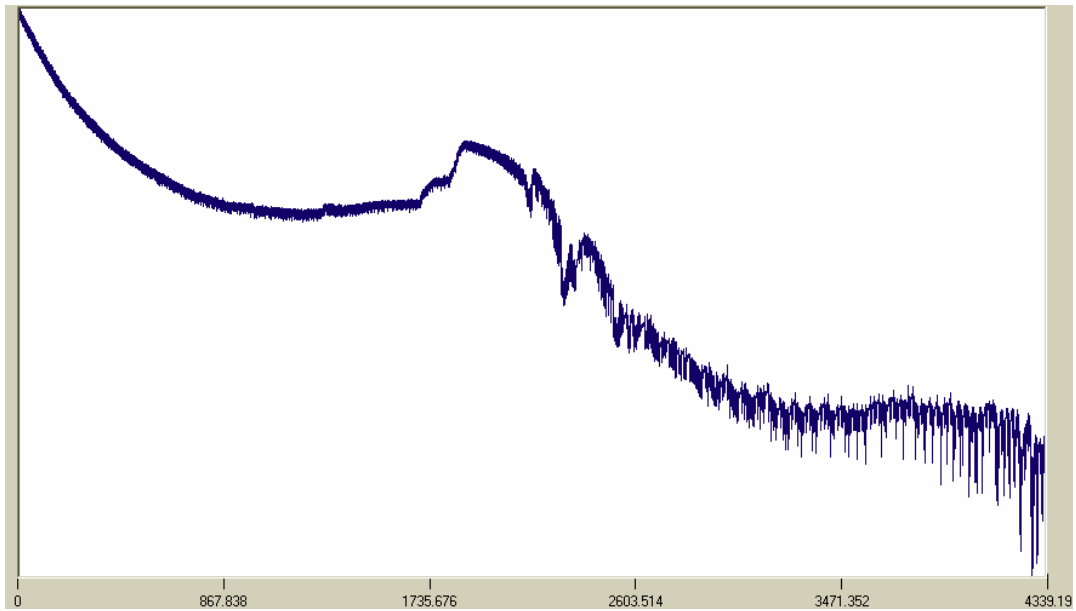
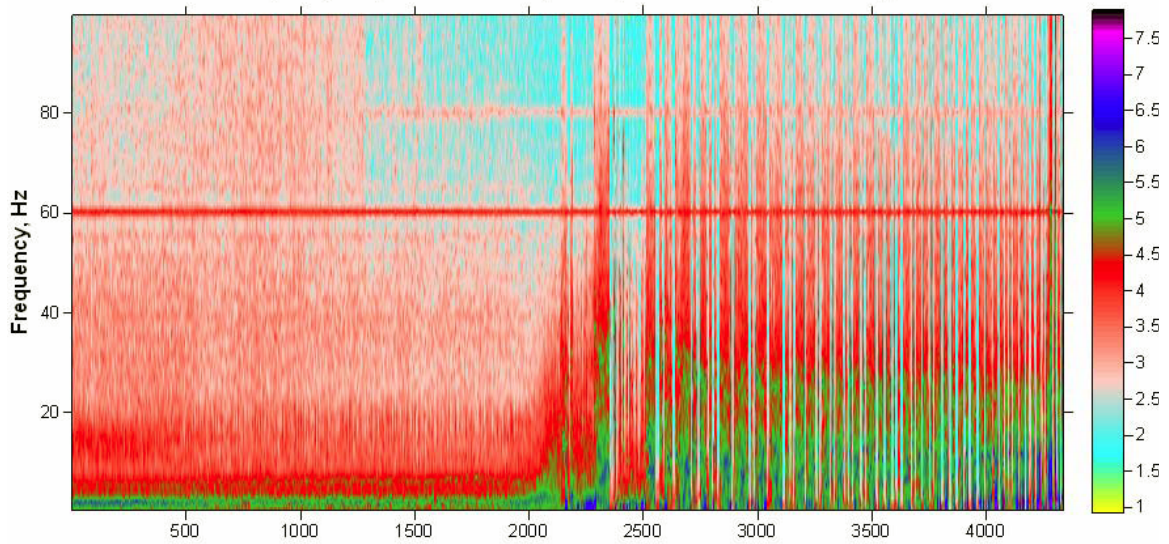


Figure 3.35 Raw ECoG data from screws on cortex (top 2 traces) and internal microdialysis electrode (bottom trace) during systemic dosing of 3-MPA (60mg/kg bolus + 50mg/kg constant infusion for 50 minutes).



Time-frequency map of evolution of power spectral density decimal logarithm



Time, right-hand end of adjacent time windows of the length 2.5 sec (500 samples with 200 Hz sampling rate)

Figure 3.36 ECoG data from screws on cortex during systemic dosing of 3-MPA (60mg/kg bolus + 50mg/kg constant infusion for 50 minutes).



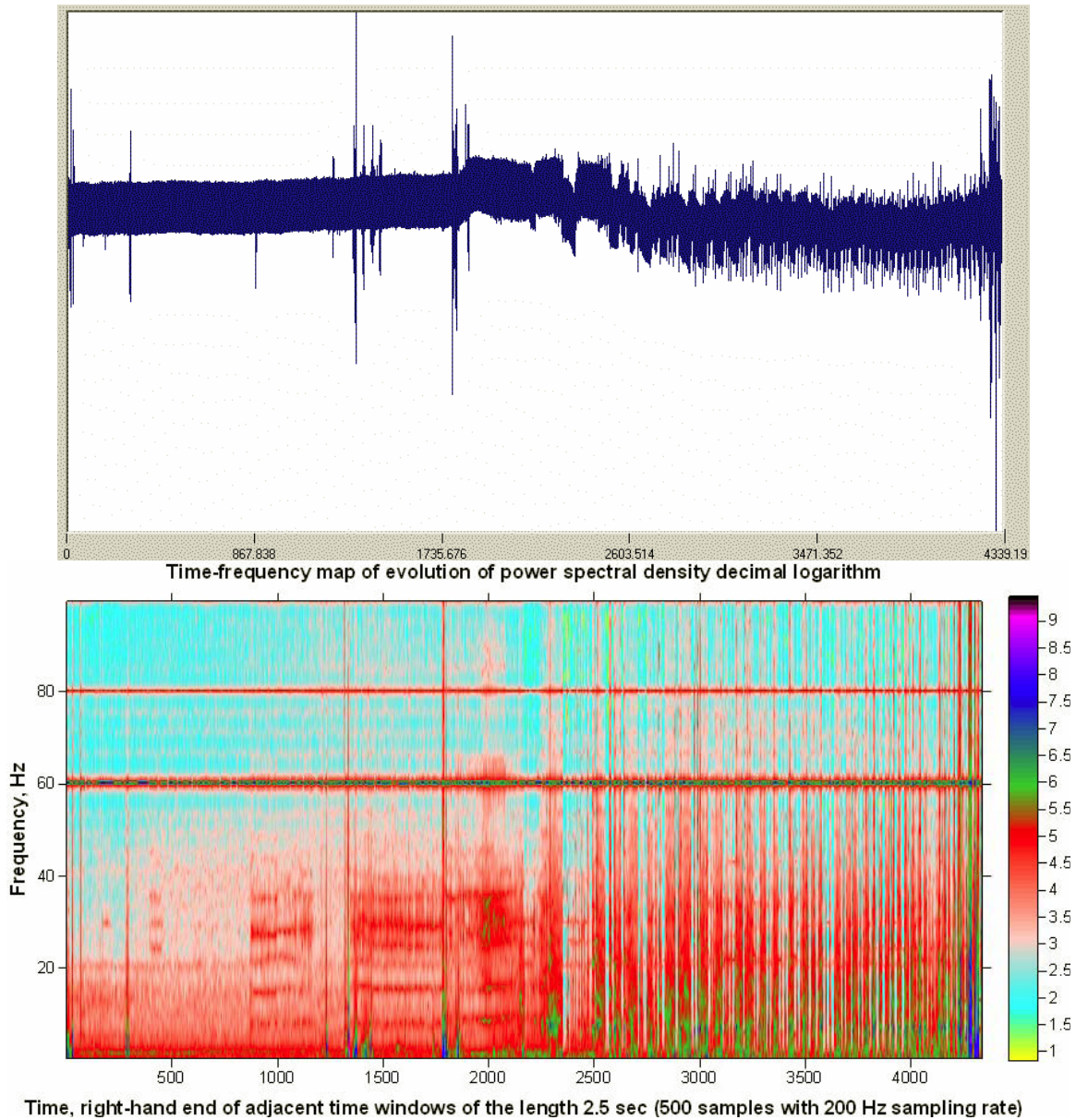


Figure 3.37 ECoG data from internal microdialysis Ag/AgCl electrode during systemic dosing of 3-MPA (60mg/kg bolus + 50mg/kg constant infusion for 50 minutes).

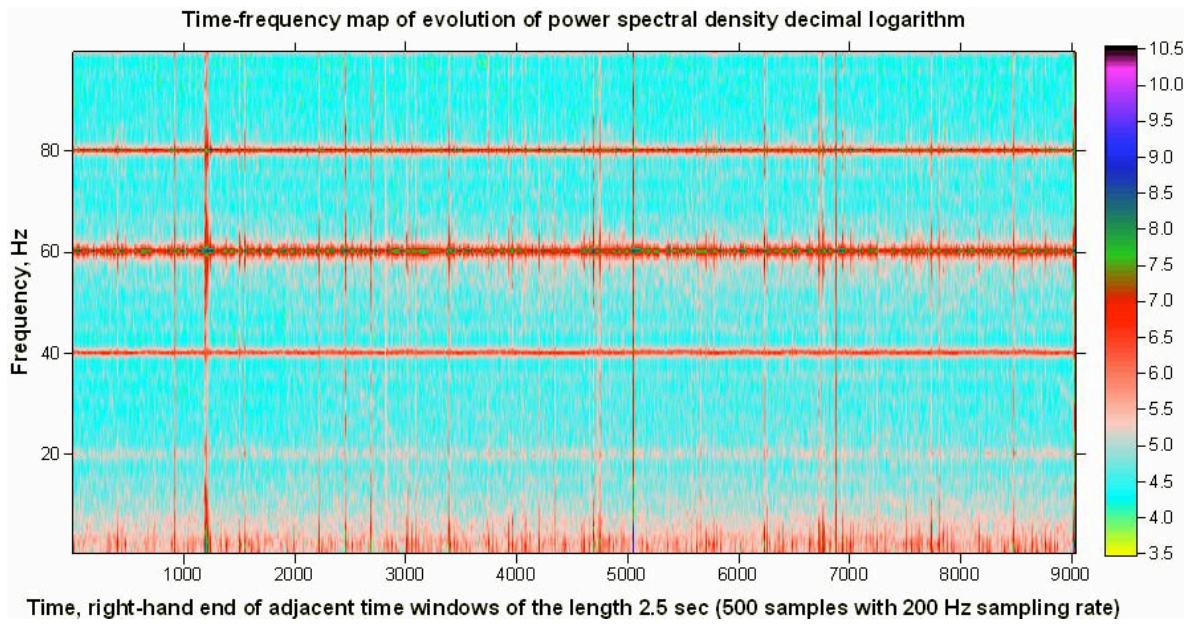


Figure 3.38 ECoG data from internal microdialysis Ag/AgCl electrode during local dosing of 10mM 3-MPA in the locus coeruleus.

### *3.2.13 Local dosing of picrotoxin*

As stated previously, one of the reasons for a local administration of 3-MPA was to induce seizures in a locally defined brain region since these types of seizures, at least initially, are more clinically relevant [3]. However, as demonstrated in previous chapters, the significant problem with the local dosing of 3-MPA has been the inability to detect seizures. It was generally thought that an increase in excitation over inhibition leads to seizures, however from the data presented here it appears that is not the whole picture. Obrenovitch et al. have explored the role of extracellular glutamate and its relationship to seizures and have shown that increasing extracellular glutamate 20-fold did not result in seizures [139]. This seem to support the data we have presented showing 5-200 fold increases in glutamate resulting in no seizure generation. In addition, there are conflicting results regarding the action of glutamate in seizure generation, where studies have shown an increase, decrease, and no change in glutamate concentrations during seizures [139-141]. There are several plausible explanations for this. It is possible that by administering 3-MPA through the probe, the number of neurons affected is so small that the signal produced from any seizure events are too small to detect. One other possibility is that there aren't any seizures being generated and an increase in excitation is only part of the picture leading to seizure generation. This idea sheds light on the fact that maybe an altered balance between excitation/inhibition is important in seizure generation, but there are other factors that are important as well. The purpose of these studies are to use a different convulsant, picrotoxin, which leads to seizure generation via a different mechanism to see if seizures can be detected. If seizures can be generated using picrotoxin, this could lead to a greater understanding of the 3-MPA model and

seizure generation in general by leading to the conclusion that 3-MPA action on the excitatory/inhibitory balance in the brain is not the cause of seizures.

Local dosing of 600 $\mu$ M picrotoxin, in aCSF, was performed in anesthetized rats, however no seizures were detected. This result indicates that more than likely there is a problem with the electrode set-up. Therefore, there is more method development that needs to be performed to measure seizures during local dosing.

#### *3.2.14 Brain histology*

After experiments, rats were sacrificed and brains were harvested for histology. The brains were placed in a 10% neutral buffered formalin solution. Probe placement as well as tissue damage was determined from brain slices. Figure 3.39 shows histological slices from a representative rat brain. These are two pictures of a 2mm probe in the hippocampus after dosing 10mM 3-MPA in this region. As can be seen in the top image, the probe is placed in the CA1 region of the hippocampus. The lower image shows no signs of cell death, leading to the conclusion that these high concentrations of 3-MPA do not significantly damage the tissue.

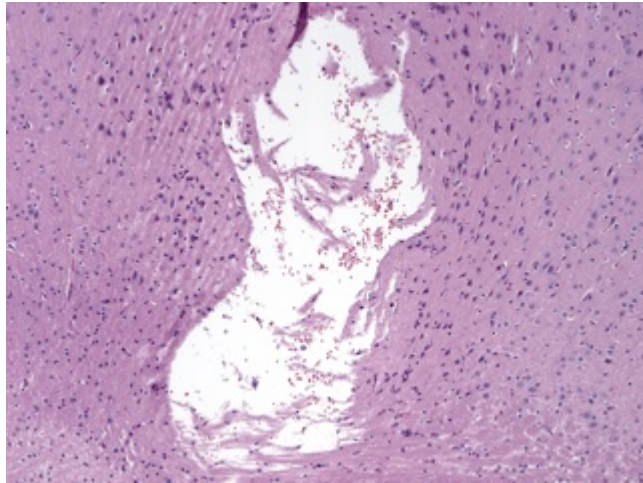
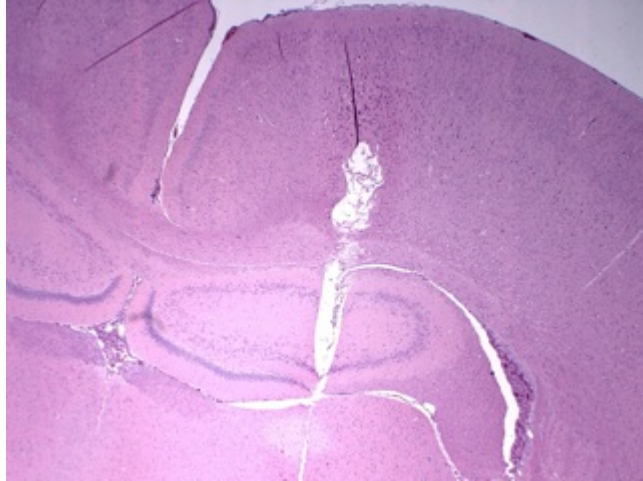


**Figure 3.39** Probe placement in CA1 of the hippocampus.

### 3.3 Conclusions

A consistent steady-state delivery of 3-MPA (in  $\mu\text{g}/\text{min}$ ) was achieved in all three brain regions in both anesthetized and awake rats. Local dosing of 3-MPA produced significant changes in amino acids and catecholamine neurotransmitters. These changes were substantially larger than those seen with systemic dosing of 3-MPA. Glutamate increased 15-fold in the striatum of anesthetized rats and 250-fold in awake rats. GABA also increased in the striatum of anesthetized and awake rats, 5-fold and 50-fold respectively. This increase in GABA was not expected based on the mechanism of action of 3-MPA on GAD. Glutamate and GABA both also increased in the hippocampus of anesthetized and awake rats, however these changes were slightly smaller than those seen in the striatum. Glutamate increased only slightly (171% of basal) in the *locus coeruleus* of anesthetized rats, while GABA increased 4-fold.

Catecholamine neurotransmitters changed as well during local dosing of 3-MPA. Dopamine and norepinephrine increased in all three brain regions in anesthetized rats, while 5-HIAA, HVA, and DOPAC remained around basal levels.

Seizures were not detected in any of the experiments using local dosing of 3-MPA. It was suggested that this was due to the small number of neurons affected by the local dose of 3-MPA as well as the significant background noise during collection.

### 3.4 References

1. Crick, E.W., *In vivo Microdialysis Coupled with Electrophysiology for the Neurochemical Analysis of Epileptic Seizures*, in *Chemistry*. 2007, The University of Kansas.
2. Crick, E.W., et al., *An investigation into the pharmacokinetics of 3-mercaptopropionic acid and development of a steady-state chemical seizure model using in vivo microdialysis and electrophysiological monitoring*. *Epilepsy Res.*, 2007. **74**(2-3): p. 116-125.
3. French, J.A. and T.A. Pedley, *Initial management of epilepsy*. *N. Engl. J. Med.*, 2008. **359**(2): p. 166-176.
4. Micahel J. Zigmond, F.E.B., Story C. Landis, James L. Roberts, Larry R. Squire, *Fundamental Neuroscience*. 1999: Academic Press.
5. Agranoff, B.W., et al., *Basic Neurochemistry. Molecular, Cellular, and Medical Aspects. 4th Ed.* 1989. 984 pp.
6. Carpenter, M.B., et al., *Connections of the subthalamic nucleus in the monkey*. *Brain Research*, 1981. **224**(1): p. 1-29.
7. Gerfen, C.R., *Synaptic organization of the striatum*. *Journal of electron microscopy technique*, 1988. **10**(3): p. 265-81.
8. Phelps, P.E., C.R. Houser, and J.E. Vaughn, *Immunocytochemical localization of choline acetyltransferase within the rat neostriatum: a correlated light and electron microscopic study of cholinergic neurons and synapses*. *The Journal of comparative neurology*, 1985. **238**(3): p. 286-307.
9. Wilson, C.J. and P.M. Groves, *Fine structure and synaptic connections of the common spiny neuron of the rat neostriatum: a study employing intracellular inject of horseradish peroxidase*. *The Journal of comparative neurology*, 1980. **194**(3): p. 599-615.
10. Kemp, J.M. and T.P. Powell, *The cortico-striate projection in the monkey*. *Brain a journal of neurology*, 1970. **93**(3): p. 525-46.

11. Bouyer, J.J., et al., *Chemical and structural analysis of the relation between cortical inputs and tyrosine hydroxylase-containing terminals in rat neostriatum*. Brain Research, 1984. **302**(2): p. 267-75.
12. Cherubini, E., et al., *Excitatory amino acids in synaptic excitation of rat striatal neurons in vitro*. Journal of Physiology (Cambridge, United Kingdom), 1988. **400**: p. 677-90.
13. Lapper, S.R. and J.P. Bolam, *Input from the frontal cortex and the parafascicular nucleus to cholinergic interneurons in the dorsal striatum of the rat*. Neuroscience, 1992. **51**(3): p. 533-45.
14. Sadikot, A.F., A. Parent, and C. Francois, *Efferent connections of the centromedian and parafascicular thalamic nuclei in the squirrel monkey: a PHA-L study of subcortical projections*. The Journal of comparative neurology, 1992. **315**(2): p. 137-59.
15. Penny, G.R., S. Afsharpour, and S.T. Kitai, *The glutamate decarboxylase-, leucine enkephalin-, methionine enkephalin- and substance P-immunoreactive neurons in the neostriatum of the rat and cat: evidence for partial population overlap*. Neuroscience (Oxford, United Kingdom), 1986. **17**(4): p. 1011-45.
16. Chang Bernard, S. and H. Lowenstein Daniel, *Epilepsy*. The New England journal of medicine, 2003. **349**(13): p. 1257-66.
17. Geddes, J.W., et al., *Altered distribution of excitatory amino acid receptors in temporal lobe epilepsy*. Experimental Neurology, 1990. **108**(3): p. 214-20.
18. Sutula, T.P., *Experimental models of temporal lobe epilepsy: new insights from the study of kindling and synaptic reorganization*. Epilepsia, 1990. **31 Suppl 3**: p. S45-54.
19. Girardi, E., et al., *Astrocytic Response in Hippocampus and Cerebral Cortex in an Experimental Epilepsy Model*. Neurochemical research, 2004. **29**(2): p. 371-377.
20. Siegel, G.J., et al., *Basic Neurochemistry. 3rd Ed.* 1981. 858 pp.
21. Anderson, P., T.V. Bliss, and K.K. Skrede, *Lamellar organization of hippocampal pathways*. Experimental brain research. Experimentelle Hirnforschung. Experimentation cerebrale, 1971. **13**(2): p. 222-38.
22. Eric R. Kandel, J.H.S., Thomas M. Jessel, *Principles of Neural Science*. 4th ed. 2000: McGraw-Hill
23. Andersen, P., et al., *The Hippocampus Book*. 2007. 832 pp.



24. Weinschenker, D., et al., *Genetic or pharmacological blockade of noradrenaline synthesis enhances the neurochemical, behavioral, and neurotoxic effects of methamphetamine*. Journal of Neurochemistry, 2008. **105**(2): p. 471-483.
25. Lambas-Senas, L., et al., *Comparative responses of the central adrenaline- and noradrenaline-containing neurons after reserpine injections*. Biochemical Pharmacology, 1986. **35**(13): p. 2207-11.
26. Singewald, N. and A. Philippu, *Release of neurotransmitters in the locus coeruleus*. Progress in Neurobiology (Oxford), 1998. **56**(2): p. 237-267.
27. Corcoran, M.E. and S.T. Mason, *Role of forebrain catecholamines in amygdaloid kindling*. Brain Research, 1980. **190**(2): p. 473-84.
28. McIntyre, D.C. and R.K. Wong, *Cellular and synaptic properties of amygdala-kindled pyriform cortex in vitro*. Journal of Neurophysiology, 1986. **55**(6): p. 1295-307.
29. McIntyre, D.C., *Amygdala kindling in rats: facilitation after local amygdala norepinephrine depletion with 6-hydroxydopamine*. Experimental Neurology, 1980. **69**(2): p. 395-407.
30. Sullivan, H.C. and I. Osorio, *Aggravation of penicillin-induced epilepsy in rats with locus ceruleus lesions*. Epilepsia, 1991. **32**(5): p. 591-6.
31. Jones, B.E., et al., *Ascending projections of the locus coeruleus in the rat. I. Axonal transport in central noradrenaline neurons*. Brain Research, 1977. **127**(1): p. 1-21.
32. Jones, B.E. and R.Y. Moore, *Ascending projections of the locus coeruleus in the rat. II. Autoradiographic study*. Brain Research, 1977. **127**(1): p. 25-53.
33. Jones, B.E. and T.Z. Yang, *The efferent projections from the reticular formation and the locus coeruleus studied by anterograde and retrograde axonal transport in the rat*. The Journal of comparative neurology, 1985. **242**(1): p. 56-92.
34. Bouret, S. and S.J. Sara, *Network reset: a simplified overarching theory of locus coeruleus noradrenaline function*. Trends in neurosciences, 2005. **28**(11): p. 574-582.
35. Ohmura, Y., et al., *The Serotonergic Projection from the Median Raphe Nucleus to the Ventral Hippocampus is Involved in the Retrieval of Fear Memory Through the Corticotropin-Releasing Factor Type 2 Receptor*. Neuropsychopharmacology. **35**(6): p. 1271-1278.

36. Pudovkina, O.L. and B.H.C. Westerink, *Release of noradrenaline in the locus coeruleus*. Dendritic Neurotransmitter Release, 2005: p. 145-154.
37. Torregrossa, M.M., X.C. Tang, and P.W. Kalivas, *The glutamatergic projection from the prefrontal cortex to the nucleus accumbens core is required for cocaine-induced decreases in ventral pallidal GABA*. Neuroscience Letters, 2008. **438**(2): p. 142-145.
38. Reperant, J., et al., *Serotonergic retinopetal projections from the dorsal raphe nucleus in the mouse demonstrated by combined [<sup>3</sup>H] 5-HT retrograde tracing and immunolabeling of endogenous 5-HT*. Brain Research, 2000. **878**(1,2): p. 213-217.
39. Grabb, M.C., et al., *Neurochemical and morphological responses to acutely and chronically implanted brain microdialysis probes*. Journal of Neuroscience Methods, 1998. **82**(1): p. 25-34.
40. Woodroffe, M.N., et al., *Detection of interleukin-1 and interleukin-6 in adult rat brain, following mechanical injury, by in vivo microdialysis: evidence of a role for microglia in cytokine production*. Journal of Neuroimmunology, 1991. **33**(3): p. 227-36.
41. Herman, J.P., A. Renda, and B. Bodie, *Norepinephrine-gamma-aminobutyric acid (GABA) interaction in limbic stress circuits: effects of reboxetine on GABAergic neurons*. Biological Psychiatry, 2003. **53**(2): p. 166-174.
42. Karbon, E.W., R. Duman, and S.J. Enna, *Biochemical identification of multiple GABAB binding sites: association with noradrenergic terminals in rat forebrain*. Brain Research, 1983. **274**(2): p. 393-6.
43. Lloyd, K.G., et al., *The potential use of GABA agonists in psychiatric disorders: evidence from studies with progabide in animal models and clinical trials*. Pharmacology, Biochemistry and Behavior, 1983. **18**(6): p. 957-66.
44. Suzdak, P.D., *Differential coupling of GABA-A and GABA-B receptors to the noradrenergic system: implications for a GABA-ergic role in depression*. 1985. p. 262 pp.
45. Suzdak, P.D. and G. Gianutsos, *Parallel changes in the sensitivity of gamma-aminobutyric acid and noradrenergic receptors following chronic administration of antidepressant and GABAergic drugs. A possible role in affective disorders*. Neuropharmacology, 1985. **24**(3): p. 217-22.

46. Anden, N.E. and H. Wachtel, *Biochemical effects of baclofen (beta - parachlorophenyl-GABA) on the dopamine and the noradrenaline in the rat brain*. *Acta Pharmacologica et Toxicologica*, 1977. **40**(2): p. 310-20.
47. Suzdak, P.D. and G. Gianutsos, *GABA-noradrenergic interaction: evidence for differential sites of action for GABA-A and GABA-B receptors*. *Journal of Neural Transmission (1972-1989)*, 1985. **64**(3-4): p. 163-72.
48. Carlsson, A., *The neurochemical circuitry of schizophrenia*. *Pharmacopsychiatry*, 2006. **39**(Suppl. 1): p. S10-S14.
49. Keinrok, Z. and R. Czajka, *The effect of endogenous and exogenous GABA on the level and turnover of noradrenaline and dopamine in rat brain*. *Acta Physiologica Polonica*, 1978. **29**(2): p. 117-21.
50. Nitz, D. and J.M. Siegel, *GABA release in the locus ceruleus as a function of sleep/wake state*. *Neuroscience (Oxford)*, 1997. **78**(3): p. 795-801.
51. Araujo de Azeredo, L., et al., *Cocaine reverses the changes in GABAA subunits and in glutamic acid decarboxylase isoenzymes mRNA expression induced by neonatal 6-hydroxydopamine*. *Behavioural Pharmacology*. **21**(4): p. 343-352.
52. Berod, A., et al., *Catecholaminergic and GABAergic anatomical relationship in the rat substantia nigra, locus coeruleus, and hypothalamic median eminence: immunocytochemical visualization of biosynthetic enzymes on serial semithin plastic-embedded sections*. *The journal of histochemistry and cytochemistry official journal of the Histochemistry Society*, 1984. **32**(12): p. 1331-8.
53. Majumdar, S. and B.N. Mallick, *Increased levels of tyrosine hydroxylase and glutamic acid decarboxylase in locus coeruleus neurons after rapid eye movement sleep deprivation in rats*. *Neuroscience Letters*, 2003. **338**(3): p. 193-196.
54. Eric R. Kandel, J.H.S., Thomas M. Jessel, *Essentials of Neural Science and Behavior*. 1995: Appleton and Lange.
55. Hudspith, M.J., *Glutamate: a role in normal brain function, anesthesia, analgesia and CNS injury*. *British Journal of Anaesthesia*, 1997. **78**(6): p. 731-747.
56. Pocock, G. and C.D. Richards, *Excitatory and inhibitory synaptic mechanisms in anesthesia*. *British Journal of Anaesthesia*, 1993. **71**(1): p. 134-47.
57. Harrison, N.L. and M.A. Simmonds, *Quantitative studies on some antagonists of N-methyl D-aspartate in slices of rat cerebral cortex*. *British Journal of Pharmacology*, 1985. **84**(2): p. 381-91.

58. Hirota, K. and D.G. Lambert, *Voltage-sensitive Ca<sup>2+</sup> channels and anesthesia*. British Journal of Anaesthesia, 1996. **76**(3): p. 344-6.
59. Lynch, C., 3rd and J.J. Pancrazio, *Snails, spiders, and stereospecificity--is there a role for calcium channels in anesthetic mechanisms?* Anesthesiology, 1994. **81**(1): p. 1-5.
60. Kitayama, M., et al., *Inhibitory effects of intravenous anaesthetic agents on K<sup>+</sup>-evoked glutamate release from rat cerebrocortical slices. Involvement of voltage-sensitive Ca<sup>2+</sup> channels and GABAA receptors*. Naunyn-Schmiedeberg's Archives of Pharmacology, 2002. **366**(3): p. 246-253.
61. Sun, X., et al., *Effects of ketamine anesthesia on neurotransmitter metabolism of cerebral ganglion in dogs*. Disi Junyi Daxue Xuebao, 2008. **29**(22): p. 2038-2040.
62. Bruehl, C. and O.W. Witte, *Cellular activity underlying altered brain metabolism during focal epileptic activity*. Annals of neurology, 1995. **38**(3): p. 414-20.
63. Chagnac-Amitai, Y. and B.W. Connors, *Horizontal spread of synchronized activity in neocortex and its control by GABA-mediated inhibition*. Journal of Neurophysiology, 1989. **61**(4): p. 747-58.
64. Golomb, D. and Y. Amitai, *Propagating neuronal discharges in neocortical slices: computational and experimental study*. Journal of Neurophysiology, 1997. **78**(3): p. 1199-211.
65. Prince, D.A., et al., *Chronic focal neocortical epileptogenesis: does disinhibition play a role?* Canadian journal of physiology and pharmacology, 1997. **75**(5): p. 500-7.
66. Olsen, R.W. and M. Avoli, *GABA and epileptogenesis*. Epilepsia, 1997. **38**(4): p. 399-407.
67. Benali, A., et al., *Excitation and inhibition jointly regulate cortical reorganization in adult rats*. Journal of Neuroscience, 2008. **28**(47): p. 12284-12293.
68. Trevelyan, A.J., et al., *epilepsModular propagation of epileptiform activity: evidence for an inhibitory veto in neocortex*. Journal of Neuroscience, 2006. **26**(48): p. 12447-12455.
69. Lothman E.W., C.R.C., *Seizures and epilepsy*. Neurobiology of Disease. 1990, New York: Oxford University Press.

70. Goldensohn, E.S. and D.P. Purpura, *Intracellular potentials of cortical neurons during focal epileptogenic discharges*. Science (New York, N.Y.), 1963. **139**: p. 840-2.
71. Li, C.L., *Cortical intracellular potentials and their responses to strychnine*. Journal of Neurophysiology, 1959. **22**(4): p. 436-50.
72. Matsumoto, H. and C.A. Marsan, *Cortical Cellular Phenomena in Experimental Epilepsy: Interictal Manifestations*. Experimental Neurology, 1964. **9**: p. 286-304.
73. Morrell, F., *Microelectrode studies in chronic epileptic foci*. Epilepsia, 1961. **2**: p. 81-8.
74. Hartline, H.K. and F. Ratliff, *Inhibitory interaction of receptor units in the eye of Limulus*. The Journal of general physiology, 1957. **40**(3): p. 357-76.
75. Kuffler, S.W., *Discharge patterns and functional organization of mammalian retina*. Journal of Neurophysiology, 1953. **16**(1): p. 37-68.
76. Mountcastle, V.B., *Modality and topographic properties of single neurons of cat's somatic sensory cortex*. Journal of Neurophysiology, 1957. **20**(4): p. 408-34.
77. Krnjevic, K., M. Randic, and D.W. Straughan, *An inhibitory process in the cerebral cortex*. The Journal of physiology, 1966. **184**(1): p. 16-48.
78. Krnjevic, K., M. Randic, and D.W. Straughan, *Nature of a cortical inhibitory process*. The Journal of physiology, 1966. **184**(1): p. 49-77.
79. Lebovitz, R.M., M. Dichter, and W.A. Spencer, *Recurrent excitation in the CA3 region of cat hippocampus*. The International journal of neuroscience, 1971. **2**(2): p. 99-107.
80. MacVicar, B.A. and F.E. Dudek, *Local synaptic circuits in rat hippocampus: interactions between pyramidal cells*. Brain Research, 1980. **184**(1): p. 220-3.
81. Andersen, P., J.C. Eccles, and Y. Loyning, *Recurrent inhibition in the hippocampus with identification of the inhibitory cell and its synapses*. Nature, 1963. **198**: p. 540-2.
82. Andersen, P., J.C. Eccles, and Y. Loyning, *Location of Postsynaptic Inhibitory Synapses on Hippocampal Pyramids*. Journal of Neurophysiology, 1964. **27**: p. 592-607.
83. Dingledine, R. and L. Gjerstad, *Penicillin blocks hippocampal IPSPs, unmasking prolonged EPSPs*. Brain Research, 1979. **168**(1): p. 205-9.

84. Dingledine, R. and L. Gjerstad, *Reduced inhibition during epileptiform activity in the in vitro hippocampal slice*. Journal of Physiology (Cambridge, United Kingdom), 1980. **305**: p. 297-313.
85. Prince, D.A. and B.J. Wilder, *Control mechanisms in cortical epileptogenic foci. "Surround" inhibition*. Archives of neurology, 1967. **16**(2): p. 194-202.
86. Traub, R.D., *Cellular mechanisms underlying the inhibitory surround of penicillin epileptogenic foci*. Brain Research, 1983. **261**(2): p. 277-84.
87. Overstreet, L.S., G.L. Westbrook, and M.V. Jones, *Measuring and modeling the spatiotemporal profile of GABA at the synapse*. Transmembrane Transporters, 2002: p. 259-275, 1 plate.
88. During, M.J., et al., *Effect of amygdala kindling on the in vivo release of GABA and 5-HT in the dorsal raphe nucleus in freely moving rats*. Brain Research, 1992. **584**(1-2): p. 36-44.
89. Osborne, P.G., et al., *An in vivo microdialysis characterization of extracellular dopamine and GABA in dorsolateral striatum of awake freely moving and halothane anesthetised rats*. Journal of Neuroscience Methods, 1990. **34**(1-3): p. 99-105.
90. Campbell, K., et al., *Extracellular gamma -aminobutyric acid levels in the rat caudate-putamen: Monitoring the neuronal and glial contribution by intracerebral microdialysis*. Brain Research, 1993. **614**(1-2): p. 241-50.
91. Drew, K.L., et al., *Characterization of gamma-aminobutyric acid and dopamine overflow following acute implantation of a microdialysis probe*. Life Sciences, 1989. **45**(14): p. 1307-17.
92. Drew, K.L. and U. Ungerstedt, *Pergolide presynaptically inhibits calcium-stimulated release of gamma -aminobutyric acid*. Journal of Neurochemistry, 1991. **57**(6): p. 1927-30.
93. Hamberger, A., et al., *Amino acid transport in isolated neurons and glia*. Advances in Experimental Medicine and Biology, 1976. **69**(Transp. Phenom. Nerv. Syst.): p. 221-36.
94. Iversen, L.L. and J.S. Kelly, *Uptake and metabolism of gamma -aminobutyric acid by neurons and glial cells*. Biochemical Pharmacology, 1975. **24**(9): p. 933-8.
95. Fonnum, F., *Determination of amino acid turnover*. Neuromethods, 1985. **3**: p. 201-237.

96. Fillenz, M., *Physiological release of excitatory amino acids*. Behavioural Brain Research, 1995. **71**(1/2): p. 51-67.
97. Esclapez, M. and C.R. Houser, *Up-regulation of GAD65 and GAD67 in remaining hippocampal GABA neurons in a model of temporal lobe epilepsy*. Journal of Comparative Neurology, 1999. **412**(3): p. 488-505.
98. Feldblum, S., R.F. Ackermann, and A.J. Tobin, *Long-term increase of glutamate decarboxylase mRNA in a rat model of temporal lobe epilepsy*. Neuron, 1990. **5**(3): p. 361-71.
99. Erlander, M.G., et al., *Two genes encode distinct glutamate decarboxylases*. Neuron, 1991. **7**(1): p. 91-100.
100. Sheikh, S.N., S.B. Martin, and D.L. Martin, *Regional distribution and relative amounts of glutamate decarboxylase isoforms in rat and mouse brain*. Neurochemistry International, 1999. **35**(1): p. 73-80.
101. Kaufman, D.L., C.R. Houser, and A.J. Tobin, *Two forms of the gamma - aminobutyric acid synthetic enzyme glutamate decarboxylase have distinct intraneuronal distributions and cofactor interactions*. Journal of Neurochemistry, 1991. **56**(2): p. 720-3.
102. Martin, D.L., et al., *Cofactor interactions and the regulation of glutamate decarboxylase activity*. Neurochemical research, 1991. **16**(3): p. 243-9.
103. Rodriguez de Lores Arnaiz, G., R. Cardoni, and A. Pellegrino de Iraldi, *Levels of norepinephrine in rat cerebellum after administration of the convulsant 3-mercaptopropionic acid*. International Journal of Neuroscience, 1976. **6**(6): p. 269-71.
104. Bengzon, J., et al., *Seizure suppression in kindling epilepsy by intrahippocampal locus coeruleus grafts: evidence for an alpha-2-adrenoreceptor mediated mechanism*. Experimental brain research. Experimentelle Hirnforschung. Experimentation cerebrale, 1990. **81**(2): p. 433-7.
105. Kokaia, M., et al., *Noradrenaline and 5-hydroxytryptamine release in the hippocampus during seizures induced by hippocampal kindling stimulation: an in vivo microdialysis study*. Neuroscience (Oxford, United Kingdom), 1989. **32**(3): p. 647-56.
106. Yan, Q.S., P.C. Jobe, and J.W. Dailey, *Thalamic deficiency in norepinephrine release detected via intracerebral microdialysis: A synaptic determinant of*

- seizure predisposition in the genetically epilepsy-prone rat*. Epilepsy Research, 1993. **14**(3): p. 229-36.
107. Eells, J.B., et al., *Fos in locus coeruleus neurons following audiogenic seizure in the genetically epilepsy-prone rat: comparison to electroshock and pentylenetetrazol seizure models*. Neuroscience Letters, 1997. **233**(1): p. 21-24.
  108. Silveira, D.C., et al., *Activation of the locus coeruleus after amygdaloid kindling*. Epilepsia, 1998. **39**(12): p. 1261-4.
  109. Silveira, D.C., et al., *Seizures in rats treated with kainic acid induce Fos-like immunoreactivity in locus coeruleus*. NeuroReport, 1998. **9**(7): p. 1353-1357.
  110. Silveira, D.C., et al., *Flurothyl-induced seizures in rats activate Fos in brainstem catecholaminergic neurons*. Epilepsy Research, 2000. **39**(1): p. 1-12.
  111. Szot, P., S.S. White, and R.C. Veith, *Effect of pentylenetetrazol on the expression of tyrosine hydroxylase mRNA and norepinephrine and dopamine transporter mRNA*. Molecular Brain Research, 1997. **44**(1): p. 46-54.
  112. Arnold, P.S., R.J. Racine, and R.A. Wise, *Effects of atropine, reserpine, 6-hydroxydopamine, and handling on seizure development in the rat*. Experimental Neurology, 1973. **40**(2): p. 457-70.
  113. Blank, D.L., *Effect of combined reserpine and ECS on electroshock seizure thresholds in mice*. Pharmacology, Biochemistry and Behavior, 1976. **4**(4): p. 485-7.
  114. Gross, R.A. and J.A. Ferrendelli, *Relationships between norepinephrine and cyclic nucleotides in brain and seizure activity*. Neuropharmacology, 1982. **21**(7): p. 655-61.
  115. Shank, R.P., et al., *Topiramate: Preclinical evaluation of a structurally novel anticonvulsant*. Epilepsia, 1994. **35**(2): p. 450-60.
  116. Corcoran, M.E., et al., *Potentiation of amygdaloid kindling and metrazol-induced seizures by 6-hydroxydopamine in rats*. Experimental Neurology, 1974. **45**(1): p. 118-33.
  117. Jerlicz, M., et al., *Audiogenic seizures susceptibility in rats with lesioned raphe nuclei and treated with p-chlorophenylalanine*. Polish Journal of Pharmacology and Pharmacy, 1978. **30**(1): p. 63-8.
  118. Applegate, C.D., S. Pretel, and D.T. Piekut, *The substantia nigra pars reticulata, seizures and Fos expression*. Epilepsy Research, 1995. **20**(1): p. 31-9.



119. White, L.E. and J.L. Price, *The functional anatomy of limbic status epilepticus in the rat. I. Patterns of 14C-2-deoxyglucose uptake and Fos immunocytochemistry*. Journal of Neuroscience, 1993. **13**(11): p. 4787-809.
120. Bonhaus, D.W., J.R. Walters, and J.O. McNamara, *Activation of substantia nigra neurons: role in the propagation of seizures in kindled rats*. The Journal of neuroscience the official journal of the Society for Neuroscience, 1986. **6**(10): p. 3024-30.
121. Csernansky, J.G., et al., *Mesolimbic dopamine receptor increases two weeks following hippocampal kindling*. Brain Research, 1988. **449**(1-2): p. 357-60.
122. Csernansky, J.G., et al., *Mesolimbic dopaminergic supersensitivity following electrical kindling of the amygdala*. Biological Psychiatry, 1988. **23**(3): p. 285-94.
123. Gelbard, H.A. and C.D. Applegate, *persistent increases in dopamine D2 receptor mRNA expression in basal ganglia following kindling*. Epilepsy Research, 1994. **17**(1): p. 23-9.
124. Castaneda, T.R., et al., *Circadian rhythms of dopamine, glutamate and GABA in the striatum and nucleus accumbens of the awake rat: modulation by light*. Journal of Pineal Research, 2004. **36**(3): p. 177-185.
125. Morari, M., et al., *Reciprocal dopamine-glutamate modulation of release in the basal ganglia*. Neurochemistry International, 1998. **33**(5): p. 383-397.
126. Aultman, J.M. and B. Moghaddam, *Distinct contributions of glutamate and dopamine receptors to temporal aspects of rodent working memory using a clinically relevant task*. Psychopharmacology (Berlin, Germany), 2001. **153**(3): p. 353-364.
127. Jedema, H.P. and B. Moghaddam, *Glutamatergic control of dopamine release during stress in the rat prefrontal cortex*. Journal of Neurochemistry, 1994. **63**(2): p. 785-8.
128. Kretschmer, B.D., *Modulation of the mesolimbic dopamine system by glutamate: role of NMDA receptors*. Journal of Neurochemistry, 1999. **73**(2): p. 839-48.
129. Nieoullon, A., L. Kerkerian, and N. Dusticier, *Presynaptic dopaminergic control of high affinity glutamate uptake in the striatum*. Neuroscience Letters, 1983. **43**(2-3): p. 191-6.
130. Shimizu, N., et al., *Glutamate modulates dopamine release in the striatum as measured by brain microdialysis*. Brain Research Bulletin, 1990. **25**(1): p. 99-102.

131. Takahata, R. and B. Moghaddam, *Target-specific glutamatergic regulation of dopamine neurons in the ventral tegmental area*. Journal of Neurochemistry, 2000. **75**(4): p. 1775-1778.
132. Youngren, K.D., D.A. Daly, and B. Moghaddam, *Distinct actions of endogenous excitatory amino acids on the outflow of dopamine in the nucleus accumbens*. Journal of Pharmacology and Experimental Therapeutics, 1993. **264**(1): p. 289-93.
133. Bamford, N.S., et al., *Heterosynaptic dopamine neurotransmission selects sets of corticostriatal terminals*. Neuron, 2004. **42**(4): p. 653-663.
134. Goldstein, D.S., et al., *Catecholamines: Bridging Basic Science with Clinical Medicine*. [In: *Adv. Pharmacol. (San Diego)*, 1998; 42]. 1998. 1083 pp.
135. Chen, B.T. and M.E. Rice, *Synaptic regulation of somatodendritic dopamine release by glutamate and GABA differs between substantia Nigra and ventral tegmental area*. Journal of Neurochemistry, 2002. **81**(1): p. 158-169.
136. Segovia, G. and F. Mora, *Role of nitric oxide in modulating the release of dopamine, glutamate, and GABA in striatum of the freely moving rat*. Brain Research Bulletin, 1998. **45**(3): p. 275-9.
137. Carlsson, A., B. Biswas, and M. Lindqvist, *Influence of GABA and GABA-like drugs on monoaminergic mechanisms*. Advances in Biochemical Psychopharmacology, 1977. **16**(Nonstriatal Dopaminergic Neurons): p. 471-5.
138. [cited 2010 10/29/2010]; Available from: [http://www.appliedneuroscience.co.uk/ME\\_lv\\_Hx.html](http://www.appliedneuroscience.co.uk/ME_lv_Hx.html).
139. Obrenovitch, T.P., J. Urenjak, and E. Zilkha, *Evidence disputing the link between seizure activity and high extracellular glutamate*. Journal of Neurochemistry, 1996. **66**(6): p. 2446-2454.
140. Millan, M.H., et al., *Changes in rat brain extracellular glutamate concentration during seizures induced by systemic picrotoxin or focal bicuculline injection: an in vivo dialysis study with on-line enzymatic detection*. Epilepsy Research, 1991. **9**(2): p. 86-91.
141. Walker, M.C., et al., *Ascorbate and glutamate release in the rat hippocampus after perforant path stimulation: a "dialysis electrode" study*. Journal of Neurochemistry, 1995. **65**(2): p. 725-31.

## **Chapter 4**

### **Multiple Dosing of 3-MPA**

#### **4.1 Introduction**

##### *4.1.1 Background and Significance*

Glutamate activates 3 types of ionotropic receptors, NMDA (N-methyl-D-aspartate), AMPA ( $\alpha$ -amino-3-hydroxy-5-methyl-4-isoxazole propionic acid), and kainite (KA) receptors. Previous work in our lab has shown the effects of both local and systemic dosing of 3-MPA on glutamate. The effects of glutamate in particular are of importance because of its role in excitotoxicity and subsequent cell death. Glutamate excitotoxicity leads to an influx of calcium into the cell [1-3], as well as an increase in reactive oxygen species and cell death [4]. There is evidence that shows cells can respond in several ways. The first possibility is desensitization. Desensitization is the process by which further binding of the ligand to a receptor leads to decreased effectiveness of the receptor [5]. If a receptor becomes desensitized, it is no longer able to gate the release or reuptake of neurotransmitters, which in the case of glutamate would lead to excitotoxicity. Another pathway is sensitization of the receptor. Sensitization refers to an increase in response over time to a stimulus that originally did not elicit a response. The third option is the idea of neural protection/neural modulation where cells respond in such a way to limit the negative effects of excitotoxicity. Neural adaptation

can be thought of as short-term depression, but can also occur over a longer period of time with modulation in enzyme activity and protein synthesis.

Investigating multiple seizure events is important because clinical studies have shown the increased likelihood of subsequent seizures following the first unprovoked event [6-8]. It is often the subsequent excitotoxicity of glutamate and  $\text{Ca}^{+2}$  that kills neurons rather than the seizures themselves [9, 10]. However, there has not been sufficient work to determine the role of the neurons during subsequent seizure and excitation events to determine their course of action. In this study 3-MPA was administered twice to determine the neuronal changes during two separate events.

#### *4.1.2 Desensitization*

Desensitization of cells can result from a variety of sources. There is evidence that with desensitization, there is poor reuptake of glutamate from the post-synaptic space [11, 12]. If glutamate remains in the AMPA receptor longer than it is gated open, excitotoxicity can result [13]. NMDA receptors desensitize relatively slowly compared to AMPA and kainic receptors, which can desensitize on the order of milliseconds [14]. One of the mechanisms of receptor desensitization appears to be a conformational change in the form of a rearrangement of the dimer interface upon binding [15]. Glutamate excitotoxicity can occur at relatively low concentrations. Excitotoxicity has been seen with extracellular levels of glutamate as low as 2-5  $\mu\text{M}$  [16, 17]. Swelling and apoptosis of the cells have been seen at levels below 25  $\mu\text{M}$  with fast necrosis setting in at concentrations of glutamate over 100  $\mu\text{M}$  [18]. The idea of excitotoxicity is important in

seizures, because upon subsequent seizure events, cells become more easily excitable. In fact in many cases, it is the excitotoxicity which is more damaging than the seizures themselves.

#### *4.1.3 Sensitization*

Sensitization is often referred to as the “kindling effect” in that the mechanism of sensitization is closely related to the kindling mechanism for seizure development. Sensitization occurs when a stimulus that initially does not elicit a response, over time generates a response [19]. In the kindling model of epilepsy, sub-convulsive doses of a convulsant are given repeatedly over a period of time. Over time the animal becomes “sensitized” to the convulsant and these sub-convulsant doses develop into seizures [20-23]. This idea was first described in 1961 by Sevillano et al. where small current stimulation in the hippocampus resulted in an intensification of seizures as a result of stimulation [24]. This idea can be applied to drug application for seizure induction. Repeated dosing of a drug which elicits an increase in glutamate, in this case 3-MPA, could result in more substantial release of glutamate upon subsequent dosing.

#### *4.1.4 Long-term potentiation*

Learning and adaptation manifest themselves in the behavior and actions of an animal. These changes, however, are due to changes in the nervous system, which are due to changes on the cellular level, neurons in particular [25]. Long-term potentiation

(LTP) was first described by Bliss et al. in 1973, where they showed that a brief period of high-frequency stimulation led to an increase in the synaptic connections between neurons in the perforant path inputs in the entorhinal cortex to the dentate granule neurons in the dentate gyrus [26]. LTP has been shown to last for months and is another hypothesis to describe learned adaptation and explain synaptic plasticity. The mechanisms of long-term potentiation, however, are still not well understood. One unresolved question is whether the mechanism involves the pre-synaptic terminal, post-synaptic terminal, or both. Alterations on the presynaptic terminal could include the amount of neurotransmitter synthesized, number of vesicles released, kinetics of release, and reuptake. Changes at the post-synaptic terminal could include up/down regulation of the number of receptors, as well as ion flow [25]. Other possible mechanisms underlying LTP include gene expression and protein synthesis, such as activity-regulated cytoskeleton-associated protein (*Arc*) [27]. Inhibiting protein synthesis has been shown to effect memory transduction [25]. LTP can be divided into two stages, early and late. Early stage LTP can last for about 1 hour and is independent of newly synthesized proteins, while late stage LTP can last for months and is dependent on protein synthesis [28]. Regardless of the mechanism, LTP is one way to describe learning and memory in cells.

#### *4.1.5 Short-term depression*

Short-term depression is often due to altered feedback mechanisms. Neurotransmitters in high concentrations post-synaptically can act upon the pre-synaptic

terminals depressing further release [29, 30]. Communication between glial cells and neurons can be depressed [31-33] and vesicle sensitivity to  $\text{Ca}^{+2}$  can be adapted [34, 35].

#### *4.1.6 Regulation of enzyme activity, proteins, and transporters*

Studies have shown the marked decrease in glutamic acid decarboxylase activity (GAD) during seizures [36-38]. Long-term studies have also shown an upregulation in GAD weeks after seizures [39, 40]. This increase in GAD activity is thought to counteract the decrease in GABA by producing more GAD that will in turn lead to increased GABA levels.

Vesicular glutamate transporter 1 (VGLUT1) and vesicular GABA transporter (VGAT) are both amino acid transporters which help to supply vesicles with the amino acids for release. Research has shown an upregulation of VGAT with a subsequent downregulation of VGLUT1, one week following pilocarpine-induced seizures [41]. Again, the purpose of this regulation is to increase the amount of GABA in the brain.

#### *4.1.7 Experimental procedure*

In past experiments, 10mM 3-MPA was perfused through the probe for 50 minutes followed by aCSF for the remaining 70 minutes. In the multiple dosing experiments, after 60 minutes of basal collection 10mM 3-MPA was perfused through the probe for 25 minutes followed by 35 minutes of aCSF, followed again with 25 minutes of

10mM 3-MPA, and finally another 35 minutes with aCSF. The sampling rate and detection schemes were the same as discussed previously.

## **4.2 Results and Discussion**

### *4.2.1 3-MPA*

The perfusion time of 3-MPA was divided into two equal 25 minute intervals. The total perfusion time of 50 minutes was held constant so that data could be compared between the single 50 minute perfusion of 3-MPA and the multiple dosing regimen. If 3-MPA was perfused longer in one experiment compared to the other, excitation and release of glutamate could not be compared directly between experiments. The perfusion was divided into two equal intervals so that the change in neurotransmitters from the first 25 minute perfusion could be compared with the changes during the second 25 minute perfusion. If one interval was longer than the other changes in neurotransmitters could then be due to the total amount of 3-MPA delivered to the brain and not any changes in synaptic plasticity of the neurons between doses.

Figure 4.1 shows the delivery of 10mM 3-MPA into the hippocampus of anesthetized rats. As expected, the delivery of 3-MPA is biphasic with removal of 3-MPA between the first and second administration and again during the final 35 minutes of the experiment. The plateau in 3-MPA is similar to that seen in the single 50 minute dose of 10mM 3-MPA. Based upon this, the total amount of 3-MPA delivered to the brain during both 25 minute administration intervals is similar to that during the single 50



minute administration. This was important to compare the multiple dosing with the single dose.

n=4 10mM 3-MPA Multiple Dosing Hippocampus

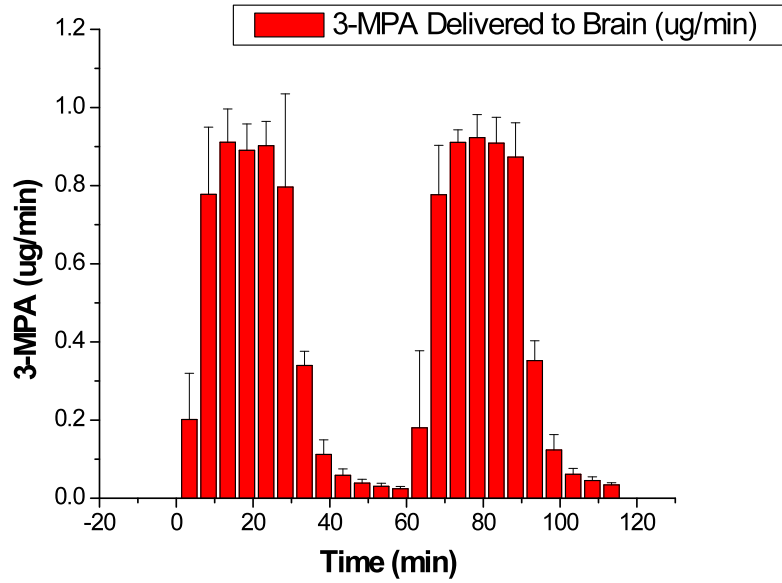


Figure 4.1 10mM 3-MPA delivered to the brain ( $\mu\text{g}/\text{min}$ ) during multiple dosing of 3-MPA (n=4 rats).

#### 4.2.2 Amino Acids

Figure 4.2 shows the changes in glutamate and GABA during the multiple dosing of 3-MPA. There were two increases in both glutamate and GABA, however the increases are attenuated during the second administration of 3-MPA. There was a 6-fold increase in glutamate during the first administration, followed by a 2.5-fold increase. GABA increased 2.5-fold during the first administration followed by almost a 2-fold increase during the second. There was a correlation between the magnitude of glutamate release during the first administration and the magnitude of the attenuation during the second administration. The error bars are significantly large due to one rat. In this one rat glutamate increased 14-fold during the first administration of 3-MPA and 6-fold during the second. The ratios for the increased glutamate release during the first administration compared to the second administration show that, although in this one rat the 14-fold increase was substantially larger than in any of the other rats, the ratio of the first increase to the second is similar, 2.76 compared to an average of  $2.13 \pm 0.71$  for all four rats combined. One reason for perfusing aCSF 35 minutes before the second administration of 3-MPA, in addition to the necessity of doing so to divide the 3-MPA administration into two equal 25 minute periods, was to allow glutamate levels to return to basal levels. In three of the rats glutamate levels returned to basal:  $101.1 \pm 8.5\%$ . The only rat where this was not the case (returned to 211%), was again the rat where the increase in glutamate was the greatest.

The area under the curve for the release of glutamate in the hippocampus of anesthetized rats for the 50 minute perfusion of 3-MPA was calculated and compared to the release of glutamate in the multiple dosing regimen of 3-MPA. The release of

glutamate was larger during the 50 minute perfusion, 39555 (% change x min), compared to 26592 (% change x min) for the multiple dosing regime. Since 3-MPA was perfused for the same period of time, and roughly the same mass of 3-MPA was perfused during the 50 minute perfusion compared to the multiple dosing regimen, these results suggest that the reason for a smaller increase in glutamate during the multiple dosing regimen is not due to a lack of glutamate available for release, but rather points towards a neuroprotective role preventing further release of glutamate.

Figure 4.3 shows the changes in the other amino acids. There was an 8-fold increase in aspartate during the first administration of 3-MPA followed by an attenuation in aspartate during the second administration, which was a more modest 2-fold increase. The large error bars are due to one rat, again the rat where the increase in glutamate was the greatest. These large error bars exist for arginine and alanine as well, both non-excitatory and non-inhibitory amino acids. With the exception of the 30 and 35 minute time points in the one rat, the alanine levels remain at basal levels, between 91 and 110 % of baseline. Since this increase was only seen in one rat, this event was not significant.

Since the depression in signal seen in these experiments is on such a short-term basis, many of the explanations regarding protein synthesis and regulation of enzymes are not applicable in this case. Upregulation in GAD was shown to occur on the timescale of one week, obviously too long to describe the changes seen here [39, 40]. Likewise, upregulation of VGAT and downregulation of VGLUT1 was shown to occur one week after seizures [41]. Therefore, there must be a short-term explanation for depression on the order of minutes and hours as opposed to days.

The most common explanations for short-term synaptic depression are vesicle depletion models. The idea behind these models is that upon stimulation a fraction of the readily releasable vesicles are depleted. Upon a second stimulation, the readily releasable pool (RRP) is a fraction of what was available upon the first stimulation [42, 43]. Synaptic depression can also be due to release probability [44, 45], and the recycling of vesicles and whether reserves lie in the readily releasable pool or the reserve pool [46-49]. Stevens et al. have shown that synaptic depression could be due to depletion of the readily releasable pool, requiring recycling and movement of vesicles from the reserve pool to the synapse for release [47]. There have been studies to determine the size of the pool. There are various ways to ensure complete emptying of the RRP, either by a large depolarizing pulse, caged  $\text{Ca}^{+2}$ , high-osmolarity solution, and repetitive stimulus trains [50-52]. In the CA1 portion of the hippocampus, the area targeted in our experiments, it has been estimated by electron microscopy that there are on average 10 vesicles in the RRP, however there is quite a bit of variability in this number even within the CA1 [52-54]. While vesicle depletion models are often used to describe short-term depression, this model cannot not explain the depression seen in these experiments. As stated above, based upon the area under the curve calculations for the release of glutamate during the 50 minute perfusion versus the multiple dosing of 3-MPA, it appears that there was sufficient glutamate that was not released during the first administration of 3-MPA, suggesting that the RRP has not been depleted.

There have been studies showing that depression is independent of the magnitude of initial release and stimulation frequency, suggesting that there are pathways of depression that are not dependent upon vesicle depletion [55-57]. Specifically in

inhibitory rat synapses, a second release was not dependent upon the magnitude of the first [58]. Synaptic release has long been connected with an influx of  $\text{Ca}^{+2}$ . There is heterogeneous sensitivity of vesicles to the concentration of  $\text{Ca}^{+2}$  needed for vesicle fusion and release. There is a hypothesis that vesicles can adapt their sensitivity to  $\text{Ca}^{+2}$ , leading to depression [34, 35]. There is also homosynaptic inhibition, where the concentration of a neurotransmitter builds up to a level where it has an action on the pre-synaptic terminal, in addition to the post-synaptic terminal, which leads to a negative feedback loop and synaptic depression [52]. One such example is the breakdown of ATP, found in high levels in vesicles, to adenosine which goes onto activate pre-synaptic adenosine receptors and leads to inhibition [29, 30]. Depression can also occur by the action of GABA on pre-synaptic  $\text{GABA}_B$  receptors which will reduce  $\text{Ca}^{+2}$  influx upon subsequent stimulation. Another possible pathway for depression is due to the interaction between neurons and glial cells. Glial cells contain neurotransmitter receptor sites. Signaling can elevate  $\text{Ca}^{+2}$  levels in glial cells which results in release of substances from astrocytes which act on the pre-synaptic terminal to regulate neurotransmitter release. Hippocampal cell culture research has shown that stimulation of glial cells leads to depression between the glial cells and neurons [32]. It is thought that this depression is due to  $\text{Ca}^{+2}$  evoked release of glutamate, which then acts on pre-synaptic metabotropic glutamate receptors [31-33].

From the studies performed here it is impossible to determine exactly what mechanism is causing this short-term depression. With such large increases in glutamate upon administration of 3-MPA, it is plausible that there is a feedback mechanism where glutamate acts on the pre-synaptic terminal, thus depressing further release of glutamate.

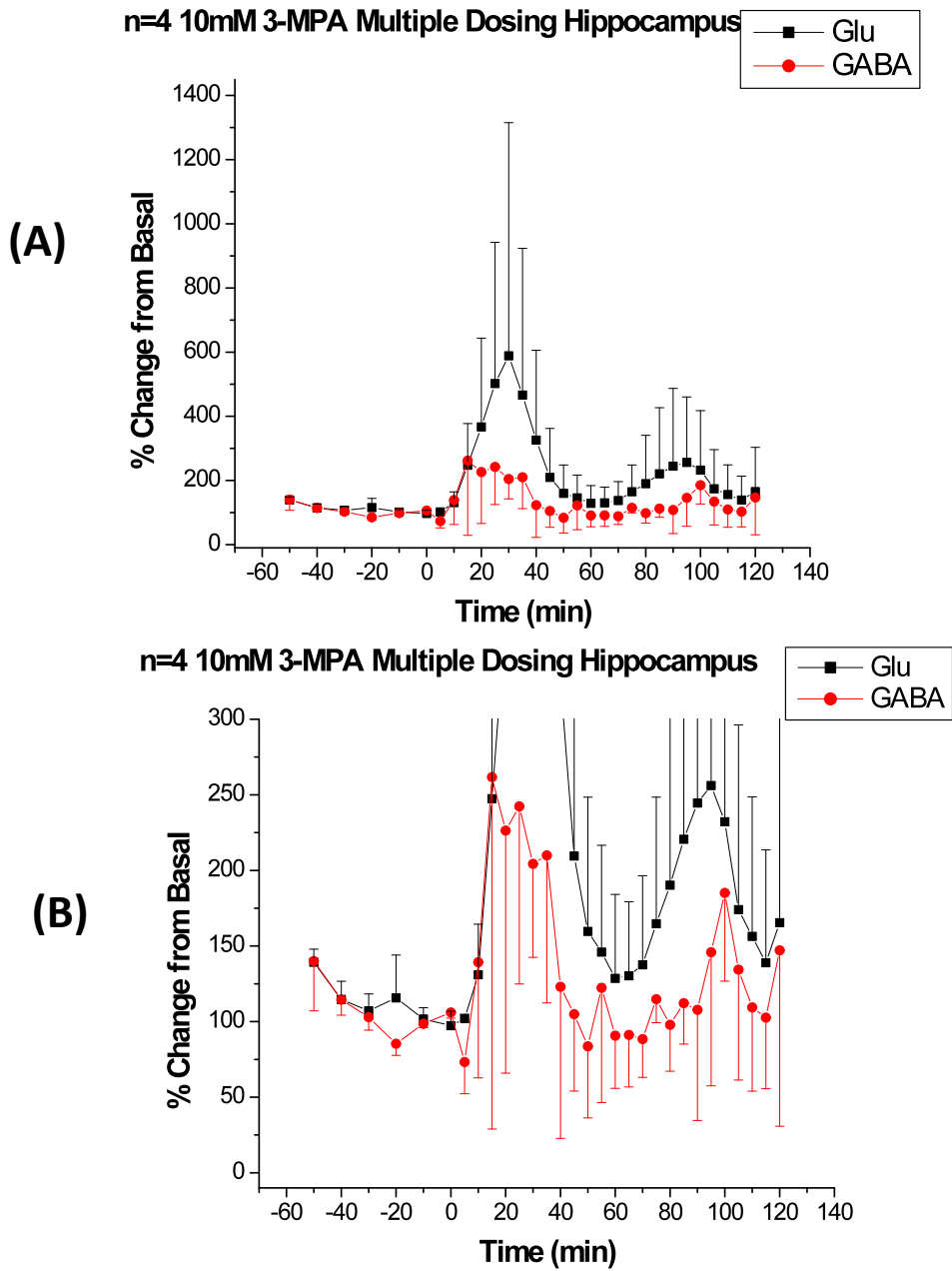


**Figure 4.2** Multiple Dosing of 10mM 3-MPA in the hippocampus of anesthetized rats. (A) Glutamate and GABA full scale and (B) zoomed picture of glutamate and GABA for better detail (n=4 rats).

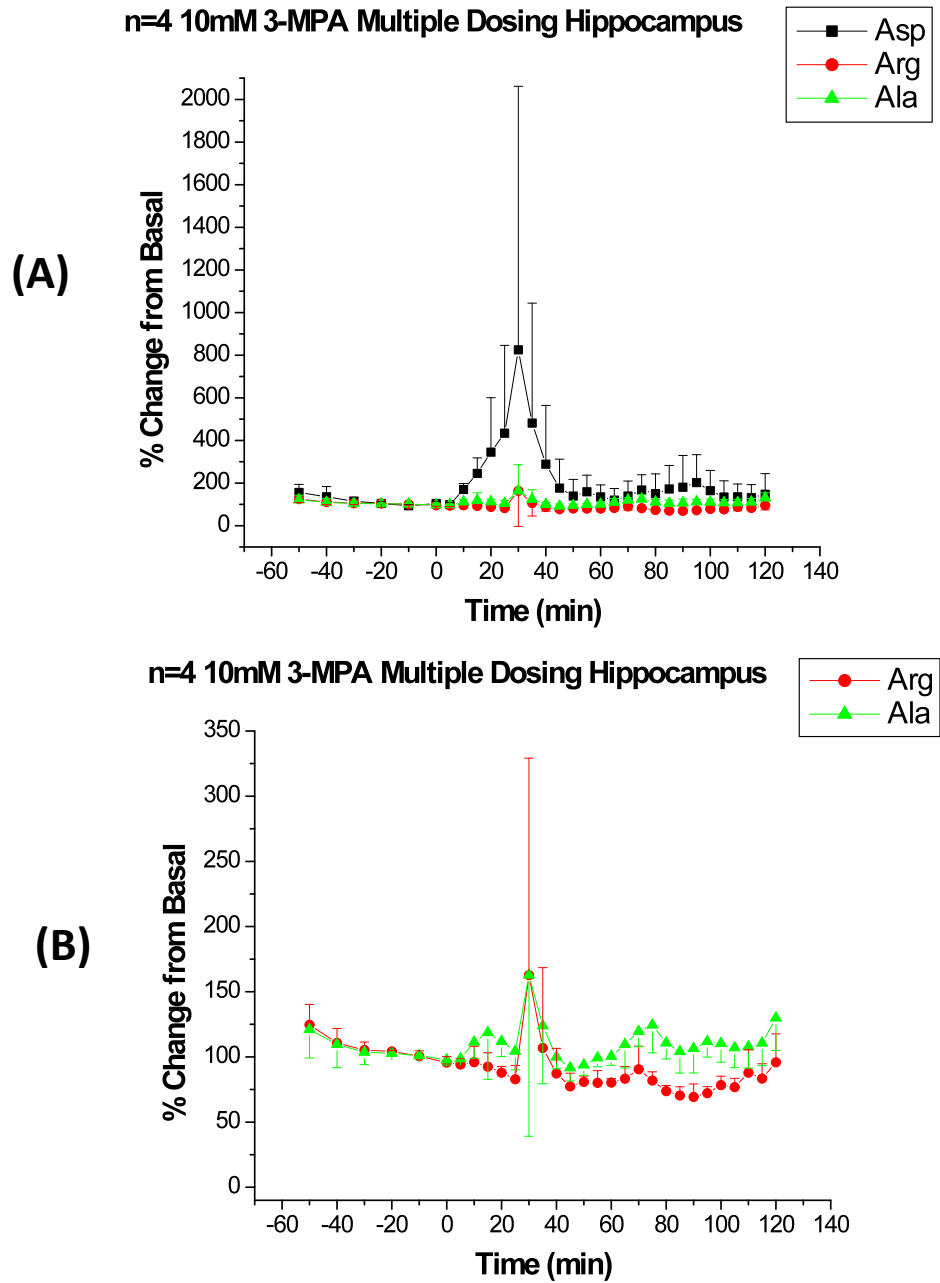


**Figure 4.3** Multiple Dosing of 10mM 3-MPA in the hippocampus of anesthetized rats. (A) aspartate, arginine, and alanine full scale and (B) zoomed picture of arginine and alanine for better detail (n=4 rats).



#### *4.2.3 Catecholamine neurotransmitters*

Figure 4.4 shows the changes in catecholamine neurotransmitters during multiple dosing of 3-MPA. There are two increase in norepinephrine, similar to that which is seen with glutamate. Norepinephrine increased 5-fold during the first administration of 3-MPA, returned to basal levels, and then increased 3.5-fold during the second administration. These increases in norepinephrine make sense, during the 50 minute perfusion of 3-MPA in the hippocampus NE remained elevated during the entire administration. This shows the relationship between 3-MPA dosing and release of NE. Dopamine increased roughly 2-fold during both administrations of 3-MPA. The metabolites DOPAC, 5-HIAA, and HVA respond similarly as they do during the 50 minute perfusion of 3-MPA, as can be seen in Figure 4.5.

Research has demonstrated a role in glutamate stimulated release of norepinephrine [59-61]. These results seem to be substantiated here, as the two increases in norepinephrine mirror the changes seen in glutamate.

#### *4.2.4 ECoG analysis*

As with the single dosing regimen of 3-MPA, no seizures were detected during multiple dosing. This can be seen in Figure 4.6. See section 3.xx for a thorough discussion of ECoG data.

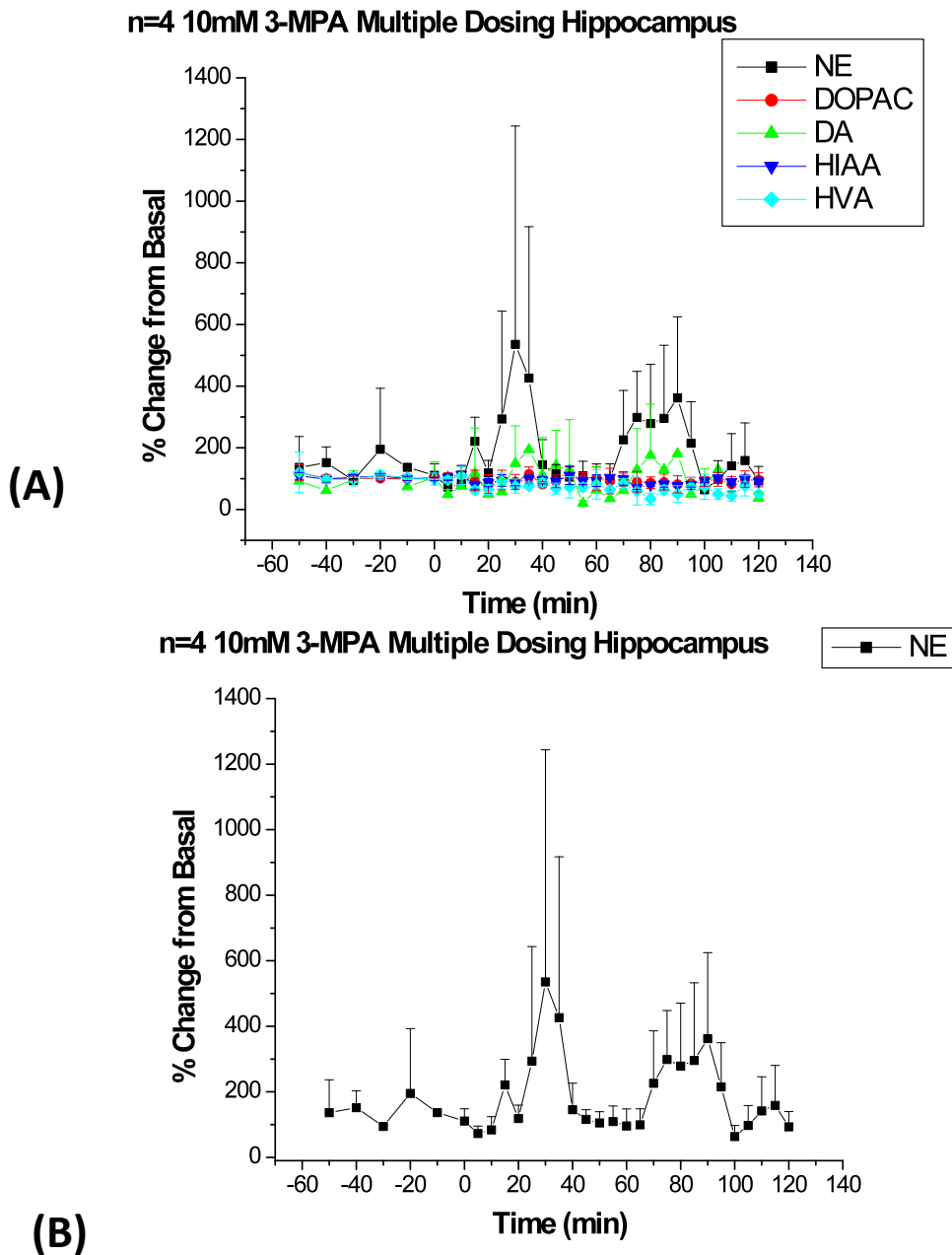
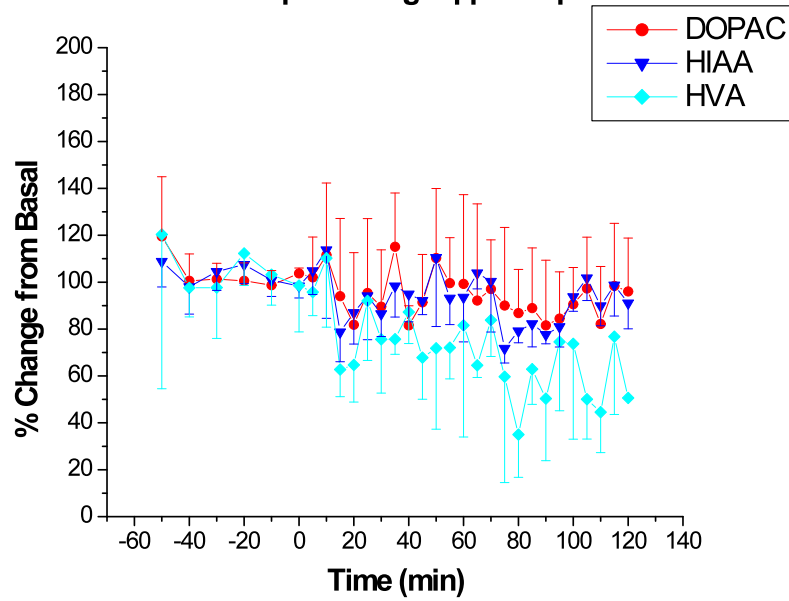


Figure 4.4 Multiple Dosing of 10mM 3-MPA in the hippocampus of anesthetized rats. (A) catecholamine neurotransmitters full scale and (B) NE for better detail (n=4 rats).

n=4 10mM 3-MPA Multiple Dosing Hippocampus



**Figure 4.5** Catecholamine metabolites during 10mM 3-MPA multiple dosing in hippocampus (n=4 rats).

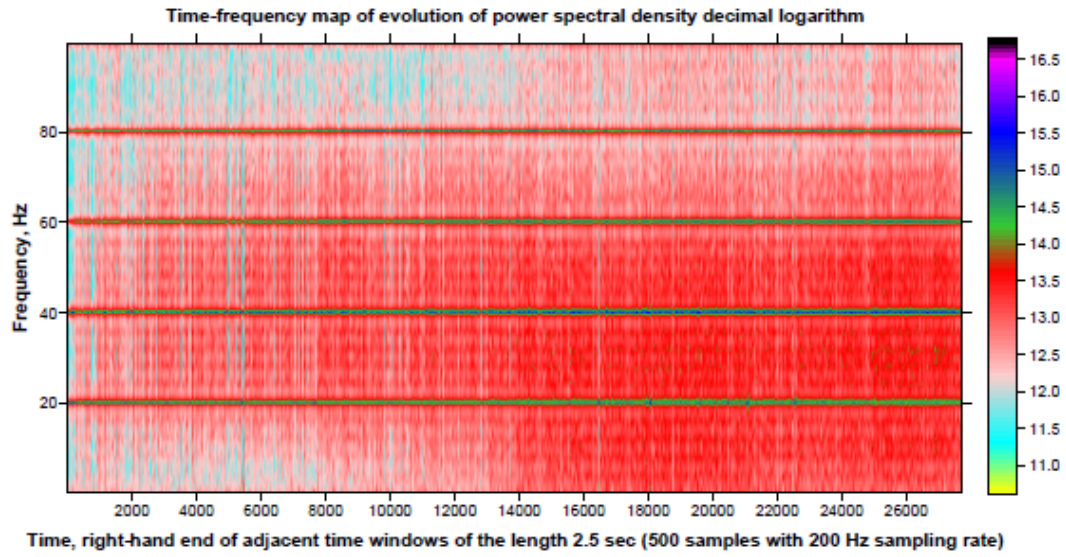


Figure 4.6 ECoG data from internal microdialysis Ag/AgCl electrode during multiple dosing of 10mM 3-MPA in the hippocampus.

### 4.3 Conclusions

Multiple dosing of 3-MPA led to a similar delivery as the 50 minute administration period. There were two increases for glutamate, corresponding to the two administration periods of 3-MPA. There was an initial 6-fold increase in glutamate, followed by an attenuated 2.5-fold increase. The area under the curve (AUC) for the second increase in glutamate was small than the first increase, however, the combined area under the curve for the two increases in glutamate was smaller than for the 50 minute perfusion. There was an attenuated increase for GABA and aspartate as well during the second administration of 3-MPA. It was suggested that the attenuation in signal was not due to a vesicle depletion, rather some protective mechanism. This short-term depression could be due to  $\text{Ca}^{+2}$  sensitivity, a negative feedback loop due to buildup of transmitter in the post-synaptic cleft, the action of GABA on pre-synaptic  $\text{GABA}_A$  receptors, and interaction between glial cells and neurons. There were also large increases in norepinephrine. It was suggested these increases could be due to the role of glutamate on norepinephrine release. As with the single dose regimen of 3-MPA no seizures were detected.

#### 4.4 References

1. Ascher, P. and L. Nowak, *The role of divalent cations in the N-methyl-D-aspartate responses of mouse central neurons in culture*. Journal of Physiology (Cambridge, United Kingdom), 1988. **399**: p. 247-66.
2. Choi, D.W., *Glutamate neurotoxicity and diseases of the nervous system*. Neuron, 1988. **1**(8): p. 623-34.
3. Konig, N., et al., *Synaptic and non-synaptic AMPA receptors permeable to calcium*. Japanese Journal of Pharmacology, 2001. **86**(1): p. 1-17.
4. Ogura, A., M. Miyamoto, and Y. Kudo, *Neuronal death in vitro: parallelism between survivability of hippocampal neurons and sustained elevation of cytosolic calcium after exposure to glutamate receptor agonist*. Experimental Brain Research, 1988. **73**(3): p. 447-58.
5. Eric R. Kandel, J.H.S., Thomas M. Jessel, *Essentials of Neural Science and Behavior*. 1995: Appleton and Lange.
6. Hauser, W.A., et al., *Seizure recurrence after a first unprovoked seizure*. The New England journal of medicine, 1982. **307**(9): p. 522-8.
7. Offringa, M., et al., *Seizure recurrence after a first febrile seizure: a multivariate approach*. Developmental medicine and child neurology, 1992. **34**(1): p. 15-24.
8. Wingkun, E.C., et al., *Natural history of recurrent seizures after resective surgery for epilepsy*. Epilepsia, 1991. **32**(6): p. 851-6.
9. Fujikawa Denson, G., *Prolonged seizures and cellular injury: understanding the connection*. Epilepsy & behavior E&B, 2005. **7 Suppl 3**: p. S3-11.
10. Wasterlain, C.G., et al., *Pathophysiological mechanisms of brain damage from status epilepticus*. Epilepsia, 1993. **34 Suppl 1**: p. S37-53.
11. Agranoff, B.W., et al., *Basic Neurochemistry. Molecular, Cellular, and Medical Aspects. 4th Ed.* 1989. 984 pp.
12. Clinckers, R., et al., *In vivo modulatory action of extracellular glutamate on the anticonvulsant effects of hippocampal dopamine and serotonin*. Epilepsia, 2005. **46**(6): p. 828-836.
13. Trussell, L.O., S. Zhang, and I.M. Raman, *Desensitization of AMPA receptors upon multiquantal neurotransmitter release*. Neuron, 1993. **10**(6): p. 1185-96.

14. Wheal, H., A. Thomson, and Editors, *Excitatory Amino Acids and Synaptic Transmission: Second Edition*. 1995. 384 pp.
15. Sun, Y., et al., *Mechanism of glutamate receptor desensitization*. Nature (London, United Kingdom), 2002. **417**(6886): p. 245-253.
16. Meldrum, B. and J. Garthwaite, *Excitatory amino acid neurotoxicity and neurodegenerative disease*. Trends in Pharmacological Sciences, 1990. **11**(9): p. 379-87.
17. Rosenberg, P.A., S. Amin, and M. Leitner, *Glutamate uptake disguises neurotoxic potency of glutamate agonists in cerebral cortex in dissociated cell culture*. Journal of Neuroscience, 1992. **12**(1): p. 56-61.
18. Cheung, N.S., et al., *Micromolar L-glutamate induces extensive apoptosis in an apoptotic-necrotic continuum of insult-dependent, excitotoxic injury in cultured cortical neurons*. Neuropharmacology, 1998. **37**(10-11): p. 1419-1429.
19. Kraus, J.E., *Sensitization phenomena in psychiatric illness: Lessons from the kindling model*. Journal of Neuropsychiatry and Clinical Neurosciences, 2000. **12**(3): p. 328-343.
20. Goddard, G.V., *Development of epileptic seizures through brain stimulation at low intensity*. Nature, 1967. **214**(5092): p. 1020-1.
21. Goddard, G.V., D.C. McIntyre, and C.K. Leech, *A permanent change in brain function resulting from daily electrical stimulation*. Experimental Neurology, 1969. **25**(3): p. 295-330.
22. McNamara, J.O., et al., *The kindling model of epilepsy: a review*. Progress in Neurobiology (Oxford, United Kingdom), 1980. **15**(2): p. 139-59.
23. McNamara, J.O., R. Morrisett, and J.V. Nadler, *Recent advances in understanding mechanisms of the kindling model*. Advances in neurology, 1992. **57**: p. 555-60.
24. McNamara, J.O., *Kindling model of epilepsy*. Advances in neurology, 1986. **44**: p. 303-18.
25. Byrne, J.H. and J.L. Roberts, *From Molecules to Networks: An Introduction to Cellular and Molecular Neuroscience*. 2004. 583 pp.
26. Bliss, T.V. and T. Lomo, *Long-lasting potentiation of synaptic transmission in the dentate area of the anaesthetized rabbit following stimulation of the perforant path*. The Journal of physiology, 1973. **232**(2): p. 331-56.

27. Steward, O. and P.F. Worley, *A cellular mechanism for targeting newly synthesized mRNAs to synaptic sites on dendrites*. Proceedings of the National Academy of Sciences of the United States of America, 2001. **98**(13): p. 7062-7068.
28. Nguyen, P.V., T. Abel, and E.R. Kandel, *Requirement of a critical period of transcription for induction of a late phase of LTP*. Science (Washington, D. C.), 1994. **265**(5175): p. 1104-1107.
29. Greene, R.W. and H.L. Haas, *The electrophysiology of adenosine in the mammalian central nervous system*. Progress in Neurobiology (Oxford, United Kingdom), 1991. **36**(4): p. 329-41.
30. Redman, R.S. and E.M. Silinsky, *ATP released together with acetylcholine as the mediator of neuromuscular depression at frog motor nerve endings*. Journal of Physiology (Cambridge, United Kingdom), 1994. **477**(1): p. 117-27.
31. Araque, A., et al., *SNARE protein-dependent glutamate release from astrocytes*. Journal of Neuroscience, 2000. **20**(2): p. 666-673.
32. Araque, A., et al., *Glutamate-dependent astrocyte modulation of synaptic transmission between cultured hippocampal neurons*. The European journal of neuroscience, 1998. **10**(6): p. 2129-42.
33. Araque, A., et al., *Calcium elevation in astrocytes causes an NMDA receptor-dependent increase in the frequency of miniature synaptic currents in cultured hippocampal neurons*. Journal of Neuroscience, 1998. **18**(17): p. 6822-6829.
34. Blank, P.S., et al., *Submaximal responses in calcium-triggered exocytosis are explained by differences in the calcium sensitivity of individual secretory vesicles*. Journal of General Physiology, 1998. **112**(5): p. 559-567.
35. Blank, P.S., et al., *The calcium sensitivity of individual secretory vesicles is invariant with the rate of calcium delivery*. The Journal of general physiology, 1998. **112**(5): p. 569-76.
36. Houser, C.R., A.B. Harris, and J.E. Vaughn, *Time course of the reduction of GABA terminals in a model of focal epilepsy: a glutamic acid decarboxylase immunocytochemical study*. Brain Research, 1986. **383**(1-2): p. 129-45.
37. Lloyd, K.G., et al., *Biochemical evidence for the alterations of GABA-mediated synaptic transmission in pathological brain tissue (stereo EEG or morphological definition) from epileptic patients*. 1981: p. 325-38.



38. Ribak, C.E., et al., *A decrease in the number of GABAergic somata is associated with the preferential loss of GABAergic terminals at epileptic foci*. Brain Research, 1986. **363**(1): p. 78-90.
39. Feldblum, S., R.F. Ackermann, and A.J. Tobin, *Long-term increase of glutamate decarboxylase mRNA in a rat model of temporal lobe epilepsy*. Neuron, 1990. **5**(3): p. 361-71.
40. Marksteiner, J. and G. Sperk, *Concomitant increase of somatostatin, neuropeptide Y and glutamate decarboxylase in the frontal cortex of rats with decreased seizure threshold*. Neuroscience (Oxford, United Kingdom), 1988. **26**(2): p. 379-85.
41. Boulland, J.-L., et al., *Changes in vesicular transporters for gamma - aminobutyric acid and glutamate reveal vulnerability and reorganization of hippocampal neurons following pilocarpine-induced seizures*. Journal of Comparative Neurology, 2007. **503**(3): p. 466-485.
42. Betz, W.J., *Depression of transmitter release at the neuromuscular junction of the frog*. The Journal of physiology, 1970. **206**(3): p. 629-44.
43. Liley, A.W. and K.A. North, *An electrical investigation of effects of repetitive stimulation on mammalian neuromuscular junction*. Journal of Neurophysiology, 1953. **16**(5): p. 509-27.
44. Tsodyks, M.V. and H. Markram, *The neural code between neocortical pyramidal neurons depends on neurotransmitter release probability*. Proceedings of the National Academy of Sciences of the United States of America, 1997. **94**(2): p. 719-723.
45. Wu, L.-G. and J.G.G. Borst, *The reduced release probability of releasable vesicles during recovery from short-term synaptic depression*. Neuron, 1999. **23**(4): p. 821-832.
46. Delgado, R., et al., *Size of vesicle pools, rates of mobilization, and recycling at neuromuscular synapses of a Drosophila mutant, shibire*. Neuron, 2000. **28**(3): p. 941-953.
47. Stevens, C.F. and J.F. Wesseling, *Identification of a novel process limiting the rate of synaptic vesicle cycling at hippocampal synapses*. Neuron, 1999. **24**(4): p. 1017-1028.
48. von Gersdorff, H. and G. Matthews, *Depletion and replenishment of vesicle pools at a ribbon-type synaptic terminal*. Journal of Neuroscience, 1997. **17**(6): p. 1919-1927.

49. Wu, L.-G. and W.J. Betz, *Kinetics of synaptic depression and vesicle recycling after tetanic stimulation of frog motor nerve terminals*. Biophysical Journal, 1998. **74**(6): p. 3003-3009.
50. Rosenmund, C. and C.F. Stevens, *Definition of the readily releasable pool of vesicles at hippocampal synapses*. Neuron, 1996. **16**(6): p. 1197-1207.
51. Stevens, C.F. and T. Tsujimoto, *Estimates for the pool size of releasable quanta at a single central synapse and for the time required to refill the pool*. Proceedings of the National Academy of Sciences of the United States of America, 1995. **92**(3): p. 846-9.
52. Zucker, R.S. and W.G. Regehr, *Short-term synaptic plasticity*. Annual Review of Physiology, 2002. **64**: p. 355-405.
53. Harris, K.M. and P. Sultan, *Variation in the number, location and size of synaptic vesicles provides an anatomical basis for the nonuniform probability of release at hippocampal CA1 synapses*. Neuropharmacology, 1995. **34**(11): p. 1387-1395.
54. Schikorski, T. and C.F. Stevens, *Quantitative ultrastructural analysis of hippocampal excitatory synapses*. Journal of Neuroscience, 1997. **17**(15): p. 5858-5867.
55. Armitage, B.A. and S.A. Siegelbaum, *Presynaptic induction and expression of homosynaptic depression at Aplysia sensorimotor neuron synapses*. Journal of Neuroscience, 1998. **18**(21): p. 8770-8779.
56. Neveu, D. and R.S. Zucker, *Long-lasting potentiation and depression without presynaptic activity*. Journal of Neurophysiology, 1996. **75**(5): p. 2157-60.
57. Parker, D., *Depression of synaptic connections between identified motor neurons in the locust*. Journal of Neurophysiology, 1995. **74**(2): p. 529-38.
58. Kraushaar, U. and P. Jonas, *Efficacy and stability of quantal GABA release at a hippocampal interneuron-principal neuron synapse*. Journal of Neuroscience, 2000. **20**(15): p. 5594-5607.
59. Howells, F.M. and V.A. Russell, *Glutamate-stimulated release of norepinephrine in hippocampal slices of animal models of attention-deficit/hyperactivity disorder (spontaneously hypertensive rat) and depression/anxiety-like behaviours (Wistar-Kyoto rat)*. Brain Research, 2008. **1200**: p. 107-115.
60. Navarro, C.E., R.J. Cabrera, and A.O. Donoso, *Release of 3H-noradrenaline by excitatory amino acids from rat mediobasal hypothalamus and the influence of aging*. Brain Research Bulletin, 1994. **33**(6): p. 677-82.

61. Ohta, K., et al., *Presynaptic glutamate receptors facilitate release of norepinephrine and 5-hydroxytryptamine as well as dopamine in the normal and ischemic striatum*. *Journal of the Autonomic Nervous System*, 1994. **49**(Suppl.): p. S195-S202.

## Chapter 5

### Conclusions and Future Work

#### 5.1 Summary of Dissertation

Previous research in our laboratory involved a pharmacokinetic/pharmacodynamic study of a chemically-induced seizure model with 3-MPA in rats [1, 2]. A steady-state model for 3-MPA administration was developed where a 60 mg/kg bolus dose was followed by a constant intravenous (i.v.) infusion of 50 mg/kgmin<sup>-1</sup> of 3-MPA for 50 minutes. The concentrations of 3-MPA were measured in the blood, striatum, and hippocampus. Steady-state concentrations of 3-MPA were achieved in the brain and the pharmacokinetics of 3-MPA in the blood and the brain were studied. This was the first known study of the pharmacokinetics of 3-MPA in a chemically-induced seizure model. By achieving steady-state concentrations of 3-MPA, the concentration/response variable was held constant when studying the neurochemical changes in the striatum and hippocampus. As expected, 3-MPA inhibited the conversion of glutamic acid to  $\gamma$ -hydroxybutyric acid *in vivo*, resulting in an increase in glutamic acid and a decrease in  $\gamma$ -hydroxybutyric acid. In addition to measuring the concentrations of 3-MPA and the subsequent neurochemical changes in the brain, ECoG recordings were made. Thus, seizure number, intensity, and duration were correlated to the neurochemical changes.

While this constant infusion model was an important first step in the development of 3-MPA epileptic seizure model, it is not very clinically relevant. Research has shown that 70% of adult onset epilepsy patients present with partial (focal) seizures [3]. This means that the seizures and the effects thereof are localized in a specific brain region. 3-MPA in this constant infusion model is administered to the entire brain, and thus its physiological and neurochemical changes are on a global scale as well. The purpose of these studies was to develop a model where 3-MPA is dosed to a specific brain region so that the physiological and neurochemical changes can be monitored in a site specific manner, while not disturbing the neurochemical balance in the brain as a whole.

#### *5.1. 3-MPA local dosing in the striatum, hippocampus, and locus coeruleus*

Delivery of 10mM 3-MPA was consistent through all three brain regions, in both awake and anesthetized rats. Upon administration of 3-MPA there was an increase in both glutamate and GABA. The increase in glutamate compared to baseline in the striatum of anesthetized rats was 15-fold following local delivery, compared to a 2-fold increase following systemic dosing of 3-MPA. Glutamate increased 7-fold in the hippocampus of anesthetized rats as well. The increases in glutamate were much larger in awake rats, 200-fold in the striatum and 25-fold in the hippocampus. It is possible that the increased levels of glutamate in awake rats are related to the use of ketamine, a NMDA antagonist, as the anesthetic utilized in these experiments has been shown to decrease excitatory transmission and inhibit voltage sensitive  $\text{Ca}^{+2}$  channels [4-10]. The increase in GABA in these experiments was unexpected and it may be due to the role of

the inhibitory surround. The inhibitory surround is the region of brain tissue surrounding the seizure focus where there is an increase in inhibition to prevent the spread of the epileptic focus to the surrounding tissue. When dosing 3-MPA through the probe, the region affected is so small that GABA released in the inhibitory surround can diffuse to the probe and would result in the increase in GABA seen at the 3-MPA dosing probe. Aspartate, another excitatory amino acid, increased as well in the striatum and hippocampus of both awake and anesthetized rats. In the *locus coeruleus*, there was again an increase in both glutamate and GABA; however, the increase in GABA was larger than glutamate. There is a significant pool of glutamate ( $\mu\text{M}$  levels) and expression of glutamic acid decarboxylase (GAD) in the *locus coeruleus*; thus this does not seem to explain the small increase in glutamate in this region, compared to the larger increases in the striatum and hippocampus [11-14].

There was an increase in norepinephrine and dopamine in all three brain regions in anesthetized rats. The increase in norepinephrine was not seen with the systemic dosing of 3-MPA and the role of norepinephrine in the *locus coeruleus* (the main synthesis site of norepinephrine in the brain) was a major reason for studying this brain region with the 3-MPA model. The increase in dopamine was not surprising, considering the increase seen with the systemic 3-MPA model, as well as the neuronal relationship between glutamate and dopamine [15-21].

As discussed above, one of the advantages of the local dosing 3-MPA model is that any seizure activity and subsequent neurotransmitter changes would be isolated to a small brain area, when compared to systemic injections where the whole brain is effected. One way to show that this was indeed the case was to dose 3-MPA through the probe in

one brain region, but also collect samples in the other two brain regions where only aCSF was being perfused, as a control. If 3-MPA was indeed acting locally, there should be minimal changes in the other brain regions, unless there were projections present from one brain region to another.

In most brain regions, administration of 3-MPA did not effect the levels of amino acids and catecholamine neurotransmitters in other regions. These results show that administration of 3-MPA through the probe produced only local neurochemical changes and does not effect the brain in a global manner.

When administering 3-MPA in either the striatum or hippocampus, there is a subsequent decrease in GABA in the *locus coeruleus*. It has been suggested this might be due to the role of norepinephrine in GABA synthesis and the interaction between GABAergic and noradrenergic neurons [22-28]. Also, when administering 3-MPA in the *locus coeruleus* there was a subsequent increase in norepinephrine in the striatum. This increase was after the termination of 3-MPA dosing and was not expected as literature has not indicated there are projections from the *locus coeruleus* to the striatum.

Seizures were detected in three rats using copper wires placed in the brain alongside the microdialysis probe. However, there were many rats in which no seizures were detected. It was thought that this might be due to the placement of the wires and their proximity to the probe itself. For this reason specially designed probes were used with an internal Ag/AgCl working electrode. These probes, along with screws placed on the cortex, detected seizures with a systemic injection of 3-MPA. However, when these probes were used with local administration of 3-MPA, no seizures were detected. This

result may be due to the small number of neurons exhibiting excitatory postsynaptic potentials (EPSPs) with the local dosing and, therefore the signal was too small to detect.

### *5.1.2 Multiple dosing of 3-MPA*

The effect of multiple doses of 3-MPA was investigated. This was an interesting set of experiments since the long-term effects of seizures have great clinical significance. The 50 minute 3-MPA administration used earlier was divided into two 25 minute periods with two 35 minute periods where aCSF was perfused through the probe following each 3-MPA administration. These experiments investigated whether neurons involved some protective mechanism to decrease excitotoxicity during the second 3-MPA administration or if neurons lost their plasticity and thus increased excitotoxicity during the second administration.

During the first administration of 3-MPA there was a 6-fold increase in glutamate followed by a 2.5-fold increase during the second administration. There were smaller increases in both GABA and aspartate during the second administration when compared with the first. There was an increase in norepinephrine during both administrations of 3-MPA as well.

While these studies are preliminary, neurons seem to incorporate a protective mechanism to reduce the amount of glutamate released during the second administration of 3-MPA. While most protective mechanisms occur over longer time periods, some protective mechanisms can apparently occur over the time period used in these studies.



## 5.2 Future directions

One of the more interesting discoveries with the local dosing of 3-MPA was the increase in GABA. 3-MPA works by inhibiting the enzyme glutamic acid decarboxylase, which is responsible for the conversion of glutamic acid to  $\gamma$ -aminobutyric acid [29-32]. This should result in an increase in glutamate and a decrease in GABA concentrations [33-37]. With a systemic injection of 3-MPA, a decrease in GABA was seen [1], however upon local administration of 3-MPA an increase in GABA was observed. It has been suggested that this increase in GABA could be a result of the inhibitory surround of the seizure focus [38-41]. The inhibitory surround is a region of inhibition surrounding the focus of a seizure that limits excitability in the surrounding tissue [42, 43]. When dosing a compound through the microdialysis probe, the effected tissue region is small enough that an increase in GABA from the inhibitory surround could diffuse towards the probe and cause the increase in GABA observed.

Several studies utilizing microdialysis could be performed to further investigate the role of the inhibitory surround and the increase in GABA seen while administering 3-MPA locally. One probe could be used to administer 3-MPA while several other probes are placed in the surrounding tissue, at an incremental distance from the dosing probe to monitor the change in GABA in the inhibitory surround. It would be expected that if an increase in inhibition in the surround is playing a role in the increased GABA at the dosing probe, then these increases in GABA should be larger in the surround than at the dosing probe, since diffusion would decrease the concentration of GABA reaching the

dosing probe. Additionally, a compound which inhibits the release of GABA could be perfused through the non-3-MPA probes to see how that changes GABA neurotransmission at the 3-MPA probe. Preventing GABA release in the inhibitory surround would prevent the inhibition and would allow epileptiform activity to spread from the region directly surrounding the probe to distant tissue [40, 41].

Preliminary studies have been performed here to assess the neurochemical changes observed with multiple doses of 3-MPA. While there is a decrease in the release of glutamate and GABA during the second administration of 3-MPA, this needs further investigation. There are explanations for these changes on a short-term time scale, including feedback mechanisms, communication between glial cells and neurons, and synaptic vesicle sensitivity to  $\text{Ca}^{+2}$  [44-50]. However, there are many long-term changes, such as protein synthesis and enzyme and transporter regulation [51-58], that will not be seen over a 2-hour experiment. Long-term awake studies must be performed, which will also provide more practical results, considering clinical outcomes and the long-term effects of epilepsy occur over a time-course of years, not hours.

### 5.3 References

1. Crick, E.W., *In vivo Microdialysis Coupled with Electrophysiology for the Neurochemical Analysis of Epileptic Seizures*, in *Chemistry*. 2007, The University of Kansas.
2. Crick, E.W., et al., *An investigation into the pharmacokinetics of 3-mercaptopropionic acid and development of a steady-state chemical seizure model using in vivo microdialysis and electrophysiological monitoring*. *Epilepsy Res.*, 2007. **74**(2-3): p. 116-125.
3. French, J.A. and T.A. Pedley, *Initial management of epilepsy*. *N. Engl. J. Med.*, 2008. **359**(2): p. 166-176.
4. Harrison, N.L. and M.A. Simmonds, *Quantitative studies on some antagonists of N-methyl D-aspartate in slices of rat cerebral cortex*. *British Journal of Pharmacology*, 1985. **84**(2): p. 381-91.
5. Hirota, K. and D.G. Lambert, *Voltage-sensitive Ca<sup>2+</sup> channels and anesthesia*. *British Journal of Anaesthesia*, 1996. **76**(3): p. 344-6.
6. Hudspith, M.J., *Glutamate: a role in normal brain function, anesthesia, analgesia and CNS injury*. *British Journal of Anaesthesia*, 1997. **78**(6): p. 731-747.
7. Kitayama, M., et al., *Inhibitory effects of intravenous anaesthetic agents on K<sup>+</sup>-evoked glutamate release from rat cerebrocortical slices. Involvement of voltage-sensitive Ca<sup>2+</sup> channels and GABAA receptors*. *Naunyn-Schmiedeberg's Archives of Pharmacology*, 2002. **366**(3): p. 246-253.
8. Lynch, C., 3rd and J.J. Pancrazio, *Snails, spiders, and stereospecificity--is there a role for calcium channels in anesthetic mechanisms?* *Anesthesiology*, 1994. **81**(1): p. 1-5.
9. Pocock, G. and C.D. Richards, *Excitatory and inhibitory synaptic mechanisms in anesthesia*. *British Journal of Anaesthesia*, 1993. **71**(1): p. 134-47.
10. Sun, X., et al., *Effects of ketamine anesthesia on neurotransmitter metabolism of cerebral ganglion in dogs*. *Disi Junyi Daxue Xuebao*, 2008. **29**(22): p. 2038-2040.
11. Berod, A., et al., *Catecholaminergic and GABAergic anatomical relationship in the rat substantia nigra, locus coeruleus, and hypothalamic median eminence: immunocytochemical visualization of biosynthetic enzymes on serial semithin plastic-embedded sections*. *The journal of histochemistry and cytochemistry official journal of the Histochemistry Society*, 1984. **32**(12): p. 1331-8.

12. Feng, Y.Z., et al., *micro - and delta -Opioid receptor antagonists precipitate similar withdrawal phenomena in butorphanol and morphine dependence*. *Neurochemical research*, 1996. **21**(1): p. 63-71.
13. Majumdar, S. and B.N. Mallick, *Increased levels of tyrosine hydroxylase and glutamic acid decarboxylase in locus coeruleus neurons after rapid eye movement sleep deprivation in rats*. *Neuroscience Letters*, 2003. **338**(3): p. 193-196.
14. Nitz, D. and J.M. Siegel, *GABA release in the locus ceruleus as a function of sleep/wake state*. *Neuroscience (Oxford)*, 1997. **78**(3): p. 795-801.
15. Aultman, J.M. and B. Moghaddam, *Distinct contributions of glutamate and dopamine receptors to temporal aspects of rodent working memory using a clinically relevant task*. *Psychopharmacology (Berlin, Germany)*, 2001. **153**(3): p. 353-364.
16. Jedema, H.P. and B. Moghaddam, *Glutamatergic control of dopamine release during stress in the rat prefrontal cortex*. *Journal of Neurochemistry*, 1994. **63**(2): p. 785-8.
17. Kretschmer, B.D., *Modulation of the mesolimbic dopamine system by glutamate: role of NMDA receptors*. *Journal of Neurochemistry*, 1999. **73**(2): p. 839-48.
18. Nieoullon, A., L. Kerkerian, and N. Dusticier, *Presynaptic dopaminergic control of high affinity glutamate uptake in the striatum*. *Neuroscience Letters*, 1983. **43**(2-3): p. 191-6.
19. Shimizu, N., et al., *Glutamate modulates dopamine release in the striatum as measured by brain microdialysis*. *Brain Research Bulletin*, 1990. **25**(1): p. 99-102.
20. Takahata, R. and B. Moghaddam, *Target-specific glutamatergic regulation of dopamine neurons in the ventral tegmental area*. *Journal of Neurochemistry*, 2000. **75**(4): p. 1775-1778.
21. Youngren, K.D., D.A. Daly, and B. Moghaddam, *Distinct actions of endogenous excitatory amino acids on the outflow of dopamine in the nucleus accumbens*. *Journal of Pharmacology and Experimental Therapeutics*, 1993. **264**(1): p. 289-93.
22. Anden, N.E. and H. Wachtel, *Biochemical effects of baclofen (beta - parachlorophenyl-GABA) on the dopamine and the noradrenaline in the rat brain*. *Acta Pharmacologica et Toxicologica*, 1977. **40**(2): p. 310-20.

23. Herman, J.P., A. Renda, and B. Bodie, *Norepinephrine-gamma-aminobutyric acid (GABA) interaction in limbic stress circuits: effects of reboxetine on GABAergic neurons*. *Biological Psychiatry*, 2003. **53**(2): p. 166-174.
24. Karbon, E.W., R.S. Duman, and S.J. Enna, *GABAB receptors and norepinephrine-stimulated cAMP production in rat brain cortex*. *Brain Research*, 1984. **306**(1-2): p. 327-32.
25. Lloyd, K.G., et al., *The potential use of GABA agonists in psychiatric disorders: evidence from studies with progabide in animal models and clinical trials*. *Pharmacology, Biochemistry and Behavior*, 1983. **18**(6): p. 957-66.
26. Suzdak, P.D., *Differential coupling of GABA-A and GABA-B receptors to the noradrenergic system: implications for a GABA-ergic role in depression*. 1985. p. 262 pp.
27. Suzdak, P.D. and G. Gianutsos, *GABA-noradrenergic interaction: evidence for differential sites of action for GABA-A and GABA-B receptors*. *Journal of Neural Transmission (1972-1989)*, 1985. **64**(3-4): p. 163-72.
28. Suzdak, P.D. and G. Gianutsos, *Parallel changes in the sensitivity of gamma -aminobutyric acid and noradrenergic receptors following chronic administration of antidepressant and GABAergic drugs. A possible role in affective disorders*. *Neuropharmacology*, 1985. **24**(3): p. 217-22.
29. Horton, R.W. and B.S. Meldrum, *Seizures induced by allylglycine, 3-mercaptopropionic acid and 4-deoxyribose in mice and photosensitive baboons, and different modes of inhibition of cerebral glutamic acid decarboxylase*. *Br J Pharmacol*, 1973. **49**(1): p. 52-63.
30. Netopilova, M., et al., *Inhibition of glutamate decarboxylase activity by 3-mercaptopropionic acid has different time course in the immature and adult rat brains*. *Neurosci. Lett.*, 1997. **226**(1): p. 68-70.
31. Netopilova, M., et al., *Differences between immature and adult rats in brain glutamate decarboxylase inhibition by 3-mercaptopropionic acid*. *Epilepsy Res.*, 1995. **20**(3): p. 179-84.
32. Sarhan, S. and N. Seiler, *Metabolic inhibitors and subcellular distribution of GABA*. *J Neurosci Res*, 1979. **4**(5-6): p. 399-421.
33. Fan, S.G., M. Wusteman, and L.L. Iversen, *3-Mercaptopropionic acid inhibits GABA release from rat brain slices in vitro*. *Brain Res.*, 1981. **229**(2): p. 371-7.

34. Herbison, A.E., R.P. Heavens, and R.G. Dyer, *Endogenous release of gamma -aminobutyric acid from the medial preoptic area measured by microdialysis in the anesthetised rat*. J. Neurochem., 1990. **55**(5): p. 1617-23.
35. Ma, D., et al., *Simultaneous determination of gamma -aminobutyric acid and glutamic acid in the brain of 3-mercaptopropionic acid-treated rats using liquid chromatography-atmospheric pressure chemical ionization mass spectrometry*. J. Chromatogr., B: Biomed. Sci. Appl., 1999. **726**(1 + 2): p. 285-290.
36. Timmerman, W., J. Zwaveling, and B.H.C. Westerink, *Characterization of extracellular GABA in the substantia nigra reticulata by means of brain microdialysis*. Naunyn-Schmiedeberg's Arch. Pharmacol., 1992. **345**(6): p. 661-5.
37. Tunnicliff, G., *Action of inhibitors on brain glutamate decarboxylase*. Int. J. Biochem., 1990. **22**(11): p. 1235-41.
38. Bruehl, C. and O.W. Witte, *Cellular activity underlying altered brain metabolism during focal epileptic activity*. Annals of neurology, 1995. **38**(3): p. 414-20.
39. Chagnac-Amitai, Y. and B.W. Connors, *Horizontal spread of synchronized activity in neocortex and its control by GABA-mediated inhibition*. Journal of Neurophysiology, 1989. **61**(4): p. 747-58.
40. Golomb, D. and Y. Amitai, *Propagating neuronal discharges in neocortical slices: computational and experimental study*. Journal of Neurophysiology, 1997. **78**(3): p. 1199-211.
41. Prince, D.A., et al., *Chronic focal neocortical epileptogenesis: does disinhibition play a role?* Canadian journal of physiology and pharmacology, 1997. **75**(5): p. 500-7.
42. Benali, A., et al., *Excitation and inhibition jointly regulate cortical reorganization in adult rats*. Journal of Neuroscience, 2008. **28**(47): p. 12284-12293.
43. Trevelyan, A.J., et al., *epilepsModular propagation of epileptiform activity: evidence for an inhibitory veto in neocortex*. Journal of Neuroscience, 2006. **26**(48): p. 12447-12455.
44. Araque, A., et al., *SNARE protein-dependent glutamate release from astrocytes*. Journal of Neuroscience, 2000. **20**(2): p. 666-673.
45. Araque, A., et al., *Glutamate-dependent astrocyte modulation of synaptic transmission between cultured hippocampal neurons*. The European journal of neuroscience, 1998. **10**(6): p. 2129-42.

46. Araque, A., et al., *Calcium elevation in astrocytes causes an NMDA receptor-dependent increase in the frequency of miniature synaptic currents in cultured hippocampal neurons*. Journal of Neuroscience, 1998. **18**(17): p. 6822-6829.
47. Blank, P.S., et al., *Submaximal responses in calcium-triggered exocytosis are explained by differences in the calcium sensitivity of individual secretory vesicles*. Journal of General Physiology, 1998. **112**(5): p. 559-567.
48. Blank, P.S., et al., *The calcium sensitivity of individual secretory vesicles is invariant with the rate of calcium delivery*. The Journal of general physiology, 1998. **112**(5): p. 569-76.
49. Greene, R.W. and H.L. Haas, *The electrophysiology of adenosine in the mammalian central nervous system*. Progress in Neurobiology (Oxford, United Kingdom), 1991. **36**(4): p. 329-41.
50. Redman, R.S. and E.M. Silinsky, *ATP released together with acetylcholine as the mediator of neuromuscular depression at frog motor nerve endings*. Journal of Physiology (Cambridge, United Kingdom), 1994. **477**(1): p. 117-27.
51. Boulland, J.-L., et al., *Changes in vesicular transporters for gamma - aminobutyric acid and glutamate reveal vulnerability and reorganization of hippocampal neurons following pilocarpine-induced seizures*. Journal of Comparative Neurology, 2007. **503**(3): p. 466-485.
52. Feldblum, S., R.F. Ackermann, and A.J. Tobin, *Long-term increase of glutamate decarboxylase mRNA in a rat model of temporal lobe epilepsy*. Neuron, 1990. **5**(3): p. 361-71.
53. Houser, C.R., A.B. Harris, and J.E. Vaughn, *Time course of the reduction of GABA terminals in a model of focal epilepsy: a glutamic acid decarboxylase immunocytochemical study*. Brain Research, 1986. **383**(1-2): p. 129-45.
54. Lloyd, K.G., et al., *Biochemical evidence for the alterations of GABA-mediated synaptic transmission in pathological brain tissue (stereo EEG or morphological definition) from epileptic patients*. 1981: p. 325-38.
55. Marksteiner, J. and G. Sperk, *Concomitant increase of somatostatin, neuropeptide Y and glutamate decarboxylase in the frontal cortex of rats with decreased seizure threshold*. Neuroscience (Oxford, United Kingdom), 1988. **26**(2): p. 379-85.
56. Nguyen, P.V., T. Abel, and E.R. Kandel, *Requirement of a critical period of transcription for induction of a late phase of LTP*. Science (Washington, D. C.), 1994. **265**(5175): p. 1104-1107.

57. Ribak, C.E., et al., *A decrease in the number of GABAergic somata is associated with the preferential loss of GABAergic terminals at epileptic foci*. Brain Research, 1986. **363**(1): p. 78-90.
58. Steward, O. and P.F. Worley, *A cellular mechanism for targeting newly synthesized mRNAs to synaptic sites on dendrites*. Proceedings of the National Academy of Sciences of the United States of America, 2001. **98**(13): p. 7062-7068.